EXAMINING THE ROLE OF ANGIOGENIC FACTORS AND EARLY DEVELOPMENTAL DEFECTS IN THE PATHOGENESIS OF PRE-ECLAMPSIA IN A MOUSE MODEL, BPH/5

A Dissertation

Presented to the Faculty of the Graduate School

of Cornell University

in Partial Fulfillment of the Requirements for the Degree of

Doctor of Philosophy

by

Ashley Kathryn Woods

January 2011

EXAMINING THE ROLE OF ANGIOGENIC FACTORS AND EARLY DEVELOPMENTAL DEFECTS IN THE PATHOGENESIS OF PRE-ECLAMPSIA IN A MOUSE MODEL, BPH/5

Ashley K. Woods, Ph.D.

Cornell University 2011

Pre-eclampsia (PE) is a devastating condition that affects 5-8% of pregnant women and is the leading cause of fetal and maternal deaths worldwide. The etiology of this disorder, however, is largely unknown. The BPH/5 mouse model is the only known rodent model that spontaneously develops the symptoms of PE as well as many of the placental pathologies associated with the human condition. As the pathogenesis of PE is known to start before the symptoms begin, this disease is very difficult to study in women. As such, this mouse model is invaluable in examining early pregnancy events and elucidating the pathophysiology of this disorder.

Angiogenic factors have been promising biomarkers of PE in women. We found that the angiogenic profile in BPH/5 mice mimics that of women at high risk of developing PE with a decrease in the pro-angiogenic factors vascular endothelial growth factor (VEGF) and related placental growth factor (PGF). Using a viral gene transfer strategy to increase systemic levels of one of these important angiogenic factors, VEGF, we provide evidence of a functional link between diminished VEGF levels and the hallmark symptoms of PE in BPH/5 mice.

The BPH/5 model of PE also exhibits significant fetal demise throughout pregnancy. One third of conceptuses are lost by mid gestation. To further characterize early pregnancy events in BPH/5, we used ultrasound to score embryos based on their health status. We were able to detect evidence of developmental challenge *in vivo* in a subset of embryos prior to previous necropsy data. Using fetoplacental units with

varying development/health status, we performed gene expression microarray studies to examine the molecular cues to fetal demise in this model. Challenged fetoplacental units show dysregulation in functional pathways related to angiogenesis, development and apoptosis.

Finally, as the placenta plays a pivotal role in the development of PE, and the BPH/5 model shows marked placental abnormalities, we examined whether these placental defects in BPH/5 could be traced to the peri-implantation period when this organ is established. We found significant pre-implantation embryo maturation delay along with premature maternal endocrine signaling in BPH/5 mice, suggesting asynchronous timing of these important events involved in implantation. This was accompanied by implantation defects as indicated by abnormal spacing of implantation sites, as well as morphological and molecular abnormalities in early BPH/5 implantation sites compared to controls. Using a protocol to artificially synchronize implantation events in BPH/5, we were able to rescue the implantation clustering defect, the molecular dysregulation in early implantation sites, and importantly, several later placental abnormalities including placental expansion toward the decidua and umbilical blood flow.

The research in this thesis highlights and confirms the important role of angiogenic factors in successful and healthy pregnancies, provides clues to the molecular signature that may underlie fetoplacental defects associated with PE, and sheds new light on early peri-implantation events that may set the stage for the development of PE and perhaps other disorders of pregnancy.

BIOGRAPHICAL SKETCH

Ashley Woods was born in Penetanguishene, Ontario, Canada in 1982. Graduating an Ontario Scholar from Havergal College, Toronto, she then pursued her undergraduate education at Mount Allison University, Sackville New Brunswick, Canada. In 2003 she earned a Bachelor of Science with first class honors in Biochemistry, and a minor in Philosophy. Her undergraduate thesis work was characterizing the kinetics of enzymes along key metabolic pathways in various tissues of the Northern Shot-tailed Shrew, *Blarina brevicauda*. Ashley then moved to Ottawa, Ontario to pursue a Masters degree under the mentorship of Dr. Ken Storey, Carleton University. Her masters work included examining post-translational modification of proteins in two models of hibernation and metabolic rate depression, the hibernating ground squirrel (*Spermophilus tridecemlineatus)* and freeze tolerant wood frog (*Rana sylvatica*). After earning her Masters in Science in Biology in 2005, she then worked in a small biotech company in Ottawa, Liponex Inc., validating animal models of cholesterol metabolism as well as designing new therapeutic compounds using cholesterol mimetics. After a year in industry, she decided to return to graduate school.

In 2006, Ashley joined the field of Pharmacology at Cornell University, and after completing her rotations, joined the lab of Dr. Robin Davisson in early 2007.

ACKNOWLEGMENTS

I have many people to thank who were able to make this research possible. First I'd like to thank Dr. Robin Davisson for the freedom to take this dissertation research in a completely new direction, and her support over the years in allowing me to forge my way in this new field. Thank-you also to my special committee: Drs Mark Roberson, Kimberly O'Brien and Jane Salmon, for their support and enthusiasm during my doctoral training.

Over the past few years I have received mentorship in many forms. I'd like to thank Dr. Darren Hoffmann for passing the torch of the BPH/5 project and his helpful conversations. Dr. Paula Cohen, for her advice and guidance on studying early developmental processes. A special thanks to Rob Munroe for passing on his surgical skills. Dr. Don Schlafer for his help in examining placental pathology. Patricia Fisher for immunohistochemistry expertise. Dr. Shari Gelber for insightful conversations.

I would also like to acknowledge my many collaborators that allowed me to be a part of very diverse studies. Collaborators include Dr. Mark Roberson, Dr Kimberly O'Brien, Dr. Fayez Safadi, Dr. Heidi Stuhlmann, Dr. Ned Place, Dr. Jane Salmon, and Dr. Lee Adamson.

I would like to acknowledge the support from my boyfriend Josh. Finally I would like to thank my family for their love and support throughout the years.

TABLE OF CONTENTS

LIST OF FIGURES

LIST OF TABLES

LIST OF ABBREVIATIONS

Ad-LacZ	Adenovirus encoding LacZ
Ad-VEGF	Adenovirus encoding VEGF
AngII	Angiotensin II
AT1-AA	Autoantibodies to the angiotensin 1 receptor
ATR	Assisted reproductive technologies
BP	Blood pressure
DAVID	Database for Annotation Visualization and Integrated Discovery
e7.5	embryonic day 7.5
ENG	Endoglin
GO	Gene ontology
HELLP	Hemolysis, Elevated Liver enzymes Low Platelets
HIF	Hypoxia Inducible Factor
HLA-G	Human leukocyte antigen-G
HUVEC	Human umbilical vein endothelial cells
IUGR	Intrauterine Growth Restriction
IVF	*in vitro* fertilization
MMP	Matrix metalloprotease
NK	Natural killer
NP	Non-pregnant
PE	Pre-eclampsia
PGF	Placental growth factor
RAS	Renin-angiotensin signaling
ROS	Reactive oxygen species

RUPP	Reduced uterine perfusion pressure
sFLT-1	Soluble form of the fms-like tyrosine kinase 1
sENG	Soluble endoglin
SOD	Superoxide dismutase
TGF-β	Transforming growth factor beta
TNFα	Tumor necrosis factor alpha
VEGF	Vascular endothelial growth factor

CHAPTER ONE:

INTRODUCTION

1.1 Pre-eclampsia

1.1.1 Hallmarks, definitions and associated disorders

Pre-eclampsia (PE) is serious pregnancy associated syndrome that affects 3-14% of pregnancies worldwide and has a recurrence rate of 7.5-65%[1]. Despite improvements in peri-natal care, the incidence of PE continues to rise, as described in the 2009 National Vital Statistics report (www.cdc.gov). It is a heterogeneous and multi-organ disorder that is the leading cause of maternal and fetal deaths in both developing and developed countries. The hallmark symptoms include new onset hypertension >140mmHg systolic blood pressure (BP) and >90mmHg diastolic BP in women who had normal BP prior to 20weeks gestation, and proteinuria ≥0.3gm in 24hr urine collection, or ≥30mg/dL of random urine determination (≥1 + reading on dipstick)[2]. Additional symptoms can include headache, blurred vision, abdominal pain and edema. Some cases of severe PE can also be accompanied by the HELLP syndrome (Hemolysis, Elevated Liver enzymes, Low Platelets). If left untreated, pre-eclampsia can progress to eclampsia which involves cerebral vasospasms resulting in tonic-clonic seizures and even death. PE is distinct from gestational hypertension, where hypertension is the only symptom. Women with gestational hypertension are often closely monitored for the early detection of PE and its more life threatening associated symptoms of HELLP and eclampsia.

Though pre-eclampsia has been documented in medical literature for hundreds of years, the treatment remains minimal. The problem lies in the unknown etiology of the disease. Without understanding the mechanism and pathological progression of the disease, it is difficult to both diagnose early, and devise a treatment strategy. Clinicians are left to manage the symptoms of PE once the syndrome has started. Treatment trials with dietary supplementation with Vitamins C and E have proven

largely ineffective at reducing the risk of development of PE with even an increase in risk of gestational hypertension, severe pre-eclampsia, eclampsia and HELLP[3, 4]. Today, women with severe-pre-eclampsia are put on strict bed-rest. If the symptoms of pre-eclampsia become too threatening to maternal health, the fetus (and placenta) is delivered. As a result, pre-eclampsia is directly responsible for 15% of pre-mature births each year in the US (www.pre-eclampsia.org).

Pre-eclampsia is a disease tremendously heterogeneous in its symptomology, organs involved and timing of the onset of these symptoms. Women can exhibit symptoms of PE as early as 28 weeks, while others do not show symptoms until term. The hallmark symptoms of PE, including new onset hypertension and proteinuria, are exhibited with all women independent of timing of onset. Yet some women go on to develop HELLP syndrome, have low-birthweight babies or poor neonatal outcomes, whereas other PE mothers deliver healthy birthweight babies with the maternal symptoms resolving soon after delivery. With the expansion in research in this area over the past 25 years, the overarching diagnosis of PE has shifted to reflect the many classifications of this syndrome. Early onset PE has symptoms beginning prior to 34 weeks gestation and is often complicated with more severe placental pathology, poor fetal outcomes, and more extreme maternal complications such as HELLP and eclampsia[5-7]. Late onset PE pregnancies show symptoms later than 34 weeks gestation and are often less severe, with symptoms resolving after delivery of usually a healthy weight neonate[5-7]. Placenta samples from early and late onset PE reveal a very different pathological origin[7, 8]. Additionally, the delivery of a small-for-gestational-age baby reflects a complication know as Intrauterine Growth Restriction (IUGR). Up to one third of PE pregnancies are associated with IUGR[9, 10]. Importantly, IUGR is not unique to PE pregnancies, as 8-14% of normal pregnancies are also affected[11]. It is

now becoming more widely accepted that though early and late onset PE as well as IUGR result from dysfunction of many of the same pathways, the etiology of these conditions is unique, and should be examined with this in mind.

1.1.2 Epidemiology : Risk Factors and Trends

Pre-eclampsia is recognized to have both a placental component as well as a maternal component. Many of the placental abnormalities are shared between PE and IUGR, and yet some women go on to have asymptomatic pregnancies with IUGR, whereas others develop PE. What has long been referred to as maternal "constitutional" factors[12] have been more itemized with the help of retrospective clinical analysis. Women that are at higher risk of developing PE have the following pre-dispositions: obesity[13], diabetes[14], hyperhomocysteinemia[15], and black ethnicity[12, 16]. Additionally, women with prior history of hypertension are at a ~20% risk of developing PE, and approximately a 30% risk of having a small-for-gestation-age fetus[17]. Interestingly, when one combines three risk factors of chronic hypertension, obesity and previous PE pregnancy, the risk of developing PE only increases to 23% and the risk for a small-for-gestation-age fetus remains the same[17]. This highlights what a large risk factor chronic hypertension is to the development of this disorder.

Though less well examined, PE is known to have some hereditary and thus genetic links. With prior PE pregnancies, mothers, daughters, sisters and granddaughters are at a 2-5 fold increased frequency of PE compared to the control population[18-20]. Despite the major and obvious contribution of the maternal genome, fetal genes, and therefore the paternal genome are also implicated in the development of this syndrome[20]. Sons born to PE pregnancies are at an increased rate of fathering their own children in pregnancies complicated with PE [20]. With such multifactorial

disease such as PE, determining the loci responsible for eliciting this syndrome would be both beneficial for genetic screening of prospective parents, but ultimately a very daunting task.

1.1.3 The causative organ of PE

Pre-eclampsia is a disease whose etiology is closely tied to the placenta. In fact, it is only upon delivery of the placenta that symptoms of PE resolve. PE is known to affect molar pregnancies[21, 22], a pregnancy disorder in which no fetus is present, implicating the placenta as the sole causative organ in this disorder.

1.2 A Disease of Theories

1.2.1 The two-stage model:

In an effort to begin to understand the multifactorial basis for the development of PE, Roberts and colleagues developed the paradigm of pre-eclampsia as a two stage disorder[23]. Within this framework, the first stage of the disease, referred to as Stage 1, reflects defects in placentation, whereas Stage 2, reflects the maternal syndrome, or the where the symptoms of PE manifest in the mother.

Stage 1: Placentation and alterations in this process in PE pregnancies

The first 12 weeks of pregnancy are crucial in the establishment of a functioning placenta. The two major cascades that have their roots in this timeframe are trophoblast differentiation and spiral artery remodeling. Trophoblast differentiation begins around 8 weeks of gestation with the cytotrophoblast differentiating into syncytiotrophoblast cells (which form a barrier between fetal and maternal blood), and the more invasive extravillous trophoblast cells. The latter cell type, influenced by a host of placental and maternal factors such as cytokines, is involved in invading and penetrating deep into the maternal decidua. Extravillous trophoblasts differentiate

further into endovascular trophoblasts and invade the maternal spiral arteries. These cells penetrate and interdigitate the smooth muscle walls of the arteries, and induce apoptosis of these cell types. Now spiral arteries are large and flaccid, maximizing blood flow to the fetus.

Both the processes of trophoblast differentiation and spiral artery remodeling are known to be deficient in PE pregnancies (Figure1.1). Increased villous and extravillous trophoblast apoptosis is observed in PE pregnancies. This is known to occur early in pregnancy and may limit interstitial and endovascular invasion by extravillous trophoblasts[2]. Alternatively, some placental defects may come from poor trophoblast differentiation from cytotrophoblast to extravillous trophoblast, leading to a smaller population of invasive trophoblasts to migrate to spiral arteries[5, 11]. During normal pregnancy these spiral arteries are converted from low capacitance, high resistance vessels to high capacitance, low resistance vessels. In PE pregnancies, this conversion does not occur (Figure1.1).

What makes this such a complicated disease to study is that the pathological cascade is known to begin in Stage 1, but this stage is largely asymptomatic, and therefore difficult to examine as clinicians don't know which women are destined to have pregnancies complicated with PE. Though the use of placental specimens is limited to term deliveries, the common characteristics of shallow invasion and reduced spiral artery remodeling have provided researchers with an insight into the placental pathology underlying the PE disease process.

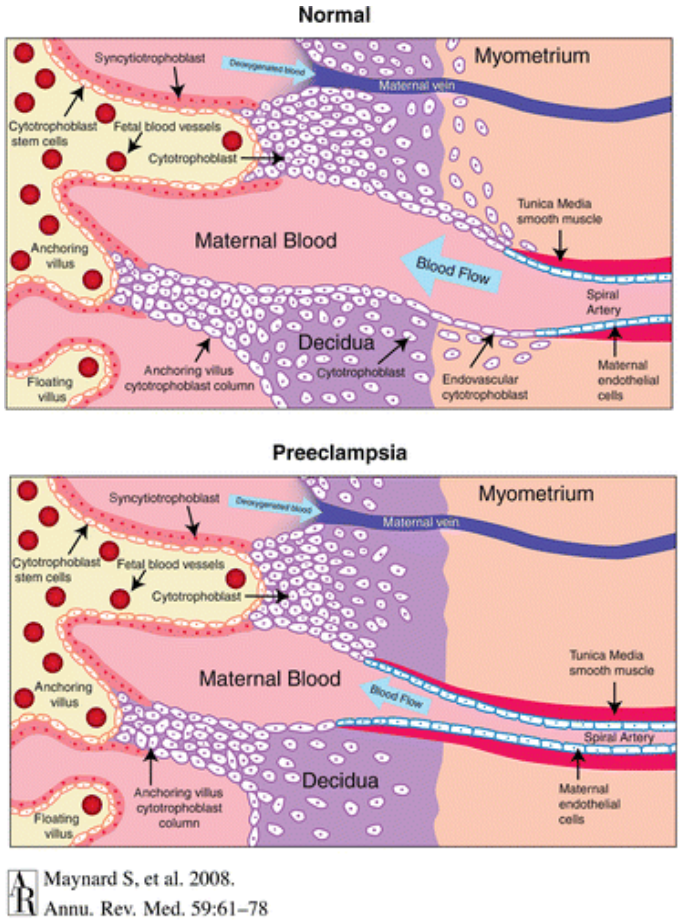

<u>Figure 1.1:</u> Schematic representation of spiral artery remodeling in normal pregnancies and pregnancies with PE. The upper panel illustrates the processes of trophoblast invasion, remodeling of the spiral arteries, and increased blood flow characteristic of normal pregnancy. The lower panel depicts the defects in these process in pregnancies complicated with PE.[24]

The "holy grail" of PE research is in determining the link between the placental defects and challenges that occur in the asymptomatic Stage 1, and the maternal syndrome of Stage 2. This would not only give us a mechanistic idea to the etiology of the disease, but provide potential venues for therapeutic intervention. It is accepted that the placenta secretes one or many factors that induce the endothelial dysfunction, global inflammation, hypertension and kidney dysfunction characteristic of Stage 2 of the syndrome. Some theories of this placental derived factor(s) include: antiangiogenic factors[25], syncytiotrophoblast knots and microparticles[26], autoantibodies to the angiotenisin 1 receptor[27], global oxidative stress and an excess of reactive oxygen species[28], the release of inflammatory cytokines[29, 30], and dysregulation of nitric oxide pathways[12, 31]. What has limited researchers to date is that no one factor is present in all PE pregnancies, highlighting the heterogeneity of this disorder[5, 32].

1.2.2 Angiogenesis and Oxidative Stress

A period of hypoxia in early pregnancy is necessary for trophoblast differentiation, invasion and proliferation. These actions are largely mediated by redox sensitive transcription factors such as hypoxia inducible factor HIF-1α[33]. Up until 10-12 weeks gestation, placental development occurs in a hypoxic state. At 10-12 weeks, trophoblast plugs that have been occluding maternal vessels into the placenta are removed and oxygenated blood begins to flow in the placental bed. One can imagine such a profound change in the physiological environment to be a point where serious damage could also occur. Prolonged exposure to hypoxia in vitro using placental explants has been shown to lead to increased apoptosis, oxidative stress, shedding of syncytiotrophoblast knots, and increased expression several anti-angiogenic factors, all of which have been shown to be key players in the pathogenesis

of PE[34, 35]. As such, prolonged oxidative stress has been a promising candidate for the link between the two stages of PE.

Recently, it has been found that cytotrophoblast cells as well as vascular endothelial cells are an important source of NADPH oxidases. Increased NADPH oxidase subunits were found in trophoblast and vascular smooth muscle tissue from women with PE implicating oxidative stress in the pathogenesis of the disease[28].

When placental explants were subjected to hypoxic conditions, one of the compounds secreted from the tissue was sFLT-1, a potent anti-angiogenic factor[34]. This finding strongly ties the oxidative stress pathogenesis to the processes of angiogenesis and vasculogenesis. During early placental development, angiogenesis and vasculogenesis are some of the major mechanisms that determine placental efficiency. Angiogenic factors from the vascular endothelial growth factor family (VEGF) including VEGF-A and closely associated placental growth factor, PGF, are extremely important during this timeframe. VEGF is expressed in uterine natural killer cells and trophoblast cells[36] and is thought to aid in vascular permeability, whereas PGFs role is less well understood. Both VEGF and PGF share a common receptor, FLT-1. What has become striking in the PE field is the finding that some women that show high levels of the soluble form of this receptor, sFLT-1, early in gestation are at a greater risk of developing PE[25], which launched angiogenic/anti-angiogenic factors on to a list of potential biomarkers of PE.

Soon after the discovery of sFLT-1, an additional soluble antiangiogenic factor, soluble endoglin (sENG), was reportedly found in women with severe PE[37]. Endoglin is a part of the transforming growth factor β (TGF-β) receptor complex. Analogous to sFLT-1: VEGF/PGF, sENG binds TGF-β and impairs its binding to cell surface receptors, and thus promoting an antiangiogenic state. The use of biomarkers

chosen from within the angiogenesis cascade has received a lot of attention in the past few decades, though its diagnostic reliability remains controversial.

1.2.3 The Role of the Inflammatory Response

An alternative theory puts the immune system as the major player in the disease progression. Sargent and colleagues proposed an immunological hypothesis of Stage I suggesting that poor invasion of trophoblasts, as a result of inadequate expression of human leukocyte antigen isoform G (HLA-G), leads to diminished decidual natural killer cell activation leading to decrease in cytokine and angiogenic factor production[38]. This is followed by Stage 2 manifested as a systemic inflammatory response involving leukocytes and the endothelial cell activation[38].

A successful pregnancy relies on specialized control of the maternal immune system. The implantation of the early embryo into the maternal uterine tissue requires significant attenuation of the normal 'non-self' response[39]. As half of the implanting fetus is paternally derived, the embryo and placenta represent a "semi-allograft"[11]. The correct modulation of the immune system requires specific events from both the uterus and embryo. The embryo's outer cells, the trophoblast, lack MHC class I and II expression, which helps the implant evade maternal immune attack[11, 40]. Trophoblasts also express HLA-G, and the uterine decidual tissue expresses Fas ligand, both known to promote feto-maternal tolerance[41].

One of the main mediators of immunotolerance, and a cell type that is gaining attention for its role in early placentation is a specialized group of leukocytes known as the uterine or decidual natural killer (NK) cells. These cells are unique compared to other NK cells and show high CD56 staining[2]. Uterine NK cells are present at the fetal-maternal milieu in great number, comprising 70% of the leukocyte population in

the decidua during early gestation[42]. The mechanism of immune evasion involves the HLA-G antigen expressed on trophoblast cells binding to NK cells and inhibiting their ability to induce cell lysis[11]. Probably the two most important roles of these cells are in a) trophoblast invasion and spiral artery remodeling (by secreting trophoblast invasion promoting cytokines such as interleukin 8 (IL-8) and interferon inducible protein 10), and b) promoting immunotolerance to the growing fetus and placenta[2, 43]. Uterine NK cells are also an important source of angiogenic factors PGF, VEGF and angiopoeitin-2, which also aid in the early vascularization of the placenta [36].

Another important cell type present in large amounts in early pregnancy is macrophages. This cell type occupies 20-25% of decidual leukocytes [44]. As cell cycling is crucial in early remodeling of the uterine tissue, macrophages are important in clearing cellular debris, as well as inducing apoptosis in unwanted cells. This promotes the invasion and growth of extraembryonic tissue [2]. Macrophages are also key mediators of angiogenesis due to their secretion of factors including VEGF, matrix metalloproteases (MMPs), TGF-β, and fibroblast growth factor[45]. Though helpful in events of early placentation, excessive activation of macrophages can result in significant secretion of pro-inflammatory cytokines. Macrophages are aberrantly activated in PE pregnancies and have roles in inhibiting trophoblast invasion[46]. The significant population of immune cells at the maternal-fetal milieu, and the balance of pro- and anti-inflammatory cytokines that mediate many of the early placentation processes closely tie the immune system with the success of a pregnancy [47]. Among the many potential cell types involved, macrophages and NK cells have received significant attention due to their potential role in the early placentation defects seen in PE pregnancies.

1.2.4 Shallow Invasion and Poor Placental Perfusion

An *in vivo* real-time assessment of shallow invasion leading to poor spiral artery remodeling, comes through the use of Doppler ultrasound. As this method is already routine in assessing fetal health in the developed world, an additional measurement, the resistance in the uterine arteries, is relatively easy to add to the standard pregnancy assessment. Analysis of the uterine artery Doppler, paying special attention to "diastolic notches" is becoming routine in sonographic examination. Diastolic notches are where the blood into the placenta shows increased resistance, resulting in the appearance of a notch during the beginning of diastole. This gives an idea of the degree of placental perfusion. It is the presence of these diastolic notches and increased resistance in uterine arteries early in gestation that has been shown to have a strong predictive value in determining which pregnancies will be complicated with PE[48]. However, similar results of Doppler analysis are predictive of IUGR, which shares many of the same placental abnormalities, diminishing the utility of this procedure to accurately predict early onset PE[5]. This diagnostic tool also shows some degree of variability[49], and hence is recommended to be used with other predictive values such as angiogenic/anti-angiogenic factors[50].

1.2.5 Fetal Stress and Trophoblast Shedding

A disease of pregnancy has potentially life threatening effects on both the mother and the fetus. As such, PE is one of the leading causes of fetal and maternal mortality worldwide. Though a lot of attention is paid to the care of the mother throughout pregnancy and the health of the unborn child, investigators are now beginning to examine the long term effects of the children born to PE pregnancies. The Barker hypothesis states that there are fetal origins of adult diseases, and that stress *in utero* can have lifelong effects [51]. In response to poor placental perfusion, the fetus can

develop compensatory strategies to overcome the challenged uterine environment. These endocrine and metabolic changes can persist well after birth and predispose infants born to PE pregnancies to cardiovascular disease later in life[52]. In fact, adolescents born to PE pregnancies have sustained hypertension compared to peers born in normal pregnancies[53, 54].

It has long been speculated that a factor secreted from the placenta is the link between placental dysfunction and eliciting the global maternal syndrome of PE (see above, Two-Stage Hypothesis). Some of the more promising candidates include syncytiotrophoblast microparticles and syncytiotrophoblast "knots"[11]. The cytotrophoblast cells can differentiate into syncytiotrophoblast layer or extravillous trophoblast cells. The syncytiotrophoblast layer is a continuous multinuclear cell layer that is the main barrier between fetal and maternal blood. As it is such a vital cell type, this layer is under constant turnover during pregnancy. As more new trophoblast cells repopulate the syncytiotrophoblast layer, older cells are sloughed off into the maternal circulation[55, 56]. Normally, the release of these multinucleated knots is initiated by apoptotic pathways[55], and the dead cells are phagocytosed without initiating an immune response. This is a normal pregnancy occurrence. The difference between this normal phenomenon and the pre-eclamptic process is two-fold. There is an increased shedding of syncytiotrophoblast knots and microparticles during pre-eclamptic pregnancies, potentially overwhelming the maternal immune cells, and the process of this shedding is not initiated by apoptotic pathways, but via necrotic pathways[57, 58]. When phagocytes engulf these products of necrosis, these cells secrete pro-inflammatory cytokines such as interleukin-6, the maternal immune response is heightened, and endothelial dysfunction progresses[58].

In summary, a significant amount of evidence indicates that there is undoubtedly a role for oxidative stress, angiogenic imbalance, the immune system, poor placental perfusion and the secretion of placental debris in the development of PE. However, the links between and among these hypotheses are not understood.

1.3 Before Placentation: the Potential Role of Implantation in PE

As the field of PE research has expanded in the past few decades, researchers are largely focused on the placenta as the causative factor in the pathophysiology of the disease. Our focus to date has been on placental defects and serum markers that are present in the maternal circulation after 12 weeks, when blood is flowing into the placenta. Huppertz, however, argues that some potential serum markers used to predict PE happen as early as 7 weeks, and hint towards an even earlier frame of investigation[5]. Huppertz challenged the way we think of PE by tracing its origins to the time of implantation. Indeed, implantation itself sets the cascade for placentation, therefore it stands to reason that defects at the time of implantation could result in poor placental outcomes. Huppertz proposes the origin of PE at the stage of trophoblast differentiation, which is in the pre-implantation period, prior to embryo invasion into the uterine wall[5]. Futhermore, he suggests that the difference in placental pathology between PE and IUGR phenotypes can be traced to the process of differentiation of villous and extravillous trophoblast, which again puts the focus of the initiation of the pathological cascade far upstream of what was previously considered[5]. Subsets of pregnancies that are at particularly high risk of developing PE are those associated with assisted reproductive technologies. Specifically, pregnancies initiated by in vitro fertilization (IVF) are at an increased risk for the development of PE[59]. In part this is due to the increase of multiple offspring as a result of this procedure[60]. Pregnancies

with multiple offspring are at a higher incidence of development of PE. However one important statistic is that singleton pregnancies initiated by IVF have a significantly increased risk of developing PE, ruling out the multiparous risk factor[60]. One of the features that sets these pregnancies apart from natural pregnancies is that processes up to and including the time of implantation are artificially induced. The process of implantation is not completely understood. With a success rate of merely 30%, this highlights a deficit in our understanding of this process. With the high incidence of PE in IVF pregnancies, it supports the shift of focus that we currently have on placentation, back to the period of implantation.

1.4 Rodents As Models of Human Pregnancy

As previously stated, studying a disease so closely associated with placentation, as is the case for PE, leads to difficulties in studying this disease in the context of the human condition. Therefore, researchers have turned to animal models, mostly rodent models, for a number of reasons. The rodent embryo, particularly the murine embryo, invades into the maternal uterine wall and induces a decidual response, much like the progression of human pregnancy and implantation. The placental architecture of mice and humans are remarkably similar with analogous structures of the chorionic villi in humans to the highly branched labyrinth in mice, and the outer extravillous cytotrophoblast in humans compared to the trophoblast giant cells in mice[61]. Murine placentae show hemochorial blood flow, much like the human placental interface [61]. As in humans, mouse trophoblast cells are involved in invading and remodeling spiral arteries, a key process in the modeling of the early stages of PE. These analogous cell types not only share functional properties with the human counterparts, but their genetic profile also shows marked similarities, allowing researchers to more thoroughly examine unique genetic contributions to placentation[62].

With the ease of a short reproductive term (roughly 20 days) come some limitations to studying murine pregnancy as a model of human pregnancy. The most obvious is the fact that mice are a litter bearing species, where the health of each implantation site could potentially affect the pregnancy as a whole. The profile of a pregnancy where many implantation sites are resorbed, versus a perfect pregnancy with 7-10 healthy conceptuses could be very different on a physiological and molecular scale. Many aspects of spacing and competition among implantation sites is seldom analogous to human pregnancies, where multiple pregnancies conceived naturally are relatively rare.

Where timing is advantageous and convenient in studying murine pregnancies, it can also be a disadvantage. In processes taking several months in a human pregnancy, researchers have only a few days to track such events in rodent models. This poses a unique challenge for researchers to track analgous potential deleterious events that may lead to the development of diseases such as PE.

A particular area which has seen great technological advancement in rodent pregnancies is in the area of imaging. Tools such as ultrasound and microCT imaging have allowed *in vivo* physiological data to be acquired on murine embryos where previous restrictions on resolution made these assessments impossible. Doppler ultrasound has enabled researchers to examine fetal heart rates and umbilical and placental blood flow in developing mouse embryos from very early embryonic stages[63, 64]. Murine pregnancies can model many of the characteristics of human PE including increased uterine artery Doppler resistance indices of poor placentation[65, 66]. Where ultrasound has given us a new tool to examine embryonic health and placental function *in utero*, microCT has seen improvement in resolution as well which allows the detection of vasculature down to 25μm, a scale now appropriate for murine

placental vasculature. This improved technique now allows for the qualitative and quantitative assessment of numerous vascular defects, including those found in placentation. This opens the door for more detailed phenotyping of genetically engineered mice[67, 68].

1.5 Rodent Models of Pre-eclampsia: Clues and Limitations

1.5.1 The rat model of placental ischemia:

One of the potential outcomes of the lack of spiral artery remodeling in PE placentae is global placental ischemia. A relatively popular rodent model of PE relies on this pathological feature as a basis of exploring how reduced placental perfusion may lead to the development of PE-like symptoms. This rat model, termed the Reduced Uterine Perfusion Pressure (or RUPP) model, is where Sprague-Dawley rats receive a uterine artery clip on day 14 of pregnancy around the aorta below the renal arteries, and to inhibit the compensatory increase in uterine flow via branches of the ovarian artery, clips are placed there as well[69]. This decreases uterine blood flow up to 40%[69]. Shortly after the clip is placed, rats exhibit an increase in maternal blood pressure and reduced kidney function[70]. Pups from this model are small, showing that despite how late in the pregnancy the clips are inserted, the restriction is still enough to elicit IUGR in this model [70]. RUPP animals also exhibit increased response to vasoactive substances, impaired vascular relaxation and global endothelial dysfunction[71]. In the angiogenic profile arena, the RUPP animals show increased sFLT1 and sENG production, and which results in reduced circulating VEGF levels[70, 72]. Interestingly, when VEGF is given to supplement the deficient circulating levels of this important angiogenic factor, the PE symptomology is largely resolved[70].

The drawback of the RUPP model is simple. In its design, RUPP only considers the response to placental ischemia as the founding basis of the development

of PE, where it is commonly accepted that the etiology of PE is probably from several early pathological events, including but not limited to poor placental perfusion. Additionally, as the RUPP model is surgically induced, animals show no endogenous placental abnormalities that illustrate what is seen in human samples. Implementing the arterial clips under anesthesia at mid-gestation, and also recording from these rats post-clipping requires significant handling stress, both of which likely confound the model significantly.

1.5.2 The sFLT-1 infusion model

A seminal study by Maynard and colleagues put the sFLT1 infusion model as another important model of PE in the field. By increasing systemic levels of this anti-angiogenic factor, pregnant rats showed increases in blood pressure and proteinuria, and glomerular endotheliosis that resembled PE pathology[25]. This intervention study also correlated with samples from women with PE that exhibited increased sFLT-1 levels and decreased PGF levels[73].

The drawbacks of this model are similar to those of the RUPP model in providing a narrow mechanistic view in the development of PE symptoms. Importantly, this model probably administers sFLT1 levels far surpassing physiological conditions. Physiologically, the placenta is an important source of sFLT1, and is completely bypassed in this model with exogenous sFLT1 administration. Additionally, it has been shown by several groups that sFLT1 is not a causative link to PE, as many women do not show an increase in sFLT1 and go on to develop PE while others show normal sFLT1 and develop the syndrome[74, 75].

1.5.3 Renin-angiotensin Transgenic Rat Model

The role of the renin angiotensin system (RAS) has also been strongly implicated in the hypertensive phenotype of the PE syndrome. During a normal pregnancy, women show increased renin and AngII in the plasma, yet show a decrease in vascular responsiveness to AngII, leading to the maintenance of basal blood pressure[76]. Women with PE, however, tend to have increased responsiveness to AngII despite significantly lower circulating AngII levels[77]. What has become important in considering the role of RAS has been the separation of global systemic activation with local utero-placental RAS signaling[77, 78]. To elucidate the role of the fetoplacental/uteroplacental RAS pathway, a specific rodent model is used in which a dam carrying a transgene for human angiotensinogen (hAogen) is mated with a sire carrying the human transgene for human renin (hRen), which results in a PE like syndrome during the second half of pregnancy, where hypertension and proteinuria are observed[79, 80]. Recent work by Dechend and colleagues have examined the question of local RAS (using the rat RAS PE model), the opposite cross, and elevating systemic AngII with osmotic mini-pumps in the development of these symptoms. The blood pressure and proteinuria phenotypes were only shown in the PE model and AngII infusion model suggesting that the increased circulating AngII is the common link among all of these phenotypes [78]. Surprisingly, the opposite cross (dam with hRen x sire with hAogen) would have only local uteroplacental increases in AngII showed increased trophoblast invasion and spiral artery remodeling. This suggests that uteroplacental AngII and not circulating AngII is important for these placental processes[78]. Uteroplacental blood flow as measured by ultrasound showed a lower resistance index for the opposite cross and the PE model, reflecting the improved invasion and remodeling.

The limitations of this model are in its placental pathology. It is commonly accepted that a *lack* of spiral artery remodeling is a common and important feature of pre-eclamptic placentae. This lack of spiral artery remodeling is linked to increased vascular resistance as seen in Doppler ultrasound, and perhaps linked to increased trophoblast shedding and placental debris (see above). If anything, this PE rat model actually shows improved and deeper invasion and remodeling of spiral arteries, followed by improved resistance indices as measured by ultrasound [78, 79, 81]. This model goes against accepted theory linking the deficiency in vessel remodeling to the development of the hallmarks of the disease, showing an increased BP and proteinuria in the presence of *improved* spiral artery remodeling.

1.5.4 Auto-antibody infusion model

Given the complications with the transgenic rat model of PE (described above) the RAS field has seen an important and promising new target to examine in the development of PE symptomology. In 1999, Wallukat *et al.* found that patients with pre-eclampsia exhibited increased circulating levels of autoantibodies against the angiotensin 1 receptor (AT1-AA)[27]. The hypothesis is that these antibodies bind to the AT1 receptor in an agonist fashion and activate the AT1 receptor leading to the increased AngII responsiveness in PE women[24, 27]. Since this finding, PE symptoms have been recapitulated in mice via an injection of autoantibodies isolated from women with PE, injected into mice mid-gestation[82]. With this AT1-AA model, mice exhibit increased blood pressure and proteinuria as well as glomerular lesions[82]. In this model, all of these phenotypes can be blocked by either losartan treatment (an AT1 receptor antagonist), or antibodies against the 7 amino acids used in antibody-receptor binding[82]. Interestingly, other rodent models have looked for autoantibodies, and AT1-AAs are present in the RUPP model, the transgenic RAS PE model as well as a

model in which low levels of tumor necrosis factor alpha (TNFα) are infused into pregnant rats[83, 84]. More recently, groups have considered the role of TNFα and AT1-AA induced PE symptomology. It is clear that the important cytokine TNFα plays a role in this model of PE[85, 86]. An interesting parallel also lies in the link between AT1-AA and TNFα induction and the increase in circulating anti-angiogenic factors sFLT1 and sENG, arguing for a role of the inflammatory response in the production of these potent anti-angiogenic factors[86].

The limitation of this new model is that the cascade leading to the source of these autoantibodies is largely unknown. Again the role of the placenta in this cascade is unclear in how placental ischemia plays a role in the development of this auto-immune condition. In vitro work has shown that AT1-AA can activate vascular cells and trophoblast, and induce reactive oxygen species via the activation of NADPH oxidase[87]. The full cascade of this auto-immune response warrants further study.

1.6 The BPH/5 model of Pre-elampsia

1.6.1 Hallmarks of PE

Part of the limitations of numerous rodent models of PE is that they require surgical, pharmacological or genetic manipulation. Though they help to elucidate potential mechanisms that may underlie the pathology, they do so with a narrow frame of reference. Many of the means to induce PE symptoms are fairly invasive which makes deciphering the cause and effect difficult.

BPH/5 is an inbred mouse model that spontaneously exhibits symptoms of PE during pregnancy[66]. This strain was derived by Schlager and colleagues from the well established hypertensive mouse strain BPH/2[88, 89]. In the non-pregnant state, BPH/5 show a mildly elevated basal blood pressure, a known risk factor for the development

of PE in humans[17]. During pregnancy, this hypertension profile increases significantly beginning late in gestation (starting at d14.5), results in frank hypertension, and resolves upon delivery of the litter[66]. Additionally, pregnant BPH/5 show increased proteinuria late in gestation which also resolves upon delivery of the pups. These hallmarks of PE mirror the timing of a human pre-eclamptic pregnancy with the onset of symptoms at the beginning of the third trimester. Additionally, significant glomerulosclerosis and endothelial dysfunction are exhibited in late gestation in this mouse model[66], which are also found in women with PE.

1.6.2 Placental Defects in BPH/5 Mimic Human Placental Samples

As discussed previously (section 1.1.3), significant placental pathology is associated with PE. The telltale reduced spiral artery remodeling and shallow trophoblast invasion into the decidua is also found in BPH/5 [90]. Additionally, the labyrithe area is severely underdeveloped showing reduced means of nutrient/oxygen exchange. Due to elevated resistance in the placental vascular bed, uterine artery Doppler late in gestation show increased resistance in the uterine vessels[90]. Taken together, the BPH/5 placental structure is severely compromised, and bears a strong resemblance to defects found in human PE placentae.

1.6.3 Oxidative stress

An additional correlation between human pregnancies and BPH/5 placental samples is evidence of oxidative stress. Prolonged hypoxia, coupled with increased production of reactive oxygen species (ROS) and deficient antioxidant capacity is thought to contribute to oxidative stress characteristic of PE pregnancies [91-93]. As shown by Hoffmann and colleagues, BPH/5 placentae show increased ROS levels and decreased antioxidant capacity compared to control strains [94]. Additionally, chronic treatment with an SOD mimetic Tempol dramatically reduced ROS levels in the

placenta as well as significantly diminishing the late gestational hypertension and proteinuria characteristic of BPH/5 pregnancies. These studies support a strong rationale for antioxidant enrichment in pregnancies complicated with PE.

1.7 Statement of the Problem

Pre-eclampsia is a serious disease of pregnancy that has seen limited progress in its understanding and treatment. Our lab discovered a mouse model that spontaneously exhibits the symptoms of PE including late gestational hypertension, proteinuria and placental pathology reminiscent of the human condition. This mouse model provides an important tool to examine specific questions in the pathology of the PE.

Initially, we began by examining the angiogenic potential in this mouse model as angiogenesis and angiogenic factors have seen increased research in recent years for their potential biomarker capability. One of the benefits of such an animal model in which the disease occurs spontaneously is that we can examine early pre-maternal syndrome timepoints that are unavailable for study in the human case and also in many of the other animal models. BPH/5 show signs of fetal stress early in gestation, and we sought to characterize this timepoint via microarray analysis to examine the molecular profile of healthy and challenged embryos. Finally, as the field focuses earlier and earlier on the pregnancy timeline in the initiation of the pathology cascade, we examined the peri-implantation period in BPH/5 mice. The goal of this research is to use the results from each of these separate studies to create a unifying hypothesis and working model to examine the causes of PE in BPH/5.

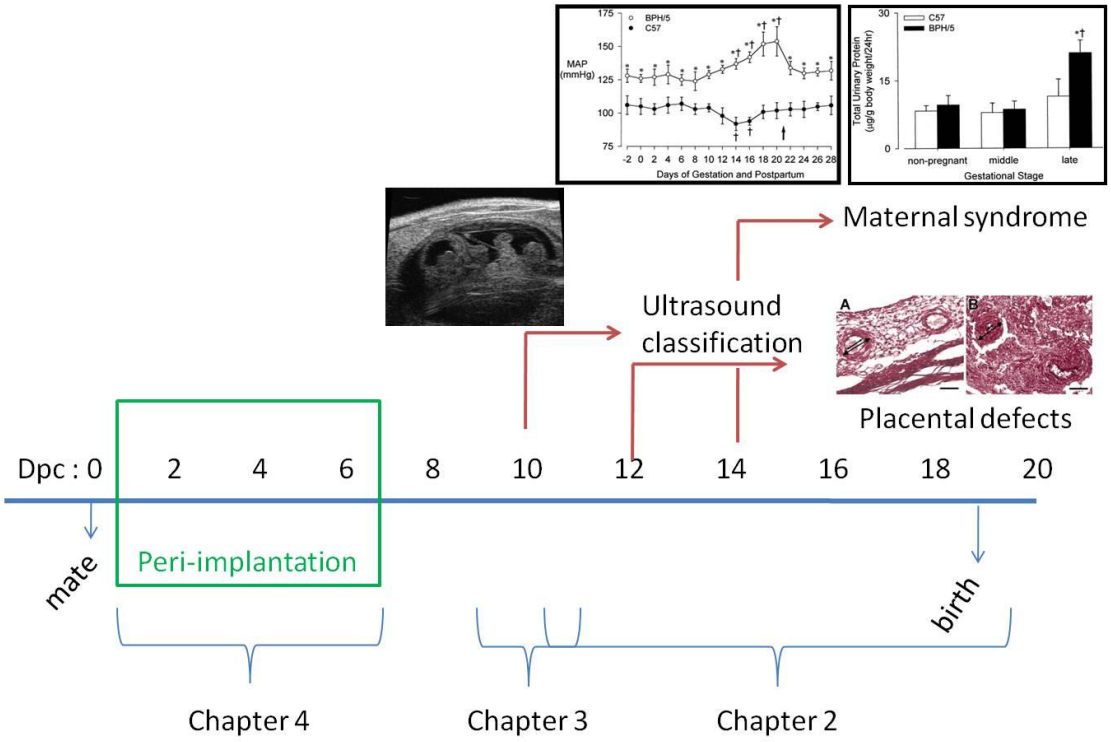

Figure 1.2: Schematic representation of a the BPH/5 pregnancy and the relevant timepoints that will be examined in the subsequent thesis chapters.

1.8 Approach

In order to test the hypothesis that there is an angiogenic defect in BPH/5 mice we employed protein and molecular assays at different gestational stages to track the angiogenic potential of BPH/5 mice. Additionally, we intervened using viral mediated gene transfer of an important angiogenic factor to determine if this factor was functionally linked to maternal and fetoplacental PE outcomes *in vivo*.

To test the hypothesis that there is a distinct molecular profile present in BPH/5 fetoplacental units early in pregnancy compared to controls, we used cutting-edge high resolution ultrasound to assess the fetal health status of BPH/5 embryos, followed by microarray analysis of these fetoplacental units.

Finally, to test the hypothesis that PE has its roots in the peri-implantation period, BPH/5 embryos were examined for their pre-implantation potential, and how those defects translate into implantation defects. Surgical reciprocal embryo transfers as well as ovariectomies with hormone supplementation were used to fully characterize the fetal and maternal components to implantation defects. Ultimately, the role of implantation in the placental pathology observed in BPH/5 was examined.

REFERENCES

1. Cudihy D, Lee RV. The pathophysiology of pre-eclampsia: Current clinical concepts. *J Obstet Gynaecol*. 2009;29:576-582.

2. Ahn H, Park J, Gilman-Sachs A, Kwak-Kim J. Immunologic characteristics of pre-eclampsia, a comprehensive review. *Am J Reprod Immunol*. 2010.

3. Rahimi R, Nikfar S, Rezaie A, Abdollahi M. A meta-analysis on the efficacy and safety of combined vitamin C and E supplementation in preeclamptic women. *Hypertens Pregnancy*. 2009;28:417-434.

4. Klemmensen A, Tabor A, Osterdal ML, Knudsen VK, Halldorsson TI, Mikkelsen TB, Olsen SF. Intake of vitamin C and E in pregnancy and risk of pre-eclampsia: Prospective study among 57 346 women. *BJOG*. 2009;116:964-974.

5. Huppertz B. Placental origins of pre-eclampsia: Challenging the current hypothesis. *Hypertension*. 2008;51:970-975.

6. Ness RB, Sibai BM. Shared and disparate components of the pathophysiologies of fetal growth restriction and pre-eclampsia. *Am J Obstet Gynecol*. 2006;195:40-49.

7. Egbor M, Ansari T, Morris N, Green CJ, Sibbons PD. Morphometric placental villous and vascular abnormalities in early- and late-onset pre-eclampsia with and without fetal growth restriction. *BJOG*. 2006;113:580-589.

8. van der Merwe JL, Hall DR, Wright C, Schubert P, Grove D. Are early and late pre-eclampsia distinct subclasses of the disease--what does the placenta reveal? *Hypertens Pregnancy*. 2010;29:457-467.

9. Eskenazi B, Fenster L, Sidney S, Elkin EP. Fetal growth retardation in infants of multiparous and nulliparous women with pre-eclampsia. *Am J Obstet Gynecol*. 1993;169:1112-1118.

10. Villar J, Carroli G, Wojdyla D, Abalos E, Giordano D, Ba'aqeel H, Farnot U, Bergsjo P, Bakketeig L, Lumbiganon P, Campodonico L, Al-Mazrou Y, Lindheimer M, Kramer M, World Health Organization Antenatal Care Trial Research Group. Pre-eclampsia, gestational hypertension and intrauterine growth restriction, related or independent conditions? *Am J Obstet Gynecol*. 2006;194:921-931.

11. James JL, Whitley GS, Cartwright JE. Pre-eclampsia: Fitting together the placental, immune and cardiovascular pieces. *J Pathol*. 2010;221:363-378.

12. Roberts JM, Catov JM. Pre-eclampsia more than 1 disease: Or is it? *Hypertension*. 2008;51:989-990.

13. Sibai BM, Gordon T, Thom E, Caritis SN, Klebanoff M, McNellis D, Paul RH. Risk factors for pre-eclampsia in healthy nulliparous women: A prospective multicenter study. the national institute of child health and human development network of maternal-fetal medicine units. *Am J Obstet Gynecol*. 1995;172:642-648.

14. Caritis S, Sibai B, Hauth J, Lindheimer MD, Klebanoff M, Thom E, VanDorsten P, Landon M, Paul R, Miodovnik M, Meis P, Thurnau G. Low-dose aspirin to prevent pre-eclampsia in women at high risk. national institute of child health and human development network of maternal-fetal medicine units. *N Engl J Med*. 1998;338:701-705.

15. Powers RW, Evans RW, Majors AK, Ojimba JI, Ness RB, Crombleholme WR, Roberts JM. Plasma homocysteine concentration is increased in pre-eclampsia and is associated with evidence of endothelial activation. *Am J Obstet Gynecol*. 1998;179:1605-1611.

16. Eskenazi B, Fenster L, Sidney S. A multivariate analysis of risk factors for pre-eclampsia. *JAMA*. 1991;266:237-241.

17. Seed PT, Chappell LC, Black MA, Poppe KK, Hwang YC, Kasabov N, McCowan L, Shennan AH, Wu SH, Poston L, North RA. Prediction of pre-eclampsia and delivery of small for gestational age babies based on a combination of clinical risk factors in high-risk women. *Hypertens Pregnancy*. 2010.

18. Carr DB, Epplein M, Johnson CO, Easterling TR, Critchlow CW. A sister's risk: Family history as a predictor of pre-eclampsia. *Am J Obstet Gynecol*. 2005;193:965-972.

19. Mogren I, Hogberg U, Winkvist A, Stenlund H. Familial occurrence of pre-eclampsia. *Epidemiology*. 1999;10:518-522.

20. Esplin MS, Fausett MB, Fraser A, Kerber R, Mineau G, Carrillo J, Varner MW. Paternal and maternal components of the predisposition to pre-eclampsia. *N Engl J Med*. 2001;344:867-872.

21. Chun D, Braga C, Chow C, Lok L. Clinical observations on some aspects of hydatidiform moles. *J Obstet Gynaecol Br Commonw*. 1964;71:180-184.

22. Goldstein DP, Berkowitz RS. Current management of complete and partial molar pregnancy. *J Reprod Med*. 1994;39:139-146.

23. Roberts JM, Gammill HS. Pre-eclampsia: Recent insights. *Hypertension*. 2005;46:1243-1249.

24. Maynard S, Epstein FH, Karumanchi SA. Pre-eclampsia and angiogenic imbalance. *Annu Rev Med*. 2008;59:61-78.

25. Maynard SE, Min JY, Merchan J, Lim KH, Li J, Mondal S, Libermann TA, Morgan JP, Sellke FW, Stillman IE, Epstein FH, Sukhatme VP, Karumanchi SA. Excess placental soluble fms-like tyrosine kinase 1 (sFlt1) may contribute to endothelial dysfunction, hypertension, and proteinuria in pre-eclampsia. *J Clin Invest*. 2003;111:649-658.

26. Redman CW, Sargent IL. Microparticles and immunomodulation in pregnancy and pre-eclampsia. *J Reprod Immunol*. 2007;76:61-67.

27. Wallukat G, Homuth V, Fischer T, Lindschau C, Horstkamp B, Jupner A, Baur E, Nissen E, Vetter K, Neichel D, Dudenhausen JW, Haller H, Luft FC. Patients with pre-eclampsia develop agonistic autoantibodies against the angiotensin AT1 receptor. *J Clin Invest*. 1999;103:945-952.

28. Raijmakers MT, Dechend R, Poston L. Oxidative stress and pre-eclampsia: Rationale for antioxidant clinical trials. *Hypertension*. 2004;44:374-380.

29. Benyo DF, Smarason A, Redman CW, Sims C, Conrad KP. Expression of inflammatory cytokines in placentas from women with pre-eclampsia. *J Clin Endocrinol Metab*. 2001;86:2505-2512.

30. Kupferminc MJ, Peaceman AM, Wigton TR, Rehnberg KA, Socol ML. Tumor necrosis factor-alpha is elevated in plasma and amniotic fluid of patients with severe pre-eclampsia. *Am J Obstet Gynecol*. 1994;170:1752-7; discussion 1757-9.

31. Noris M, Todeschini M, Cassis P, Pasta F, Cappellini A, Bonazzola S, Macconi D, Maucci R, Porrati F, Benigni A, Picciolo C, Remuzzi G. L-arginine depletion in pre-eclampsia orients nitric oxide synthase toward oxidant species. *Hypertension*. 2004;43:614-622.

32. LaMarca BD, Gilbert J, Granger JP. Recent progress toward the understanding of the pathophysiology of hypertension during pre-eclampsia. *Hypertension*. 2008;51:982-988.

33. Maltepe E, Krampitz GW, Okazaki KM, Red-Horse K, Mak W, Simon MC, Fisher SJ. Hypoxia-inducible factor-dependent histone deacetylase activity determines stem cell fate in the placenta. *Development*. 2005;132:3393-3403.

34. Nevo O, Soleymanlou N, Wu Y, Xu J, Kingdom J, Many A, Zamudio S, Caniggia I. Increased expression of sFlt-1 in in vivo and in vitro models of human placental hypoxia is mediated by HIF-1. *Am J Physiol Regul Integr Comp Physiol*. 2006;291:R1085-93.

35. Redman CW, Sargent IL. Placental stress and pre-eclampsia: A revised view. *Placenta*. 2009.

36. Tabiasco J, Rabot M, Aguerre-Girr M, El Costa H, Berrebi A, Parant O, Laskarin G, Juretic K, Bensussan A, Rukavina D, Le Bouteiller P. Human decidual NK cells: Unique phenotype and functional properties -- a review. *Placenta*. 2006;27 Suppl A:S34-9.

37. Levine RJ, Lam C, Qian C, Yu KF, Maynard SE, Sachs BP, Sibai BM, Epstein FH, Romero R, Thadhani R. Soluble endoglin and other circulating antiangiogenic factors in pre-eclampsia. *N Engl J Med*. 2006;355:992.

38. Sargent IL, Borzychowski AM, Redman CW. Immunoregulation in normal pregnancy and pre-eclampsia: An overview. *Reprod Biomed Online*. 2006;13:680-686.

39. Trowsdale J, Betz AG. Mother's little helpers: Mechanisms of maternal-fetal tolerance. *Nat Immunol*. 2006;7:241-246.

40. Blaschitz A, Hutter H, Dohr G. HLA class I protein expression in the human placenta. *Early Pregnancy*. 2001;5:67-69.

41. Guleria I, Sayegh MH. Maternal acceptance of the fetus: True human tolerance. *J Immunol*. 2007;178:3345-3351.

42. Bulmer JN, Lash GE. Human uterine natural killer cells: A reappraisal. *Mol Immunol*. 2005;42:511-521.

43. Trundley A, Moffett A. Human uterine leukocytes and pregnancy. *Tissue Antigens*. 2004;63:1-12.

44. Williams PJ, Searle RF, Robson SC, Innes BA, Bulmer JN. Decidual leucocyte populations in early to late gestation normal human pregnancy. *J Reprod Immunol*. 2009;82:24-31.

45. Sunderkotter C, Steinbrink K, Goebeler M, Bhardwaj R, Sorg C. Macrophages and angiogenesis. *J Leukoc Biol*. 1994;55:410-422.

46. Renaud SJ, Graham CH. The role of macrophages in utero-placental interactions during normal and pathological pregnancy. *Immunol Invest*. 2008;37:535-564.

47. Laresgoiti-Servitje E, Gomez-Lopez N, Olson DM. An immunological insight into the origins of pre-eclampsia. *Hum Reprod Update*. 2010;16:510-524.

48. Papageorghiou AT, Yu CK, Bindra R, Pandis G, Nicolaides KH, Fetal Medicine Foundation Second Trimester Screening Group. Multicenter screening for pre-eclampsia and fetal growth restriction by transvaginal uterine artery doppler at 23 weeks of gestation. *Ultrasound Obstet Gynecol*. 2001;18:441-449.

49. Pilalis A, Souka AP, Antsaklis P, Basayiannis K, Benardis P, Haidopoulos D, Papantoniou N, Mesogitis S, Antsaklis A. Screening for pre-eclampsia and small for gestational age fetuses at the 11-14 weeks scan by uterine artery dopplers. *Acta Obstet Gynecol Scand*. 2007;86:530-534.

50. Espinoza J, Romero R, Nien JK, Gomez R, Kusanovic JP, Goncalves LF, Medina L, Edwin S, Hassan S, Carstens M, Gonzalez R. Identification of patients at risk for early onset and/or severe pre-eclampsia with the use of uterine artery doppler velocimetry and placental growth factor. *Am J Obstet Gynecol*. 2007;196:326.e1-326.13.

51. Alexander BT. Fetal programming of hypertension. *Am J Physiol Regul Integr Comp Physiol*. 2006;290:R1-R10.

52. Geelhoed JJ, Fraser A, Tilling K, Benfield L, Davey Smith G, Sattar N, Nelson SM, Lawlor DA. Pre-eclampsia and gestational hypertension are associated with childhood blood pressure independently of family adiposity measures: The avon longitudinal study of parents and children. *Circulation*. 2010;122:1192-1199.

53. Oglaend B, Forman MR, Romundstad PR, Nilsen ST, Vatten LJ. Blood pressure in early adolescence in the offspring of preeclamptic and normotensive pregnancies. *J Hypertens*. 2009;27:2051-2054.

54. Ferreira I, Peeters LL, Stehouwer CD. Pre-eclampsia and increased blood pressure in the offspring: Meta-analysis and critical review of the evidence. *J Hypertens*. 2009;27:1955-1959.

55. Huppertz B, Frank HG, Reister F, Kingdom J, Korr H, Kaufmann P. Apoptosis cascade progresses during turnover of human trophoblast: Analysis of villous cytotrophoblast and syncytial fragments in vitro. *Lab Invest*. 1999;79:1687-1702.

56. Huppertz B, Frank HG, Kingdom JC, Reister F, Kaufmann P. Villous cytotrophoblast regulation of the syncytial apoptotic cascade in the human placenta. *Histochem Cell Biol*. 1998;110:495-508.

57. Abumaree MH, Stone PR, Chamley LW. The effects of apoptotic, deported human placental trophoblast on macrophages: Possible consequences for pregnancy. *J Reprod Immunol*. 2006;72:33-45.

58. Chen Q, Ding JX, Liu B, Stone P, Feng YJ, Chamley L. Spreading endothelial cell dysfunction in response to necrotic trophoblasts. soluble factors released from endothelial cells that have phagocytosed necrotic shed trophoblasts reduce the proliferation of additional endothelial cells. *Placenta*. 2010;31:976-981.

59. Chen XK, Wen SW, Bottomley J, Smith GN, Leader A, Walker MC. In vitro fertilization is associated with an increased risk for pre-eclampsia. *Hypertens Pregnancy*. 2009;28:1-12.

60. Kalra SK, Molinaro TA. The association of in vitro fertilization and perinatal morbidity. *Semin Reprod Med*. 2008;26:423-435.

61. Cross JC. The genetics of pre-eclampsia: A feto-placental or maternal problem? *Clin Genet*. 2003;64:96-103.

62. Hemberger M, Cross JC. Genes governing placental development. *Trends Endocrinol Metab*. 2001;12:162-168.

63. Mu J, Qu D, Bartczak A, Phillips MJ, Manuel J, He W, Koscik C, Mendicino M, Zhang L, Clark DA, Grant DR, Backx PH, Levy GA, Adamson SL. Fgl2 deficiency causes neonatal death and cardiac dysfunction during embryonic and postnatal development in mice. *Physiol Genomics*. 2007;31:53-62.

64. Mu J, Adamson SL. Developmental changes in hemodynamics of uterine artery, utero- and umbilicoplacental, and vitelline circulations in mouse throughout gestation. *Am J Physiol Heart Circ Physiol*. 2006;291:H1421-8.

65. Boukerrou M, Bresson S, Collinet P, Delelis A, Deruelle P, Houfflin-Debarge V, Dufour P, Subtil D. Factors associated with uterine artery doppler anomalies in patients with pre-eclampsia. *Hypertens Pregnancy*. 2009;28:178-189.

66. Davisson RL, Hoffmann DS, Butz GM, Aldape G, Schlager G, Merrill DC, Sethi S, Weiss RM, Bates JN. Discovery of a spontaneous genetic mouse model of pre-eclampsia. *Hypertension*. 2002;39:337-342.

67. Rennie MY, Whiteley KJ, Kulandavelu S, Adamson SL, Sled JG. 3D visualisation and quantification by microcomputed tomography of late gestational changes in the arterial and venous feto-placental vasculature of the mouse. *Placenta*. 2007;28:833-840.

68. Kulandavelu S, Qu D, Sunn N, Mu J, Rennie MY, Whiteley KJ, Walls JR, Bock NA, Sun JC, Covelli A, Sled JG, Adamson SL. Embryonic and neonatal phenotyping of genetically engineered mice. *ILAR J*. 2006;47:103-117.

69. Granger JP, LaMarca BB, Cockrell K, Sedeek M, Balzi C, Chandler D, Bennett W. Reduced uterine perfusion pressure (RUPP) model for studying cardiovascular-renal dysfunction in response to placental ischemia. *Methods Mol Med*. 2006;122:383-392.

70. Gilbert JS, Verzwyvelt J, Colson D, Arany M, Karumanchi SA, Granger JP. Recombinant vascular endothelial growth factor 121 infusion lowers blood pressure and improves renal function in rats with placentalischemia-induced hypertension. *Hypertension*. 2010;55:380-385.

71. Crews JK, Herrington JN, Granger JP, Khalil RA. Decreased endothelium-dependent vascular relaxation during reduction of uterine perfusion pressure in pregnant rat. *Hypertension*. 2000;35:367-372.

72. Gilbert JS, Gilbert SA, Arany M, Granger JP. Hypertension produced by placental ischemia in pregnant rats is associated with increased soluble endoglin expression. *Hypertension*. 2009;53:399-403.

73. Levine RJ, Maynard SE, Qian C, Lim KH, England LJ, Yu KF, Schisterman EF, Thadhani R, Sachs BP, Epstein FH, Sibai BM, Sukhatme VP, Karumanchi SA. Circulating angiogenic factors and the risk of pre-eclampsia. *N Engl J Med*. 2004;350:672-683.

74. Powers RW, Roberts JM, Cooper KM, Gallaher MJ, Frank MP, Harger GF, Ness RB. Maternal serum soluble fms-like tyrosine kinase 1 concentrations are not increased in early pregnancy and decrease more slowly postpartum in women who develop pre-eclampsia. *Am J Obstet Gynecol*. 2005;193:185-191.

75. Smith GC, Crossley JA, Aitken DA, Jenkins N, Lyall F, Cameron AD, Connor JM, Dobbie R. Circulating angiogenic factors in early pregnancy and the risk of pre-eclampsia, intrauterine growth restriction, spontaneous preterm birth, and stillbirth. *Obstet Gynecol*. 2007;109:1316-1324.

76. Shah DM. Role of the renin-angiotensin system in the pathogenesis of pre-eclampsia. *Am J Physiol Renal Physiol*. 2005;288:F614-25.

77. Herse F, Staff AC, Hering L, Muller DN, Luft FC, Dechend R. AT1-receptor autoantibodies and uteroplacental RAS in pregnancy and pre-eclampsia. *J Mol Med*. 2008;86:697-703.

78. Hering L, Herse F, Geusens N, Verlohren S, Wenzel K, Staff AC, Brosnihan KB, Huppertz B, Luft FC, Muller DN, Pijnenborg R, Cartwright JE, Dechend R. Effects of circulating and local uteroplacental angiotensin II in rat pregnancy. *Hypertension*. 2010;56:311-318.

79. Verlohren S, Niehoff M, Hering L, Geusens N, Herse F, Tintu AN, Plagemann A, LeNoble F, Pijnenborg R, Muller DN, Luft FC, Dudenhausen JW, Gollasch M, Dechend R. Uterine vascular function in a transgenic pre-eclampsia rat model. *Hypertension*. 2008;51:547-553.

80. Bohlender J, Ganten D, Luft FC. Rats transgenic for human renin and human angiotensinogen as a model for gestational hypertension. *J Am Soc Nephrol*. 2000;11:2056-2061.

81. Verlohren S, Geusens N, Morton J, Verhaegen I, Hering L, Herse F, Dudenhausen JW, Muller DN, Luft FC, Cartwright JE, Davidge ST, Pijnenborg R, Dechend R. Inhibition of trophoblast-induced spiral artery remodeling reduces placental perfusion in rat pregnancy. *Hypertension*. 2010;56:304-310.

82. Zhou CC, Zhang Y, Irani RA, Zhang H, Mi T, Popek EJ, Hicks MJ, Ramin SM, Kellems RE, Xia Y. Angiotensin receptor agonistic autoantibodies induce pre-eclampsia in pregnant mice. *Nat Med*. 2008;14:855-862.

83. LaMarca B, Wallukat G, Llinas M, Herse F, Dechend R, Granger JP. Autoantibodies to the angiotensin type I receptor in response to placental ischemia and tumor necrosis factor alpha in pregnant rats. *Hypertension*. 2008;52:1168-1172.

84. Dechend R, Gratze P, Wallukat G, Shagdarsuren E, Plehm R, Brasen JH, Fiebeler A, Schneider W, Caluwaerts S, Vercruysse L, Pijnenborg R, Luft FC, Muller DN. Agonistic autoantibodies to the AT1 receptor in a transgenic rat model of pre-eclampsia. *Hypertension*. 2005;45:742-746.

85. Irani RA, Zhang Y, Zhou CC, Blackwell SC, Hicks MJ, Ramin SM, Kellems RE, Xia Y. Autoantibody-mediated angiotensin receptor activation contributes to pre-eclampsia through tumor necrosis factor-alpha signaling. *Hypertension*. 2010;55:1246-1253.

86. Parrish MR, Murphy SR, Rutland S, Wallace K, Wenzel K, Wallukat G, Keiser S, Ray LF, Dechend R, Martin JN, Granger JP, LaMarca B. The effect of immune factors, tumor necrosis factor-alpha, and agonistic autoantibodies to the angiotensin II type I receptor on soluble fms-like tyrosine-1 and soluble endoglin production in response to hypertension during pregnancy. *Am J Hypertens*. 2010;23:911-916.

87. Dechend R, Viedt C, Muller DN, Ugele B, Brandes RP, Wallukat G, Park JK, Janke J, Barta P, Theuer J, Fiebeler A, Homuth V, Dietz R, Haller H, Kreuzer J, Luft FC. AT1 receptor agonistic antibodies from preeclamptic patients stimulate NADPH oxidase. *Circulation*. 2003;107:1632-1639.

88. Wright FA, O'Connor DT, Roberts E, Kutey G, Berry CC, Yoneda LU, Timberlake D, Schlager G. Genome scan for blood pressure loci in mice. *Hypertension*. 1999;34:625-630.

89. Schlager G, Sides J. Characterization of hypertensive and hypotensive inbred strains of mice. *Lab Anim Sci*. 1997;47:288-292.

90. Dokras A, Hoffmann DS, Eastvold JS, Kienzle MF, Gruman LM, Kirby PA, Weiss RM, Davisson RL. Severe feto-placental abnormalities precede the onset of hypertension and proteinuria in a mouse model of pre-eclampsia. *Biol Reprod*. 2006;75:899-907.

91. Burton GJ, Jauniaux E. Placental oxidative stress: From miscarriage to pre-eclampsia. *J Soc Gynecol Investig*. 2004;11:342-352.

92. Gupta S, Agarwal A, Sharma RK. The role of placental oxidative stress and lipid peroxidation in pre-eclampsia. *Obstet Gynecol Surv*. 2005;60:807-816.

93. Chappell LC, Seed PT, Kelly FJ, Briley A, Hunt BJ, Charnock-Jones DS, Mallet A, Poston L. Vitamin C and E supplementation in women at risk of pre-eclampsia is associated with changes in indices of oxidative stress and placental function. *Am J Obstet Gynecol*. 2002;187:777-784.

94. Hoffmann DS, Weydert CJ, Lazartigues E, Kutschke WJ, Kienzle MF, Leach JE, Sharma JA, Sharma RV, Davisson RL. Chronic tempol prevents hypertension, proteinuria, and poor feto-placental outcomes in BPH/5 mouse model of pre-eclampsia. *Hypertension*. 2008;51:1058-1065.

CHAPTER TWO:

ADENOVIRAL DELIVERY OF $VEGF_{121}$ EARLY IN PREGNANCY PREVENTS SPONTANEOUS DEVELOPMENT OF PRE-ECLAMPSIA IN BPH/5 MICE*

*Most of the work in this chapter is published in Woods, A.K., Hoffmann, D.S, Weydert, C.J., Butler, S.D., Zhou, Y., Sharma, R.V., Davisson, R.L. *Hypertension* (in press)

SUMMARY

An imbalance in circulating pro-angiogenic and anti-angiogenic factors is postulated to play a causal role in pre-eclampsia (PE). We have described an inbred mouse strain, BPH/5, which spontaneously develops a PE-like syndrome including late-gestational hypertension, proteinuria, and poor fetoplacental outcomes. Here we tested the hypothesis that an angiogenic imbalance during pregnancy in BPH/5 mice leads to the development of PE-like phenotypes in this model. Similar to clinical findings, plasma from pregnant BPH/5 showed reduced levels of free vascular endothelial growth factor (VEGF) and placental growth factor (PGF) compared to C57BL/6 controls. This was paralleled by a marked decrease in VEGF protein and *Pgf* mRNA in BPH/5 placentae. Surprisingly, antagonism by the soluble form of the FLT1 receptor (sFLT1) did not appear to be the cause of this reduction, as sFLT1 levels were unchanged or even reduced in BPH/5 compared to controls. Adenoviral-mediated delivery of $VEGF_{121}$ (Ad-VEGF) via tail vein at e7.5 normalized both the plasma free VEGF levels in BPH/5 and restored the *in vitro* angiogenic capacity of serum from these mice. Ad-VEGF also reduced the incidence of fetal resorptions and prevented the late-gestational spike in blood pressure and proteinuria observed in BPH/5. These data underscore the importance of dysregulation of angiogenic factors in the pathogenesis of PE, and suggest the potential utility of early pro-angiogenic therapies in treating this disease.

INTRODUCTION

Pre-eclampsia (PE) is a pregnancy-specific syndrome defined by sudden onset of hypertension and proteinuria after 20 weeks gestation. A multi-system disorder that impacts both mother and fetus, PE is a major public health problem. Worldwide, PE affects 5-8% of pregnancies and is the leading cause of maternal and fetal deaths[1, 2]. In developing countries, the incidence of PE is even higher[3]. Despite its common occurrence and serious consequences, treatment of PE has not changed over the last century. Even today, the only known effective means to avoid progression to eclampsia is delivery of the fetus and placenta. As such, PE accounts for up to 20% of preterm births worldwide[3].

The etiology of PE remains unclear, however there is growing evidence that an imbalance in several members of the vascular endothelial growth factor (VEGF) family and its receptors is linked to the clinical syndrome[1, 4]. VEGF-A (VEGF), critical to angiogenesis and vasculogenesis required for placentation, is present in numerous isoforms[5]. $VEGF_{121}$, the predominant isoform, lacks a membrane-bound motif, making it freely diffusible and therefore having the greatest therapeutic potential[5]. The closely related placental growth factor (PGF) shares 42% sequence homology to VEGF and shares a common receptor, VEGFR-1 (i.e. Fms-like tyrosine kinase 1, FLT1)[6, 7]. Many women who develop PE show decreases in circulating free VEGF and PGF starting in early- to mid-gestation[1, 2, 8]. In addition, high levels of the soluble form of the FLT1 receptor (sFLT1) and soluble endoglin (sENG), both anti-angiogenic factors, are also reported in PE patients at various times during pregnancy[9-11]. On the other hand, increased serum sFLT1 levels are not always observed in women with PE[12], and a recent study showed that not only were elevated sFLT1 levels at 11-14 weeks not predictive of PE in women, but were in fact associated with reduced risk for delivery of a small-for-gestational-age baby[13].

Despite discrepancies in clinical findings, significant progress in basic research has been made to support the hypothesis that an imbalance between pro-angiogenic and anti-angiogenic factors is involved in the pathogenesis of PE. Maynard et al. found that adenoviral-mediated increases in circulating sFLT1 levels in normal pregnant rats induced a PE-like syndrome[9]. A similar study in mice confirmed that exogenous delivery of sFLT1 during pregnancy can induce late-gestational hypertension[14]. To determine if the effects of exogenous sFLT1 could be counterbalanced by increasing pro-angiogenic factors, Li et al. used repeated subcutaneous injections of $VEGF_{121}$ and found that this attenuated PE symptoms in pregnant rats previously made pre-eclamptic by an adenovirus encoding sFLT1[15]. A similar strategy was adopted by Gilbert et al. in the context of a rat model in which the uteroplacental circulation is disrupted at mid-gestation, and increased circulating levels of sFLT1 late in pregnancy were observed[16]. These studies provide important proof-of-concept that an angiogenic imbalance can induce some aspects of PE, however the experimental design is somewhat predictive of the outcome. Testing whether there is endogenous angiogenic imbalance in an animal model that spontaneously develops PE is an important next step.

Several years ago we described an inbred murine strain, BPH/5, which spontaneously develops a maternal and fetoplacental syndrome that bears striking resemblance to PE[17]. The model is characterized by late-gestational hypertension, proteinuria, renal glomerular lesions and endothelial dysfunction[17, 18]. In addition to the maternal systemic disorder, BPH/5 also show fetoplacental defects reminiscent of human PE, including defective trophoblast invasion of the maternal decidua and diminished remodeling of maternal spiral arteries[19]. This translates into dramatic decreases in end-diastolic blood flow in uterine arteries[19], taken clinically to indicate placental vascular insufficiency[20]. BPH/5 also exhibit impaired endothelial cell

branching and development of the fetal labyrinth, which is associated with fetal growth restriction, intrauterine fetal demise and small litters of low birth-weight pups[17-19].

Based on our findings of fetoplacental defects indicative of poor angiogenesis/vasculogenesis in the BPH/5 model, together with clinical evidence of an angiogenic imbalance in women with PE, we hypothesized that BPH/5 would exhibit altered levels of endogenous pro- and anti-angiogenic factors during pregnancy, and this would translate into a maternal and fetoplacental syndrome that resembles human PE. Here we demonstrate that an angiogenic imbalance is present in BPH/5 mice during early-to-mid gestation, and this is due to decreased levels of pro-angiogenic VEGF and PGF, but not increased levels of anti-angiogenic sFLT1. Adenovirus-mediated delivery of $VEGF_{121}$ early in pregnancy (e7.5) in BPH/5 normalized VEGF levels, reduced fetal resorptions and prevented spontaneous development of late-gestational hypertension and proteinuria in this model. These data underscore the importance of angiogenic imbalance in the pathogenesis of PE, and further suggest the potential utility of early pro-angiogenic therapies in treating this disease.

METHODS

Animals and Husbandry. Experiments were performed in 8-12 wk old BPH/5 and control C57Bl/6 (C57) mice obtained from in-house colonies. Animals were housed and maintained as previously described[17]. BPH/5 is an inbred strain derived from the spontaneously hypertensive BPH/2 strain, which was originally established through an eight-way cross that included C57Bl/6[17, 21]. Mice underwent strain-matched mating and presence of a vaginal plug in the morning was defined as gestational day e0.5[17]. Gestational stages were defined as early: e9.5-12.5; middle: e13.5-15.5; and late: e18.5-19.5. All animal procedures were approved by the Institutional Animal Care and

Use Committees at The University of Iowa and Cornell University, and are in accordance with the PHS Guide for the Care and Use of Laboratory Animals, USDA regulations and the AUMA panel on Euthanasia.

Adenovirus delivery. Adenoviral vectors encoding $VEGF_{121}$ (Ad-VEGF) and a control gene β-galactosidase (Ad-LacZ) were prepared by the University of Iowa Gene Transfer Vector Core as described previously[22] Briefly, cDNA for $VEGFA_{121}$ was cloned into the E1-deleted region of the replication-deficient E1/E3 deleted Ad5 adenovirus vector backbone[23]. Expression of the $VEGF_{121}$ gene in this viral construct was driven by the RSV promoter[22]. Virus was double-purified and the titer determined as described[22]. Ad-VEGF or Ad-LacZ were injected into C57 and BPH/5 via tail vein on e7.5 (100 µl, 10^9 plaque forming units).

Enzyme-Linked Immunosorbent Assay (ELISA). To determine circulating levels of VEGF, PGF, sFLT1 and sENG, blood was collected from non-pregnant (NP), early, and mid-gestation BPH/5 and C57 females via cardiac puncture and fractionated using EDTA collection tubes. Plasma was isolated from blood samples spun within 30 minutes of collection at 3500 RPM for 15 minutes at 4ºC and immediately frozen at -80ºC. All ELISA kits were purchased from R&D systems and assays were performed according to manufacturer's instructions. For measuring free VEGF, plasma was diluted 2-fold for NP mice and 5- to 10-fold for pregnant mice using assay diluent. The sensitivity for this assay was 3 pg/mL. To determine plasma free levels of PGF, ELISA analysis of undiluted plasma samples from NP, early, and mid-gestation were performed. The sensitivity for this assay was 2 pg/mL. Circulating levels of sFLT1 were determined by ELISA on plasma samples diluted 2-fold for NP mice and diluted 10-fold for pregnant mice. The sensitivity of this assay was 15 pg/mL. Finally, to

measure sENG, ELISA was performed on plasma diluted 5-fold for NP, early- and mid-gestation samples. The sensitivity of this assay was 60 pg/mL.

Quantitative real-time PCR. BPH/5 and C57 mouse placentae were collected at e9.5, e12.5, e14.5 and e18.5 (sFlt-1 only). Samples contained extraembryonic tissues including the decidua basalis and placenta, but excluded the umbilical cord and embryo proper. Placentae from each litter were pooled to create one biological sample (n=1) and total RNA was isolated utilizing a RNeasy kit according to manufacturer's instructions (Qiagen). Quality of RNA samples was determined by denaturing agarose gel electrophoresis and total RNA content quantified by spectrophotometry. Quantitation of *Vegf, Pgf* and *sFlt1* expression levels were performed by amplification of cDNA (equivalent to 10 ng input RNA) using SYBR Green and primers specific to each gene (ABI 7700, PE Biosystems). Primers were selected using a combination of Primer Express software (Applied Biosystems) and Primer Bank (Harvard University http://pga.mgh.harvard.edu/cgi-bin/primerbank). All primers were purchased from integrated DNA technologies (IDT). The primers used were as follows: *Vegf* (NM_001025250): forward 5'-CTT GTT CAG AGC GGA GAA AGC-3', reverse: 5'-ACA TCT GCA AGT ACG TTC GTT-3'; *Pgf* (NM_008827): forward 5'-TCT GCT GGG AAC AAC TCA ACA-3', reverse 5'-GTG AGA CAC CTC ATC AGG GTA T-3'; *sFlt-1* (D88690): forward 5'-ACG TGT GTT TCC TGC TGT GT-3' and reverse 5'- TCA AAG CTT GGT GAA GGG CT-3'; and beta actin: forward 5'CAT CCT CTT CCT CCC TGG AGA AGA 3' and reverse: 5' ACA GGA TTC CAT ACC CAA GAA GGA AGG 3'. Samples were subjected to forty cycles of PCR (50°, 2 min; 95°, 10 min; 40X [95°, 0:15 min; 60°, 1 min]) followed by a dissociation protocol. Each sample was run in triplicate and gene expression was analyzed using the ddCt method. mRNA levels were normalized to *β-actin* (to generate dCt) and compared to C57 e9.5

(to generate ddCt). Sequence-specific amplification was confirmed by a single peak during the dissociation protocol following amplification.

Western blot analysis. Placentae were collected at early and mid-gestation from BPH/5 and C57 mice as described above. Samples were weighed, pooled from each litter (n=1) and homogenized in 50 mM potassium phosphate buffer (pH 7.8). Homogenates were sonicated for 30s at 30% amplitude (Sonics and Materials). Protein concentration was determined with the Bradford assay as previously described.[18] Equal amounts of protein (30 μg protein) were separated on a 12.5% SDS-PAGE gel and were transferred to PVDF membrane. Membranes were blocked in 5% dry milk in TBST (0.01 mol/L Tris, 0.15mol/L NaCl buffer pH8.0 and 0.1% Tween 20) for 2 hours.[18] VEGF levels were measured using an antibody that recognized both $VEGF_{121}$ and $VEGF_{165}$ isoforms (anti-goat VEGF, 1:500, Sigma-Aldrich, St. Louis, MO). Blots were incubated for 1h at room temperature with primary antibody, washed three times in TBST, followed by incubation with secondary antibody for an additional hour (donkey anti-goat IgG peroxidase
1:10 000, Santa Cruz). Blots were stripped and re-probed with a monoclonal anti-actin antibody (Sigma Aldrich). Densitometry of VEGF and actin blots was performed utilizing the BioRad Quantity One. Band intensities were normalized to actin. Values were normalized to the early gestation C57 band for each blot. Experiments were run in triplicate.

In Vitro Angiogenesis Assay. The *in vitro* angiogenesis assay was performed utilizing human umbilical vein endothelial cells (HUVEC) using an *In Vitro* Angiogenesis Kit (Trevigen) according to manufacturer's instructions. Briefly, black Optilux 96 well plates (Falcon) were coated with growth factor reduced matrigel (Trevigen) and were

stored for 30 mins at 37^{o}C to allow polymerization. HUVEC cells obtained from B&D Biosciences were cultured in 75mm culture flasks according to manufacturer's instructions. Confluent cells in flasks were incubated with Calcein AM for 30 mins and trypsinized. Approximately 25,000 cells were plated in matrigel-coated 96 well plates and cultured for 18-20hrs in medium supplemented with either 5% FBS or serum collected from different experimental animals. Plates were imaged using 1.25x objective on a Leica DMI 6000B inverted microscope equipped with green fluorescent protein imaging filters. Total tube lengths in the entire well were measured by experimenters blind to the treatments using Image J software. Data are normalized to the positive FBS control for total tube length.

Radiotelemetric measurement of blood pressure throughout pregnancy. For longitudinal blood pressure measurements, NP female BPH/5 and C57 mice were surgically implanted with radiotelemeters as described previously.[24] Mice were allowed to recover fully for 7 days prior to baseline recording and strain-matched mating. Arterial blood pressure was recorded for 3 consecutive days prior to mating utilizing Dataquest ART data acquisition system (Data Sciences Int). Following strain-matched breeding and detection of a vaginal plug (e0.5), blood pressure was recorded as described previously[17, 18]. Titer-matched Ad-VEGF or Ad-LacZ control vector (100 µL, 1x10^{9} pfu) was injected via tail vein on e7.5 in both strains and arterial pressure recording was continued throughout the duration of pregnancy (~20 days) and for an additional week post-partum.

Urine protein analysis. Urine samples were collected from mid- and late-gestation C57 and BPH/5 females injected with Ad-VEGF or Ad-LacZ on e7.5 and frozen at -

20°C until analysis as described[17, 18]. Protein analysis was performed using Bradford reagent as described[17, 18].

Analysis of pregnancy outcomes. C57 and BPH/5 females treated with Ad-LacZ or Ad-VEGF on e7.5 were euthanized at mid-gestation. The uterine horns were exposed, and the fetuses were counted. Fetal resorptions were identified by necrotic/hemorrhagic appearance compared with normal viable fetuses[17, 18]. In two additional cohorts of both strains treated with Ad-LacZ or Ad-VEGF at e7.5, placental and fetal weights at e14.5 and e18.5 were recorded for all pups from each litter. Finally, the numbers of live pups born were recorded in yet another cohort of BPH/5 and C57 females treated with Ad-LacZ or Ad-VEGF and allowed to deliver.

Morphometric analysis and Immunohistochemistry. C57 and BPH/5 females that had been treated with Ad-LacZ or Ad-VEGF on e7.5 were euthanized at e12.5. Fetoplacental units were removed, fixed in 10% neutral buffered formalin, and paraffin embedded using standard procedures. Tissues were sectioned at 5μm, and stained with isolectin B4 to stain the basement membrane of endothelial cells in the labyrinth and maternal deciduas, and Masson's Trichrome stain to stain the vessels in the placenta as previously described [19]. Placental depth, labryrinth area and junctional zone area were measured as described in [19]. Spiral arteries were imaged and quantified by the ratio of the outer lumen diameter (OD) to the lumen diameter (LD), measured at the point where the OD was the largest.

Statistical analysis. Data are expressed as mean ± SEM. ANOVA followed by Newman-Keuls test for significance was performed for all data sets. $p<0.05$ was considered statistically significant.

RESULTS

Angiogenic imbalance in pregnant BPH/5 is due to decreased pro-angiogenic factors. Free VEGF levels were compared in BPH/5 and C57 plasma from early- and mid-gestation. We focused on these time-points since clinical data points to early- or mid-gestational decreases in VEGF in women with PE[1, 8]. There was a marked increase in circulating free VEGF in C57 controls at both early- and mid-gestation compared to NP levels (Figure 2.1A). BPH/5 also showed pregnancy-induced increases in plasma VEGF, however this was significantly blunted at both time-points compared to C57 (Figure 2.1A). Since the placenta is an important source of angiogenic factors during pregnancy[25], we next compared *Vegf* mRNA levels in placental samples from C57 and BPH/5 at three time-points. Summary data presented in Figure 2.1B shows no differences in *Vegf* transcript levels between C57 and BPH/5 at any of the gestational time-points examined. Since emerging evidence suggests that VEGF expression is regulated via miRNA-mediated repression of *Vegf* mRNA translation[26], we next measured VEGF protein in placentae using Western analysis. As seen in Figure 2.1C and 2.1D, VEGF protein expression was significantly decreased in BPH/5 placentae at both early- and mid-gestational time-points compared to C57 controls, consistent with the plasma VEGF data.

We next compared circulating free PGF in BPH/5 and C57 at early- and mid-gestation since decreased levels of this growth factor at these time-points is associated with PE in women.[8] There was a marked early increase in plasma PGF levels in C57, and this returned to NP levels by mid-gestation (Figure 2.2A). Although BPH/5 showed a significant elevation in free PGF levels at early gestation compared to NP levels, this pregnancy-induced PGF increase was significantly reduced compared to C57 controls (Figure 2.2A). Since this suggested that BPH/5 placentae produce only modest levels of PGF, we next examined *Pgf* transcript levels in this tissue using real-

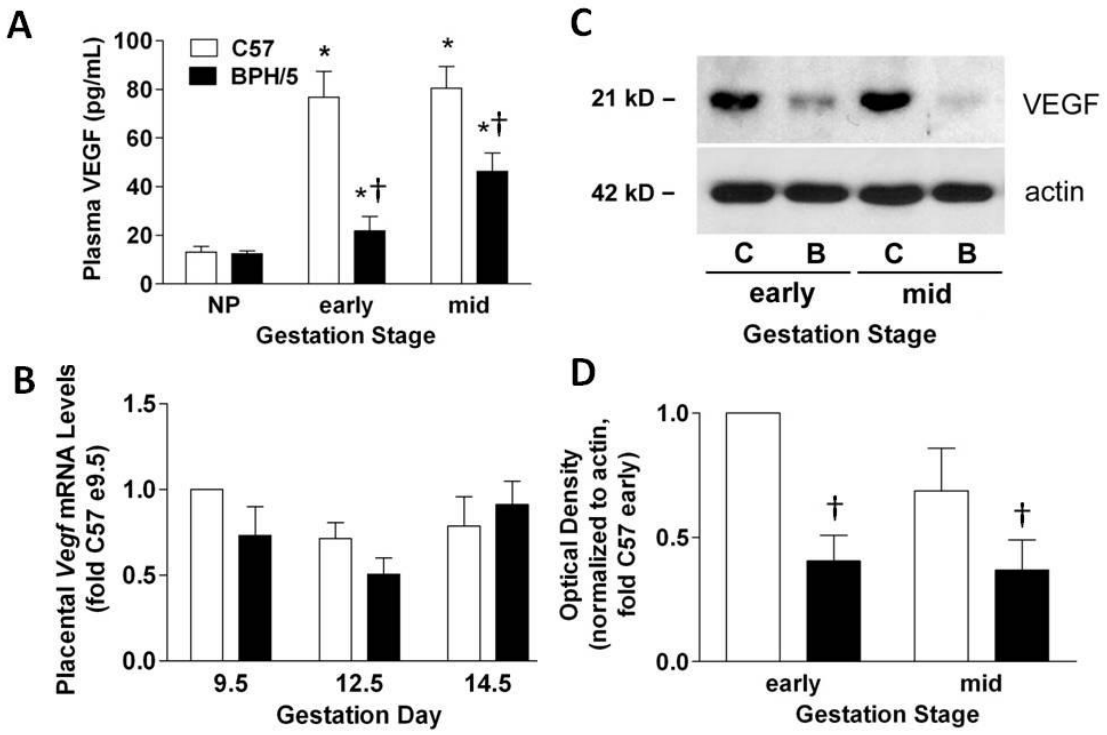

<u>Figure 2.1:</u> Circulating and placental VEGF levels are decreased in BPH/5. A) Summary of circulating free VEGF as determined by ELISA in non-pregnant (NP) and at early and mid-gestation C57 and BPH/5 (n=4-6 per group). B) Summary of real-time qPCR analysis of placental *Vegf* mRNA levels at different days of gestation (n=5 per group). Data are expressed relative to C57 at e9.5 C) Representative Western blot of VEGF protein levels in placenta samples from C57 (C) and BPH/5 (B) at early and mid-gestation. β-actin served as loading control. D) Summary of Western blot quantification (n=3 per group at each time-point) normalized to actin and expressed relative to C57 early. *$p<0.05$ vs NP in matched strain; †$p<0.05$ vs. time-matched C57.

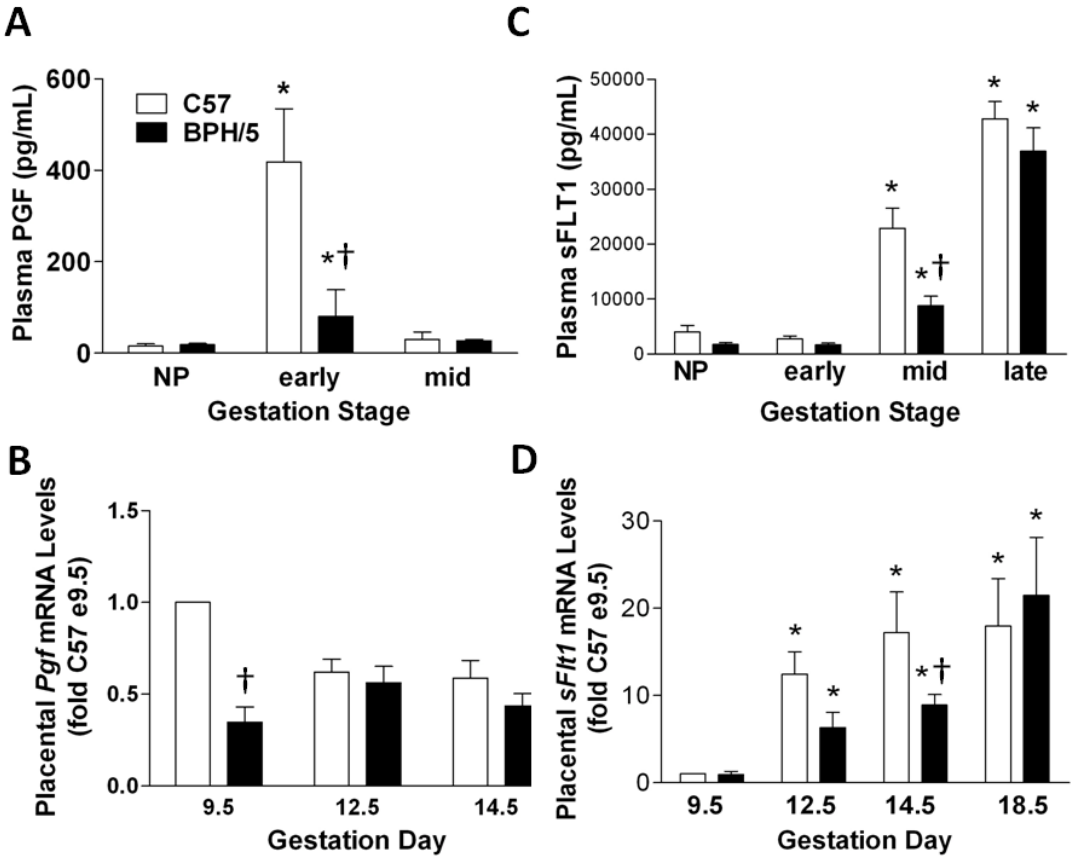

Figure 2.2: Pro-angiogenic PGF is downregulated, whereas anti-angiogenic sFLT1 is unchanged or even decreased in BPH/5. A) Summary of free plasma PGF levels as determined by ELISA in non-pregnant (NP) and at different gestational stages of C57 and BPH/5 (n=4-6 per group). B) Summary of *Pgf* mRNA expression from placental tissue at different gestational days (n=5 per group). Data are expressed relative to C57 at e9.5. C) Summary of circulating sFLT1 levels as determined by ELISA in NP and at different gestational stages of C57 and BPH/5 (n=4-6 per group). D) Summary of real-time qPCR analysis of *sFlt1* from placental tissue of C57 and BPH/5 at different gestational days (n=5 per group). *p<0.05 vs NP in matched strain; †p<0.05 vs. time-matched C57.

time PCR. As shown in Figure 2.2B, placental *Pgf* mRNA was reduced in BPH/5 compared to gestation-matched controls at e9.5 but not at other time-points, reflecting the plasma PGF data.

Since a decrease in VEGF and PGF levels can be accompanied by an elevation in sFLT1 levels in women with PE[1, 9], next we compared the sFLT1 profile in BPH/5 and C57 at early-, mid- and late-gestation. Circulating sFLT1 levels were increased at mid- and late-gestation in both strains relative to NP levels, however the increases in BPH/5 were either not different (late) or even decreased (mid) relative to C57 (Figure 2.2C). Since the placenta is the major source of sFLT1 during pregnancy[27], we further analyzed placental *sFlt1* mRNA. Data in Figure 2.2D show that placental expression of *sFlt1* increased throughout pregnancy in C57 starting at e12.5, and although the temporal profile in BPH/5 mirrors that of C57, mRNA levels were either not altered or even decreased (e14.5) in BPH/5.

Recently, soluble endoglin (sENG) has emerged clinically as a potentially important anti-angiogenic factor in PE[11]. Therefore, plasma sENG levels were compared in BPH/5 and C57 at early- and mid-gestation. As shown in Figure 2.3, sENG was modestly elevated in BPH/5 at e9.5, but not at the other time-points examined.

Adenoviral delivery of $VEGF_{121}$ restores circulating free VEGF levels in BPH/5 and rescues the angiogenic potential of serum from pregnant BPH/5. Based on our findings of decreased pro-angiogenic factors in BPH/5, along with the promise of $VEGF_{121}$ as a therapeutic agent[5, 15, 16], next we determined whether administration of an adenovirus encoding $VEGF_{121}$ (Ad-VEGF) early in pregnancy in BPH/5 would normalize circulating free VEGF levels. We utilized an adenovirus rather than repeated daily injections of recombinant $VEGF_{121}$[15, 16] in order to effect stable, long-term circulating levels of $VEGF_{121}$[28]. As shown in Figure 2.4, tail vein injection of

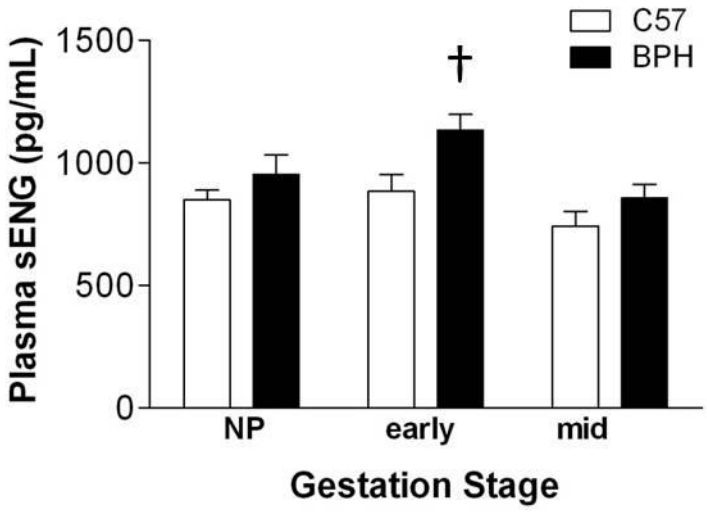

Figure 2.3: Soluble Endoglin levels show slight increase at early gestation in BPH/5. Summary of circulating sENG levels as determined by ELISA in non-pregnant (NP) and at early- and mid- gestation C57 and BPH/5 (n=5-9 per group). † $p<0.05$ vs time-matched C57.

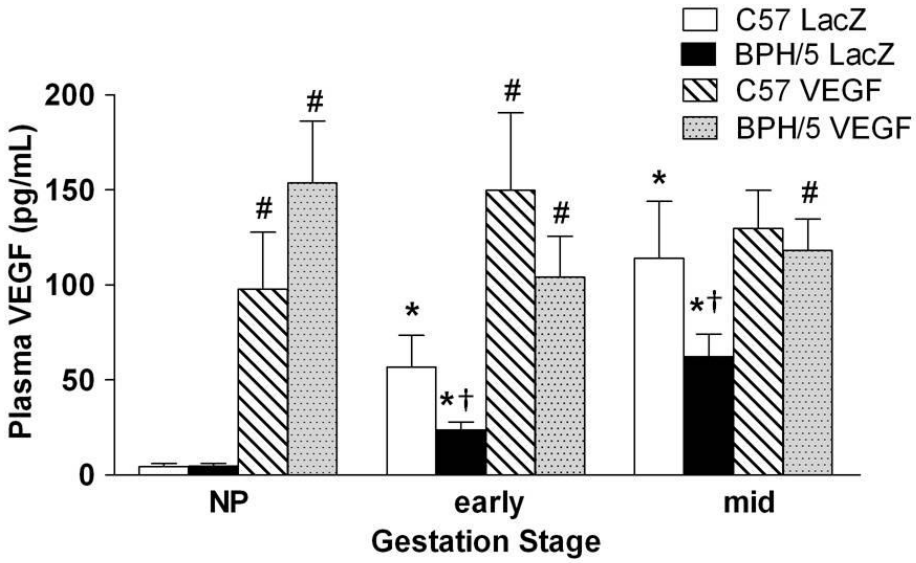

<u>Figure 2.4</u>: Adenoviral-mediated delivery of $VEGF_{121}$ normalizes plasma VEGF levels in BPH/5. Summary of circulating free VEGF levels as determined by ELISA in non-pregnant (NP, 3 days post-injection), early or mid-gestation C57 and BPH/5 mice that underwent tail vein injections of Ad-LacZ or Ad-VEGF. In pregnant mice, viral injections occurred on e7.5. NP: n=4-7 per group; early gestation: n=5-8 per group; mid gestation: n=5-10 per group. *$p<0.05$ vs NP in matched strain and treatment; †$p<0.05$ vs time-matched C57 Ad-LacZ; #$p<0.05$ vs. Ad-LacZ in matched strain and time-point.

Ad-VEGF in NP C57 and BPH/5 females increased plasma VEGF levels more than 20-fold in both strains. Further, Ad-VEGF injected at e7.5 increased circulating VEGF in BPH/5 to levels that were comparable to gestation-matched C57 controls at both early- and mid-gestation (Figure 2.4). Free VEGF levels of Ad-LacZ-treated mice of both strains were similar to those without viral treatments (Figure 2.1A), confirming that the viral vector itself had no effect on circulating free VEGF levels.

To confirm that the Ad-VEGF-induced elevation in circulating free VEGF leads to functionally active VEGF, we performed a well established *in vitro* angiogenesis assay in HUVEC cells[9] using serum collected from NP or pregnant C57 and BPH/5 mice (e12.5) that had been treated with Ad-LacZ or Ad-VEGF (or no treatment) on e7.5. As seen in representative images and summary data in Figure 2.5, endothelial tube formation was significantly decreased with e12.5 serum from BPH/5 that had received no viral treatment or had been injected with the Ad-LacZ vector. Ad-VEGF treatment significantly enhanced tube formation elicited by BPH/5 serum compared to that of Ad-LacZ-treated controls, such that there were no differences in tube formation between serum of these mice and C57 controls (all treatments, Figure 2.5). These results demonstrate that there was functional reconstitution of the angiogenic potential of serum from BPH/5 by systemic Ad-VEGF treatment.

Ad-VEGF therapy early in pregnancy prevents the hallmark maternal PE symptoms and ameliorates fetal resorptions in BPH/5 mice. Next we tested the hypothesis that Ad-VEGF administered early in pregnancy in BPH/5 would ameliorate late-gestational hypertension and proteinuria in this model. NP female BPH/5 and C57 mice were implanted with radiotelemeters for continuous measurement of BP before, during and after pregnancy[17, 18]. After 1 week recovery,

<u>Figure 2.5:</u> Ad-VEGF therapy rescues the angiogenic potential of BPH/5 serum as measured in an endothelial tube formation assay. A) Representative images of individual wells of HUVEC cells treated with serum collected from e12.5 C57 and BPH/5 that had undergone tail vein injections of Ad-LacZ or Ad-VEGF on e7.5. White bar (upper right) indicates a representative measurement of tube length. B) Summary of tube lengths normalized to 5% FBS in cells treated with serum from non-pregnant (NP) mice or from e12.5 C57 and BPH/5 mice given no treatment (none) or administered Ad-LacZ or Ad-VEGF on e7.5. NP: n=8 per strain; no treatment and Ad-LacZ: n=5-8 per group and strain; Ad-VEGF: n=5-12 per group and strain. *$p<0.05$ vs NP matched strain; † $p<0.05$ vs. C57 in matched treatment; # $p<0.05$ vs BPH/5 none or Ad-LacZ.

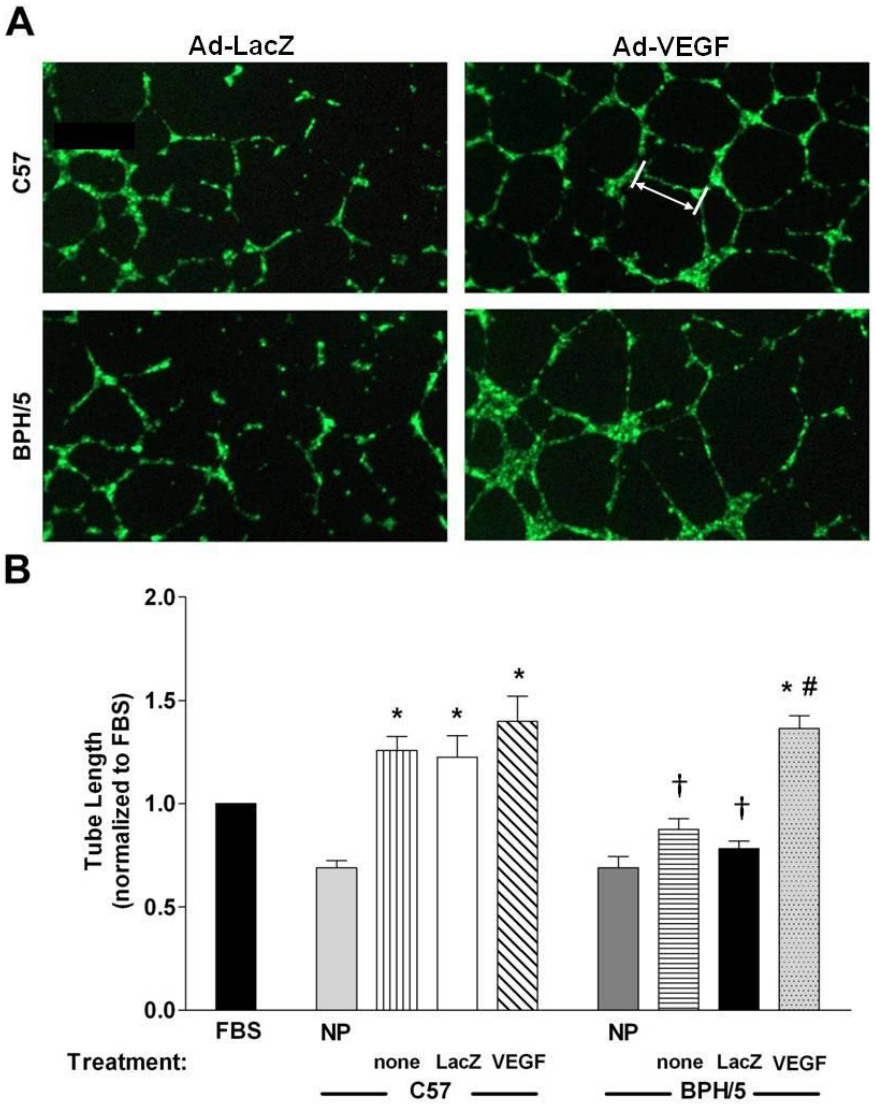
A
Ad-LacZ
Ad-VEGF
C57
BPH/5
B
Tube Length
(normalized to FBS)
2.0
1.5
1.0
0.5
0.0
*
*
*
†
†
* #
FBS
NP
NP
Treatment:
none
LacZ
VEGF
none
LacZ
VEGF
C57
BPH/5

baseline BP was recorded for 3 days before timed strain-matched matings and the start of continuous BP measurements. On e7.5, BPH/5 and C57 mice underwent tail vein injections of Ad-VEGF or Ad-LacZ as above. As seen in Figure 2.6A and 2.6B, baseline mean arterial pressure (MAP) was significantly elevated in Ad-LacZ-treated BPH/5 compared to treatment-matched C57 (120±3 vs. 95±4 mmHg, $p<0.05$), consistent with our earlier reports that BPH/5 have mildly elevated BP before pregnancy[17, 18]. Importantly, neither viral vector altered baseline MAP in either strain (Figure 2.6A,2.6B). However, pregnancy caused a late-gestational rise in MAP over baseline (days 16-20) in Ad-LacZ-treated BPH/5 mice, which is characteristic of this strain[17, 18], and this was prevented by Ad-VEGF therapy (Figure 2.6A). Notably, MAP returned to baseline following delivery in Ad-LacZ-treated BPH/5 mice, consistent with what we have shown previously[17, 18] and with what occurs in women with PE[29]. MAP in C57 controls remained steady throughout pregnancy, and was unaffected by either viral vector (Figure 2.6B).

In a separate cohort of C57 and BPH/5 mice that had undergone Ad-VEGF or Ad-LacZ injections at e7.5, 24-hr urine samples were collected at mid- and late-gestation and subjected to protein analysis. Proteinuria is detected only during late-gestation in BPH/5 mice[17, 18]. These data were confirmed here, wherein urinary protein levels were significantly elevated in Ad-LacZ-treated BPH/5 compared to treatment-matched C57 controls at late- but not mid-gestation (Figure 2.6C). Furthermore, similar to its effects on BP, Ad-VEGF administered early in pregnancy prevented development of proteinuria during late-gestation in BPH/5 (Figure 2.6C). Ad-VEGF did not alter urinary protein levels in C57 mice at either gestational time (Figure 2.6C).

Figure 2.6: Adenoviral-mediated delivery of $VEGF_{121}$ early in pregnancy prevents the hallmark maternal symptoms and rescues fetal demise in BPH/5. Summary of radiotelemetric measurements of mean arterial pressure (MAP) before, during and after pregnancy in BPH/5 (panel A) and C57 (panel B) mice. Ad-VEGF or Ad-LacZ were injected by tail vein on e7.5; n=6-8 for each strain and treatment. C) Summary of urinary protein levels at mid- and late-gestation in BPH/5 and C57 mice that had undergone virus injections on e7.5; n=6-12 per group at each time-point. D) Summary of incidence of fetal resorptions at e14.5 in C57 and BPH/5 mice that had undergone virus injections on e7.5; n=8-11 per group. E) Term litter sizes in each of the strains and virus treatment groups; n=11-18 litters per group. *$p<0.05$ vs baseline in matched strain; #$p<0.05$ vs BPH/5 Ad-LacZ; †$p<0.05$ vs C57 in matched treatment.

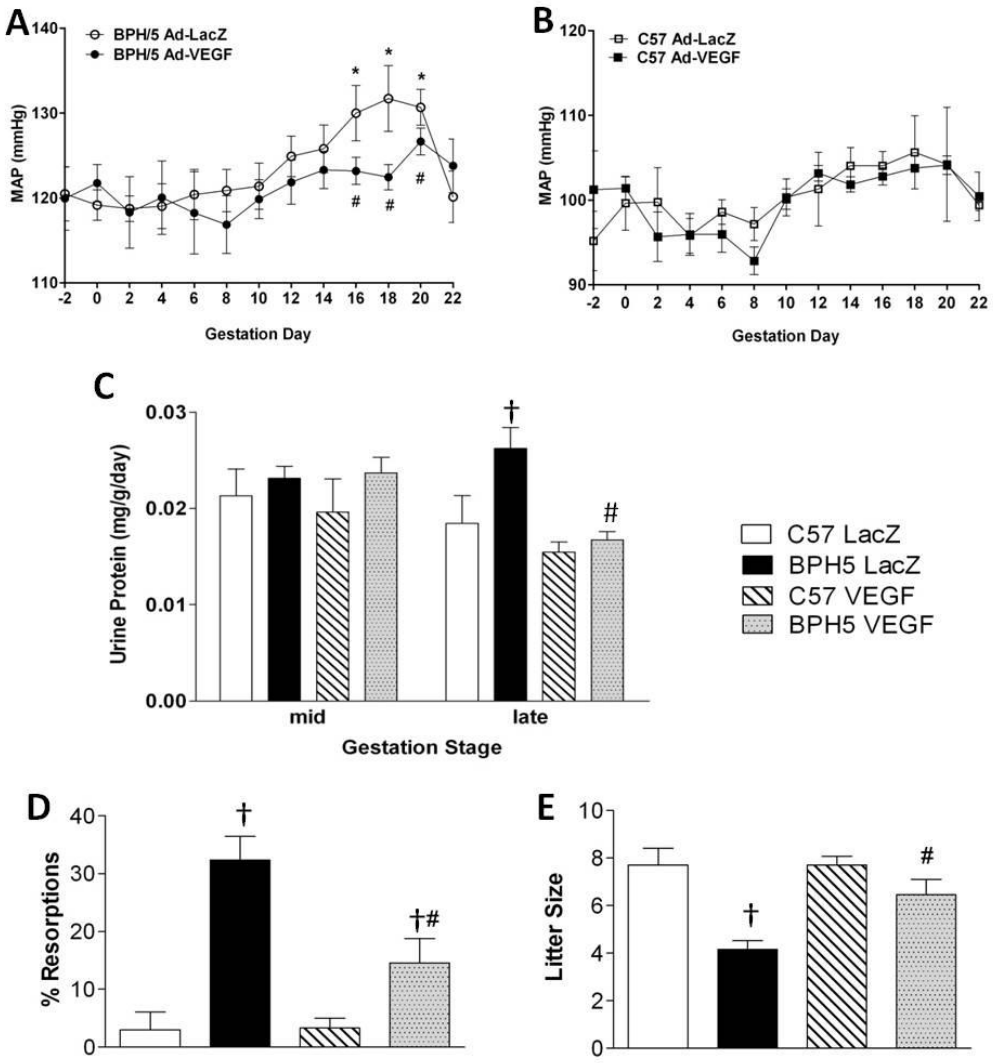
A
BPH/5 Ad-LacZ
BPH/5 Ad-VEGF
MAP (mmHg)
Gestation Day
B
C57 Ad-LacZ
C57 Ad-VEGF
MAP (mmHg)
Gestation Day
C
Urine Protein (mg/g/day)
mid
late
Gestation Stage
C57 LacZ
BPH5 LacZ
C57 VEGF
BPH5 VEGF
D
% Resorptions
E
Litter Size

To determine whether decreased VEGF production during early pregnancy is an important contributor to fetoplacental defects observed in BPH/5 mice[17, 19], we examined several fetoplacental outcomes in BPH/5 and C57 mice treated with Ad-VEGF or Ad-LacZ on e7.5 as above. Data presented in Figure 2.6D show that a third of fetoplacental units in BPH/5 mice treated with the control vector were resorbed, whereas resorptions in Ad-LacZ-treated C57 mice were extremely rare. These results are consistent with our earlier report of fetal resorption incidence in BPH/5[17], and confirm that systemic delivery of adenovirus itself does not elicit resorptions. Importantly, Ad-VEGF reduced this fetal demise observed in BPH/5 by ~50% (Figure 2.6D), which resulted in a significant increase in term litter size compared to Ad-LacZ-treated mice (Figure 2.6E). On the other hand, VEGF therapy did not restore mid- or late-gestational placental or fetal weights in BPH/5 (Table 2.1). It should be noted that in C57 mice, Ad-VEGF treatment had no significant effect on fetoplacental outcomes except a small reduction in fetal weight at e14.5 (Figure 2.6 and Table 2.1).

Potential effects of VEGF therapy: As circulating levels of VEGF significantly improved the hallmark symptoms of pre-eclampsia (Figure 2.6), and since the BPH/5 have significant placental abnormalities associated with the development of the symptoms of pre-eclampsia [17, 19], we examined placentae from VEGF treated animals compared to LacZ controls. An increase in circulating VEGF had no effect on overall placental morphology, with no change in labyrinth area, and global implantation depth (data not shown). VEGF, however, had a positive impact on spiral artery remodeling in BPH/5, with a significant increase in the lumen diameter to outer diameter ratio in VEGF treated BPH/5 animals vs LacZ treated controls (Figure 2.7). VEGF therapy had no effect on spiral artery remodeling in C57 mice.

Table 2.1: Placental and fetal weights (mg)

Gestation day and Sample	Treatment	Strain	Mean ± SEM	n
e14.5 Placental Weight (mg)	Ad-LacZ	C57	103.1±3.9	26
		BPH/5	81.7±5.1 †	40
	Ad-VEGF	C57	109.4±4.2	19
		BPH/5	93.4±3.8 †	13
e14.5 Fetal Weight (mg)	Ad-LacZ	C57	293.4±12.9	20
		BPH/5	196.4±6.8 †	29
	Ad-VEGF	C57	236.9±5.4 #	28
		BPH/5	174.1±8.6 †	15
e18.5 Placental Weight (mg)	Ad-LacZ	C57	91.3±3.1	35
		BPH/5	105.3±4.1 †	26
	Ad-VEGF	C57	90.8±3.1	42
		BPH/5	99.4±3.2	32
e18.5 Fetal Weight (mg)	Ad-LacZ	C57	1168±19.0	35
		BPH/5	1053±40.5 †	23
	Ad-VEGF	C57	1193±18.5	44
		BPH/5	1022±22.3 †	29

Data are expressed as mean ± SEM of n given in table for each treatment and strain. †$p<0.05$ vs. C57 in matched treatment, #$p<0.05$ vs C57 Ad-LacZ.

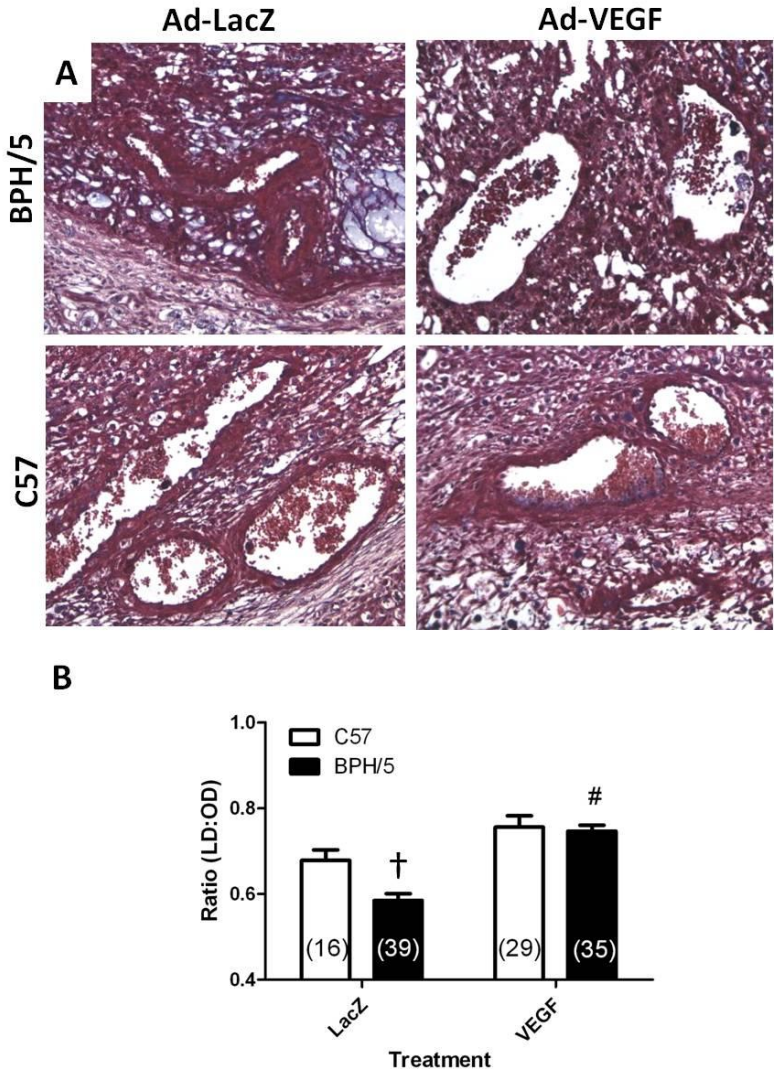

Figure 2.7: Adenoviral-mediated increase in VEGF has positive effects on spiral artery remodeling in BPH/5 mice. A) Representative images of spiral arteries from sectioned placentae stained with Masson's Trichrome of samples taken at e12.5 from mice that received a tail vein injection of Ad-VEGF or Ad-LacZ at e7.5. B) Summary of measurements of the ratio of Lumen Diameter (LD) to Outer Diameter (OD). #$p<0.05$ vs BPH/5 Ad-LacZ; †$p<0.05$ vs C57 in matched treatment.

DISCUSSION

The angiogenic imbalance theory of PE, first posited by Karumanchi and colleagues, has gained significant traction over the years. Their landmark study in 2003 showed that the VEGF and PGF antagonist sFLT1 is upregulated in placentae of PE patients, and this is associated with increased circulating levels of sFLT1 and decreased free plasma VEGF and PGF[9]. A number of follow-up clinical studies supported these findings[1, 10, 30], and an era began of determining whether these factors could be used as biomarkers and/or therapeutic targets in PE[30, 31]. However, more recent clinical data[13, 32] and retrospective reviews of clinical studies such as that by Widmer et al.[33] reveal a much more complex picture. In parallel to the clinical studies, basic research in animal models has yielded important proof-of-concept support for this hypothesis[9,14,15]. However, the experiments have involved exogenous delivery or experimental induction of sFLT1 and subsequent injections of $VEGF_{121}$ to ameliorate sFLT1-mediated responses, which complicates interpretation about the endogenous role of these factors in PE. We employed an animal model that spontaneously develops a PE-like syndrome to rigorously test the angiogenic imbalance hypothesis in the laboratory.

First, we found that the increase in plasma free VEGF levels that occurs normally during early- and mid-gestation in murine (C57) pregnancies is significantly attenuated in BPH/5. This appears to be due at least in part to decreased translation of VEGF mRNA in the placenta. The decreased free VEGF levels observed in BPH/5 mice is consistent with human disease data[9], however our finding of diminished placental VEGF protein is in contrast with some reports in PE patients in which VEGF protein and total VEGF circulating levels may actually be higher than in normal pregnancies (but this is compromised by excess sFLT1)[34]. Second, our results show that the normal pregnancy-induced increase in circulating free PGF in C57 is limited

to early gestation, which mirrors the temporal expression pattern of this growth factor in murine placenta observed in this study and others[35]. Placental expression and plasma free PGF are also markedly blunted in BPH/5 pregnancies. Third, unlike the increased expression and circulating levels of sFLT1 that have been suggested as a causative factor in PE in women[1, 9, 10], this anti-angiogenic factor is either unchanged or even decreased in BPH/5 placentae and plasma relative to controls. This suggests that while there is marked angiogenic imbalance in the BPH/5 model, it may be due to decreased production of pro-angiogenic VEGF and PGF independent of sFLT1-mediated sequestration of these factors. However, it should be noted that sFLT1 is now known to have at least 4 isoforms, and the isoform that is most dominantly expressed in human PE placentae is not expressed in mice[36].

Fourth, sENG is modestly elevated transiently at early gestation in BPH/5, suggesting it is not a major contributor to the PE-like syndrome in BPH/5. Finally, we show that decreased expression of VEGF is functionally linked to the development of fetal demise and the maternal PE-like syndrome in BPH/5 mice since early (e7.5) systemic delivery of Ad-VEGF normalized circulating free VEGF, rescued the angiogenic capacity of serum from pregnant BPH/5, decreased fetal resportions and prevented the hallmark late-gestational hypertension and proteinuria observed in this model.

Although it is widely accepted that the placenta is the major source of angiogenic factors during pregnancy[19, 25, 35], it has been difficult to directly link changes observed in plasma from PE patients to dysregulation of these genes in the placenta due to lack of availability of placental tissue from PE patients at early time points. However, a few studies have demonstrated that cytotrophoblasts from preeclamptic patients show lower staining of VEGF and its receptors, suggesting dysregulation of angiogenic genes in the placenta[34, 38]. Our data highlight the possibility of post-transcriptional regulation of VEGF in the placenta because while

there is a marked decrease in VEGF protein levels in BPH/5 placentae, mRNA levels of VEGF are not significantly changed at any time-point compared to controls. Several mechanisms for post-transcriptional regulation of VEGF in other tissues have been postulated, including down-regulation by microRNAs and translational regulation by cMyc[26]. In addition, hypoxia is known to stabilize *Vegf* mRNA,[39] and a stress-responsive 'switch' in the 3' UTR of *Vegf* has been shown to regulate its expression during hypoxia[40]. This is interesting since it has been postulated that PE is associated with premature breach of the trophoblast shell in early placental development and a subsequent burst of hyperoxia in the developing placental tissue[41]. Although decreased PGF in BPH/5 appears to be due to decreased placental transcription during early gestation, similar to VEGF, PGF regulation by miRNA-mediated repression of translation cannot be ruled out. Our unpublished data shows that in early-gestational BPH/5 placentae, there is marked upregulation of several microRNAs that are known to bind and repress translation of both VEGF and PGF mRNA (Zhou, Guruju, Woods, Sharma and Davisson, unpublished results).

The mechanisms by which decreased circulating free VEGF or PGF during early and mid-gestation result in the multi-system dysfunction observed in PE are not yet fully understood. Given their importance in angiogenesis and vascular remodeling during fetoplacental development, as well as in maintaining maternal cardiovascular and renal function, there are several possibilities. First, a decrease in placental synthesis and secretion of VEGF and PGF by villous cytotrophoblasts, fetal macrophages and fetal fibroblasts may lead to decreases in vasculogenesis and angiogenesis, causing poor placentation[25, 42]. Early defects in placentation due to decreased production of these pro-angiogenic factors could cause the so-called "Stage 1" of the disease, characterized by reduced fetoplacental perfusion and a reduction in spiral artery remodeling, placental oxidative stress and inflammation[42, 43]. Preliminary

placental morphological analyses suggest VEGF has an effect at the level of spiral artery remodeling (Figure 2.7). As spiral artery remodeling is decreased in BPH/5, one might speculate a decrease in uterine natural killer (NK) cells, as they are shown to be involved in this process[44, 45]. Through secretion of angiogenic factors VEGF, PGF and angiopoeitin-II, NK cells are important mediators of early placental development, including trophoblast invasion and facilitating spiral artery remodeling[46]. Though a preliminary analysis of NK cells has been carried out in BPH/5 showed no global reduction in the number of these cells[19], perhaps their distribution or activation is not optimal. Additionally, recent work has demonstrated several sup-populations of uNK cells by histology [47, 48] which can be classified based on size and degree of granulation as well as DBA lectin and PAS staining status (positive or negative). Further classification and examination of uNK cells in BPH/5 is warranted. Shallow trophoblast invasion, deficient spiral artery remodeling, and low levels of angiogenic factors present in BPH/5 placentae (Figure 2.1, [19]), may argue a potential defect in uterine NK proliferation or differentiation[49]. If this hypothesis were true, perhaps by increasing circulating levels of VEGF, as performed in this study, the deficiency of angiogenic factors as a result of the defective NK population is bypassed and spiral artery remodeling improved to normal levels. Indeed, it is interesting to speculate that Ad-VEGF, by ameliorating poor placentation and spiral artery remodeling in the BPH/5 model, leads to reduced fetal resorptions as reported in Figure 2.4D, and that this may be the critical upstream event in Ad-VEGF's beneficial effects on maternal symptoms in this model. It should also be noted that another splice variant of the gene encoding a soluble form of the VEGF receptor-2 has recently been identified and shown to inhibit angiogenesis[50]. It will be intriguing to determine if this isoform is altered in BPH/5 placentae.

In addition to the placenta, angiogenic factors play an important role in various other organ systems. For example, VEGF expression is critical to maintaining the fenestrated and sinusoidal endothelium of the kidney and choroid plexus of the brain and liver, three distinct areas that are affected in PE patients[1, 51]. Podocytes, renal epithelial cells that form the outermost glomerular filtration barrier, synthesize large amounts of VEGF, which is required for development and function of the glomerular filtration barrier[51, 52]. Decreased circulating or local podocyte levels of VEGF could lead to damage of glomerular endothelium and increased protein secretion into the urine[1, 51]. VEGF is also known to regulate vascular permeability, and dysregulation of this process can result in edema, another distinct feature of PE[1]. Furthermore, evidence from anti-angiogenic cancer clinical trials using anti-VEGF antibodies shows that VEGF antagonism results in hypertension, glomerular endotheliosis and proteinuria,[53] again reinforcing the potential role of decreased VEGF in the development of gestational hypertension and proteinuria. Given the powerful effects of early Ad-VEGF treatment on BPH/5 fetal outcomes and maternal endpoints in this study, it will be important to determine the site(s) and mechanisms by which increased levels of this pro-angiogenic factor mediates its effects.

Emerging evidence suggests that decreased levels of circulating VEGF may also contribute to oxidative stress-induced endothelial dysfunction. Recent work from Granger and colleagues has shown that exogenous delivery of recombinant sFLT1 into pregnant rats results in reduced plasma free VEGF levels, increased vascular oxidative stress, decreased NO-dependent vasorelaxation and increased blood pressure[54]. Previous work from our laboratory has shown that increased reactive oxygen species scavenging by Tempol starting before and continuing throughout pregnancy ameliorates fetoplacental defects and development of PE symptoms in BPH/5 model[18]. These results, along with our current findings of decreased placental and plasma free

VEGF in BPH/5 and our previous data showing that BPH/5 exhibit late-gestational endothelial dysfunction[17] suggest that dysregulation of VEGF production in this model may lead to maternal oxidative stress and endothelial dysfunction. Certainly many previous studies have implicated both increased oxidative stress and angiogenic imbalance in the development of PE, however the pathogenic mechanisms have mostly been considered in parallel[42, 43, 55]. The studies discussed above suggest a possible connection between these two pathways.

We have shown that an angiogenic imbalance in BPH/5 mice precedes the onset of maternal PE-like symptoms in this model, and this imbalance is likely due to decreased placental synthesis and circulation of VEGF and PGF independent of increased antagonism by sFLT1. Furthermore, our studies suggest a causal link between decreased VEGF levels and the development of fetoplacental defects and maternal PE-like symptoms since early viral delivery of $VEGF_{121}$ was sufficient to reduce fetal resorptions and prevent late-gestational hypertension and proteinuria in this model. Since fetal loss occurs in advance of hypertension and proteinuria in this model, it is interesting to speculate that Ad-VEGF's beneficial effects on fetal status contributed to amelioration of the maternal syndrome in this study. We believe the BPH/5 model will provide a unique opportunity to now examine the precise molecular underpinnings of changes in the angiogenic profile in the context of PE.

*** Figures 2.4 and 2.6 as well as Table 2.1 reflect experiments performed by D. Hoffmann and C. Weydert, co-authors of this manuscript.****

REFERENCES

1. Maynard S, Epstein FH, Karumanchi SA. Pre-eclampsia and angiogenic imbalance. *Annu Rev Med*. 2008;59:61-78.

2. Roberts JM, Pearson G, Cutler J, Lindheimer M, NHLBI Working Group on Research on Hypertension During Pregnancy. Summary of the NHLBI working group on research on hypertension during pregnancy. *Hypertension*. 2003;41:437-445.

3. Duley L. The global impact of pre-eclampsia and eclampsia. *Semin Perinatol*. 2009;33:130-137.

4. Myatt L, Webster RP. Vascular biology of pre-eclampsia. *J Thromb Haemost*. 2009;7:375-384.

5. Ferrara N. Vascular endothelial growth factor: Basic science and clinical progress. *Endocr Rev*. 2004;25:581-611.

6. De Falco S, Gigante B, Persico MG. Structure and function of placental growth factor. *Trends Cardiovasc Med*. 2002;12:241-246.

7. Shibuya M. Vascular endothelial growth factor receptor-1 (VEGFR-1/Flt-1): A dual regulator for angiogenesis. *Angiogenesis*. 2006;9:225-30; discussion 231.

8. Torry DS, Wang HS, Wang TH, Caudle MR, Torry RJ. Pre-eclampsia is associated with reduced serum levels of placenta growth factor. *Am J Obstet Gynecol*. 1998;179:1539-1544.

9. Maynard SE, Min JY, Merchan J, Lim KH, Li J, Mondal S, Libermann TA, Morgan JP, Sellke FW, Stillman IE, Epstein FH, Sukhatme VP, Karumanchi SA. Excess placental soluble fms-like tyrosine kinase 1 (sFlt1) may contribute to endothelial dysfunction, hypertension, and proteinuria in pre-eclampsia. *J Clin Invest*. 2003;111:649-658.

10. Hertig A, Berkane N, Lefevre G, Toumi K, Marti HP, Capeau J, Uzan S, Rondeau E. Maternal serum sFlt1 concentration is an early and reliable predictive marker of pre-eclampsia. *Clin Chem*. 2004;50:1702-1703.

11. Venkatesha S, Toporsian M, Lam C, Hanai J, Mammoto T, Kim YM, Bdolah Y, Lim KH, Yuan HT, Libermann TA, Stillman IE, Roberts D, D'Amore PA, Epstein FH, Sellke FW, Romero R, Sukhatme VP, Letarte M, Karumanchi SA. Soluble endoglin contributes to the pathogenesis of pre-eclampsia. *Nat Med*. 2006;12:642-649.

12. Powers RW, Roberts JM, Cooper KM, Gallaher MJ, Frank MP, Harger GF, Ness RB. Maternal serum soluble fms-like tyrosine kinase 1 concentrations are not increased in early pregnancy and decrease more slowly postpartum in women who develop pre-eclampsia. *Am J Obstet Gynecol*. 2005;193:185-191.

13. Smith GC, Crossley JA, Aitken DA, Jenkins N, Lyall F, Cameron AD, Connor JM, Dobbie R. Circulating angiogenic factors in early pregnancy and the risk of pre-eclampsia, intrauterine growth restriction, spontaneous preterm birth, and stillbirth. *Obstet Gynecol*. 2007;109:1316-1324.

14. Lu F, Longo M, Tamayo E, Maner W, Al-Hendy A, Anderson GD, Hankins GD, Saade GR. The effect of over-expression of sFlt-1 on blood pressure and the occurrence of other manifestations of pre-eclampsia in unrestrained conscious pregnant mice. *Am J Obstet Gynecol*. 2007;196:396.e1-7; discussion 396.e7.

15. Li Z, Zhang Y, Ying Ma J, Kapoun AM, Shao Q, Kerr I, Lam A, O'Young G, Sannajust F, Stathis P, Schreiner G, Karumanchi SA, Protter AA, Pollitt NS. Recombinant vascular endothelial growth factor 121 attenuates hypertension and improves kidney damage in a rat model of pre-eclampsia. *Hypertension*. 2007;50:686-692.

16. Gilbert JS, Verzwyvelt J, Colson D, Arany M, Karumanchi SA, Granger JP. Recombinant vascular endothelial growth factor 121 infusion lowers blood pressure and improves renal function in rats with placentalischemia-induced hypertension. *Hypertension*. 2010;55:380-385.

17. Davisson RL, Hoffmann DS, Butz GM, Aldape G, Schlager G, Merrill DC, Sethi S, Weiss RM, Bates JN. Discovery of a spontaneous genetic mouse model of pre-eclampsia. *Hypertension*. 2002;39:337-342.

18. Hoffmann DS, Weydert CJ, Lazartigues E, Kutschke WJ, Kienzle MF, Leach JE, Sharma JA, Sharma RV, Davisson RL. Chronic tempol prevents hypertension, proteinuria, and poor feto-placental outcomes in BPH/5 mouse model of pre-eclampsia. *Hypertension*. 2008;51:1058-1065.

19. Dokras A, Hoffmann DS, Eastvold JS, Kienzle MF, Gruman LM, Kirby PA, Weiss RM, Davisson RL. Severe feto-placental abnormalities precede the onset of hypertension and proteinuria in a mouse model of pre-eclampsia. *Biol Reprod*. 2006;75:899-907.

20. Parra M, Rodrigo R, Barja P, Bosco C, Fernandez V, Munoz H, Soto-Chacon E. Screening test for pre-eclampsia through assessment of uteroplacental blood flow and biochemical markers of oxidative stress and endothelial dysfunction. *Am J Obstet Gynecol*. 2005;193:1486-1491.

21. Schlager G, Sides J. Characterization of hypertensive and hypotensive inbred strains of mice. *Lab Anim Sci*. 1997;47:288-292.

22. Anderson RD, Haskell RE, Xia H, Roessler BJ, Davidson BL. A simple method for the rapid generation of recombinant adenovirus vectors. *Gene Ther*. 2000;7:1034-1038.

23. Shima DT, Gougos A, Miller JW, Tolentino M, Robinson G, Adamis AP, D'Amore PA. Cloning and mRNA expression of vascular endothelial growth factor in ischemic retinas of macaca fascicularis. *Invest Ophthalmol Vis Sci*. 1996;37:1334-1340.

24. Butz GM, Davisson RL. Chronic blood pressure recording in pregnant mice by radiotelemetry. *Physiol Genomics*. 2001.

25. Burton GJ, Charnock-Jones DS, Jauniaux E. Regulation of vascular growth and function in the human placenta. *Reproduction*. 2009;138:895-902.

26. Hua Z, Lv Q, Ye W, Wong CK, Cai G, Gu D, Ji Y, Zhao C, Wang J, Yang BB, Zhang Y. MiRNA-directed regulation of VEGF and other angiogenic factors under hypoxia. *PLoS One*. 2006;1:e116.

27. Clark DE, Smith SK, He Y, Day KA, Licence DR, Corps AN, Lammoglia R, Charnock-Jones DS. A vascular endothelial growth factor antagonist is produced by the human placenta and released into the maternal circulation. *Biol Reprod*. 1998;59:1540-1548.

28. Jalkanen J, Leppanen P, Narvanen O, Greaves DR, Yla-Herttuala S. Adenovirus-mediated gene transfer of a secreted decoy human macrophage scavenger receptor (SR-AI) in LDL receptor knock-out mice. *Atherosclerosis*. 2003;169:95-103.

29. Berks D, Steegers EA, Molas M, Visser W. Resolution of hypertension and proteinuria after pre-eclampsia. *Obstet Gynecol*. 2009;114:1307-1314.

30. Levine RJ, Maynard SE, Qian C, Lim KH, England LJ, Yu KF, Schisterman EF, Thadhani R, Sachs BP, Epstein FH, Sibai BM, Sukhatme VP, Karumanchi SA. Circulating angiogenic factors and the risk of pre-eclampsia. *N Engl J Med*. 2004;350:672-683.

31. Thadhani R, Mutter WP, Wolf M, Levine RJ, Taylor RN, Sukhatme VP, Ecker J, Karumanchi SA. First trimester placental growth factor and soluble fms-like tyrosine kinase 1 and risk for pre-eclampsia. *J Clin Endocrinol Metab*. 2004;89:770-775.

32. Savvidou MD, Yu CK, Harland LC, Hingorani AD, Nicolaides KH. Maternal serum concentration of soluble fms-like tyrosine kinase 1 and vascular endothelial growth factor in women with abnormal uterine artery doppler and in those with fetal growth restriction. *Am J Obstet Gynecol*. 2006;195:1668-1673.

33. Widmer M, Villar J, Benigni A, Conde-Agudelo A, Karumanchi SA, Lindheimer M. Mapping the theories of pre-eclampsia and the role of angiogenic factors: A systematic review. *Obstet Gynecol*. 2007;109:168-180.

34. Tsatsaris V, Goffin F, Munaut C, Brichant JF, Pignon MR, Noel A, Schaaps JP, Cabrol D, Frankenne F, Foidart JM. Overexpression of the soluble vascular endothelial growth factor receptor in preeclamptic patients: Pathophysiological consequences. *J Clin Endocrinol Metab*. 2003;88:5555-5563.

35. Achen MG, Gad JM, Stacker SA, Wilks AF. Placenta growth factor and vascular endothelial growth factor are co-expressed during early embryonic development. *Growth Factors*. 1997;15:69-80.

36. Sela S, Itin A, Natanson-Yaron S, Greenfield C, Goldman-Wohl D, Yagel S, Keshet E. A novel human-specific soluble vascular endothelial growth factor receptor 1: Cell-type-specific splicing and implications to vascular endothelial growth factor homeostasis and pre-eclampsia. *Circ Res*. 2008;102:1566-1574.

37. Heydarian M, McCaffrey T, Florea L, Yang Z, Ross MM, Zhou W, Maynard SE. Novel splice variants of sFlt1 are upregulated in pre-eclampsia. *Placenta*. 2009;30:250-255.

38. Zhou Y, McMaster M, Woo K, Janatpour M, Perry J, Karpanen T, Alitalo K, Damsky C, Fisher SJ. Vascular endothelial growth factor ligands and receptors that regulate human cytotrophoblast survival are dysregulated in severe pre-eclampsia and hemolysis, elevated liver enzymes, and low platelets syndrome. *Am J Pathol*. 2002;160:1405-1423.

39. Liu LX, Lu H, Luo Y, Date T, Belanger AJ, Vincent KA, Akita GY, Goldberg M, Cheng SH, Gregory RJ, Jiang C. Stabilization of vascular endothelial growth factor mRNA by hypoxia-inducible factor 1. *Biochem Biophys Res Commun*. 2002;291:908-914.

40. Ray PS, Jia J, Yao P, Majumder M, Hatzoglou M, Fox PL. A stress-responsive RNA switch regulates VEGFA expression. *Nature*. 2009;457:915-919.

41. Jauniaux E, Watson AL, Hempstock J, Bao YP, Skepper JN, Burton GJ. Onset of maternal arterial blood flow and placental oxidative stress. A possible factor in human early pregnancy failure. *Am J Pathol*. 2000;157:2111-2122.

42. Redman CW, Sargent IL. Placental stress and pre-eclampsia: A revised view. *Placenta*. 2009.

43. Roberts JM, Hubel CA. The two stage model of pre-eclampsia: Variations on the theme. *Placenta*. 2009;30 Suppl A:S32-7.

44. Trundley A, Moffett A. Human uterine leukocytes and pregnancy. *Tissue Antigens*. 2004;63:1-12.

45. Ahn H, Park J, Gilman-Sachs A, Kwak-Kim J. Immunologic characteristics of pre-eclampsia, a comprehensive review. *Am J Reprod Immunol*. 2010.

46. Tabiasco J, Rabot M, Aguerre-Girr M, El Costa H, Berrebi A, Parant O, Laskarin G, Juretic K, Bensussan A, Rukavina D, Le Bouteiller P. Human decidual NK cells: Unique phenotype and functional properties -- a review. *Placenta*. 2006;27 Suppl A:S34-9.

47. Paffaro VA,Jr, Bizinotto MC, Joazeiro PP, Yamada AT. Subset classification of mouse uterine natural killer cells by DBA lectin reactivity. *Placenta*. 2003;24:479-488.

48. Croy BA, Zhang J, Tayade C, Colucci F, Yadi H, Yamada AT. Analysis of uterine natural killer cells in mice. *Methods Mol Biol*. 2010;612:465-503.

49. Tayade C, Hilchie D, He H, Fang Y, Moons L, Carmeliet P, Foster RA, Croy BA. Genetic deletion of placenta growth factor in mice alters uterine NK cells. *J Immunol*. 2007;178:4267-4275.

50. Albuquerque RJ, Hayashi T, Cho WG, Kleinman ME, Dridi S, Takeda A, Baffi JZ, Yamada K, Kaneko H, Green MG, Chappell J, Wilting J, Weich HA, Yamagami S, Amano S, Mizuki N, Alexander JS, Peterson ML, Brekken RA, Hirashima M, Capoor S, Usui T, Ambati BK, Ambati J. Alternatively spliced vascular endothelial growth factor receptor-2 is an essential endogenous inhibitor of lymphatic vessel growth. *Nat Med*. 2009;15:1023-1030.

51. Eremina V, Baelde HJ, Quaggin SE. Role of the VEGF--a signaling pathway in the glomerulus: Evidence for crosstalk between components of the glomerular filtration barrier. *Nephron Physiol*. 2007;106:p32-7.

52. Robert B, Zhao X, Abrahamson DR. Coexpression of neuropilin-1, Flk1, and VEGF(164) in developing and mature mouse kidney glomeruli. *Am J Physiol Renal Physiol*. 2000;279:F275-82.

53. Sugimoto H, Hamano Y, Charytan D, Cosgrove D, Kieran M, Sudhakar A, Kalluri R. Neutralization of circulating vascular endothelial growth factor (VEGF) by anti-VEGF antibodies and soluble VEGF receptor 1 (sFlt-1) induces proteinuria. *J Biol Chem*. 2003;278:12605-12608.

54. Bridges JP, Gilbert JS, Colson D, Gilbert SA, Dukes MP, Ryan MJ, Granger JP. Oxidative stress contributes to soluble fms-like tyrosine kinase-1 induced vascular dysfunction in pregnant rats. *Am J Hypertens*. 2009;22:564-568.

55. Cindrova-Davies T. Gabor than award lecture 2008: Pre-eclampsia - from placental oxidative stress to maternal endothelial dysfunction. *Placenta*. 2009;30 Suppl A:S55-65.

CHAPTER THREE:

GENE EXPRESSION PROFILING OF SONOGRAPHICALLY PHENOTYPED FETOPLACENTAL UNITS REVEALS A BROAD ARRAY OF DIFFERENTIALLY REGULATED PATHWAYS IN THE BPH/5 MOUSE MODEL OF PRE-ECLAMPSIA

SUMMARY

Pregnancies in BPH/5, a murine model of PE, are characterized by abnormal placentation and progressive fetal loss. To identify at-risk embryos *in utero*, ultra-high frequency ultrasound (VEVO 770) was used to phenotype BPH/5 embryos at e10.5. Pregnant BPH/5 and C57were anesthetized, the uterine horns exteriorized, and sonographic data collected from each embryo using a 40MHz scanhead. Three distinct fetoplacental phenotypes emerged in BPH/5 when compared to C57: Class I (normal HR and development); Class II (slow or irregular HR, reduced size); Class III (no development past e7.5). Scored fetoplacental units were then dissected and tissues from each of the three classes of BPH/5, as well as C57 implantation sites, were collected. Total RNA was extracted and gene expression microarray experiments were run. Separate arrays were used comparing each BPH/5 class to a C57 reference, and genes were considered dysregulated with >1.5-fold change and $p<0.05$. A total of 2350 dysregulated genes were identified across the three BPH/5 classes, with Class II showing the greatest proportion of differentially expressed genes. The more developmentally challenged classes showed dysregulation in functional pathways of angiogenesis, development and apoptosis. Review of the gene lists revealed that 6 different imprinted genes were among the dysregulated genes, with 4 of paternal origin (insulin growth factor 2, delta-like 1, paternally expressed gene 3 and the amino acid transporter Slc38a4) and 2 of maternal origin (H19 and Decorin). Together, these data reveal that a significant proportion of BPH/5 fetoplacental units exhibit compromised development and health at e10.5, and this is associated with marked gene dysregulation, including several imprinted genes.

INTRODUCTION

Pre-eclampsia (PE) is a pregnancy-associated disorder affecting 8-10% of women worldwide. It is characterized by new onset high blood pressure and proteinuria late in gestation. Fetoplacental abnormalities often complicate PE pregnancies. Early onset PE is associated with increased risk of intra-uterine growth restriction (IUGR) of the fetus[1]. Additionally, pregnancies complicated by severe PE have an increase risk of fetal mortality[2]. Placentae from PE pregnancies often show shallow trophoblast invasion into the maternal decidua and reduced spiral artery remodeling[3, 4]. Though the etiology of PE remains unknown, major recent hypotheses include abnormal placentation and angiogenic imbalance[5]. However, there are still very few treatment options beyond early delivery of the placenta and fetus.

Several years ago we described the BPH/5 model, a murine strain that spontaneously develops a syndrome that bears close resemblance to human PE. These mice develop pregnancy-induced hypertension, proteinuria, and placental defects with time-courses similar to the human condition[6, 7]. BPH/5 is also a model of intrauterine growth restriction and fetal loss[6, 7]. Determining the cause of fetal demise in this model, and how this may relate to the development of the maternal syndrome in later pregnancy could provide very important clues in our understanding of the pathophysiology of PE.

The use of gene expression profiling of cells and tissues has become a major tool for determining disease progression, identification of diagnostic or prognostic biomarkers and classification of diseases. In recent years, this technology has been used to investigate the molecular mechanisms of normal placental development in human and mouse[8, 9] as well as placental abnormalities in human pregnancies complicated with PE[10-17]. A number of differentially regulated genes were identified as

potential biomarkers for predicting PE, however, a limitation of these human studies comes from the scarcity of samples collected at different gestational time points. The molecular profile of term PE placentae provides a snapshot of endpoint dysregulated pathways, however it does not aid in identifying differentially expressed genes in what is likely a long cascade of gestational events leading up to manifestation of the disease.

A significant advancement in the field of PE research could come with the understanding of early pathological events that lead to the maternal syndrome. The BPH/5 mouse model provides a unique tool for understanding early fetoplacental defects that may underlie the development of PE later in gestation. Since some but not all BPH/5 fetuses succumb during gestation, we turned to ultra-high frequency ultrasound in order to track fetoplacental status *in utero*. Clinical ultrasounds have long been used to monitor human pregnancies, however the resolution of these systems is limited in the study of murine pregnancy. The availability of dedicated ultrasound imaging systems for rodents, such as the VEVO 770 (Visualsonics), have provided unique opportunities to examine developmental defects in fetoplacental units starting early in gestation. With these systems, transducers capable of operating at eight times higher frequency than clinical ultrasounds have allowed researchers to visualize miniature structures in a non-invasive manner (*in utero*)[18]. With these improvements in resolution, murine embryos can be imaged as early as e5.5, with embryonic heart rates detected as early as e9.5[19, 20]. In this study, we hypothesized that BPH/5 fetoplacental units would exhibit differential gene expression at early gestation (e10.5). Examining BPH/5 fetoplacental units via ultra-high frequency ultrasound provides a powerful tool to assess embryonic health *in utero* and provides a platform for molecular characterization and understanding the genetic underpinnings of fetal demise in this model. We focused on this timepoint since previous work in our group

shows increased incidence of fetal demise starting at mid-gestation, coincident with the development of PE-like symptoms in this mouse model[6, 7]. By focusing earlier in gestation, our goal was to elucidate potential pathways underlying fetal demise, and perhaps the PE-like syndrome in this model. Using Vevo 770 for ultra-high frequency ultrasound, we scored and separated embryos into three categories based on fetal health and development. Using RNA isolated from these three classes of fetoplacental units, along with gestation-matched C57Bl/6 units, we performed genome-wide expression profiling using DNA microarray technology.

METHODS

Ultra-high frequency ultrasonagraphic analysis of BPH/5 and C57 mouse feto-placenta units. Strain-matched matings were set up for C57Bl/6 (C57) controls and BPH/5 mice. The day vaginal plug was detected was denoted e0.5. Initial experiments showed that gestation day 10.5 was the earliest time point in which the greatest variation in embryonic health was examined prior to fetal death and necrosis (data not shown). Pregnant BPH/5 and C57 females at e10.5 were anaesthetized with 2% isofluorane and the abdominal hair was chemically removed as described in Slevin and colleagues[21]. Maternal physiology was closely followed by monitoring core body temperature, heart rate and respiration rates. Briefly, a ventral incision was made and the uterine horns were exteriorized and each individual embryo was interrogated using a 40MHz frequency scanhead (Visualsonics VEVO 770). Fetal and maternal heart rates (HR) were measured using pulse-wave Doppler (expressed as fetal/maternal HR), and crown-rump measurements were taken when the orientation permitted the maximum distance between head and tail (as described in [22]). Fetuses were placed in one of 3 categories: Class I (normal HR and development); Class II (slow or irregular HR, reduced size); Class III (no embryonic dvelopment, HR often not detected but not

necrotic). After embryos were categorized, the female was quickly euthanized via cervical dislocation and individual implantation sites (fetus, placental tissue and surrounding uterine wall) were excised and placed in RNA stabilizing RNAlater (Qiagen) and stored at -80ºC for future RNA extraction (see below). All animal protocols were approved by the Cornell University Animal Care and Use Committee.

Immunohistochemistry. Isolectin staining was performed as described previously [6]. Briefly, implantation sites were fixed in 10% formalin before paraffin embedding using a standard procedure. Paraffin sections were cut at 5μm, and stained using Isolectin-B4 staining (1:125, Vector Laboratories), which labels basement membranes. Sections were counterstained with DAB+ (Dako) and photographed.

Total RNA extraction. Total RNA was isolated from the entire fetoplacental unit using QIAGEN RNeasy Mini kit (QIAGEN) in accordance with manufacturer's protocols. Total RNA was quantified with NanoDrop ND-1000 spectrophotometer (Thermo Scientific). The quality and integrity of total RNA were assessed using Agilent 2100 Bioanalyzer (Agilent Technologies). The RNA integrity number (RIN) equal to or higher than 9 was acceptable for microarray and real time qPCR analysis.

DNA microarray. The microarray experiments were performed with a dual-channel reference[23] design in which the C57 mouse fetoplacental units were used as a reference. Array analysis was carried out with a subset of embryos collected from three pregnancies where a BPH/5 female carried embryos from each class (I, II, and III). Three such litters were used for these studies. C57 embryos (all Class I) were used as controls. Labeling was carried out using the indirect cDNA labeling method in which 20μg of total RNA was labeled with Cy5 or Cy3 and purified prior to

hybridization on the array (cDNA synthesis using Superscript III, Invitrogen, purification with columns from QIAGEN). The labeling efficiency and quantification of Cy3 and Cy5 dye were assessed on NanoDrop ND-1000. Prior to hybridization, the mouse OneArray™ with 29,922 mouse genome probes and 1880 experimental control probes which are highly sensitive to 70-mer sense-strand polynucleotide probes (Phalanx Biotech) were prehybridized for 1 hour followed manufacturer's instructions. The labeled cDNA was resuspended in mouse OneArray hybridization buffer and the arrays were incubated in hybridization chambers (Corning) and hybridization was performed for 16 to 20 hours at 42°C. Each array was scanned with the GenPix 4000B microarray scanner (Molecular Devices) at two channels of wavelengths, 532 and 635nm. The scanned images were analyzed and each spot quantified using Genepix Pro 6.0 program (Molecular Devices).

Microarray data analysis. For the microarray data normalization and differential expression analysis, R software 2.6.0 (http://www.r-project.org/) and LIMMA (Linear Models for Microarray Data) software was used. The p-values were adjusted for multiple test corrections across all genes and comparisons with the Benjamini-Hochberg method to control for false-discovery rate (FDR) at less than 5% with moderate stringency with a fold change cutoff of ≥ 1.5 or ≤ -1.5. These criteria were used as a threshold to determine genes with significant differential expression.

Real Time Quantitative PCR validation. A number of differentially expressed genes from the microarray study were validated with real-time quantitative PCR. First strand cDNA was prepared using High Capacity cDNA Reverse Transcription it (Applied Biosystems) followed the manufacturer's protocol. An equivalent to 25 ng of total RNA was used in real time quantitative PCR. The primers for real time quantitative

PCR (see Table 3.1) were designed. The housekeeping gene, β-actin, was used as an internal control for normalization. Real-time PCR reactions were performed in a 96-well plate with a total volume of 25 µl containing 1X Power SYBR Green PCR Master Mix and the ABI 7500 Fast Real-Time PCR System (Applied Biosystems). The quantification of gene expression was analyzed with ΔΔCt method[24]. The relative expression of each gene with fold changes in mRNA was calculated as $2^{-\Delta\Delta Ct}$.

Functional Analysis

Gene Ontology analysis. To interpret the function of differentially expressed genes in Class I, II and III of BPH/5 mouse fetoplacental units associated with the biological processes, the analysis tool, Database for Annotation, Visualization and Integrated Discovery DAVID (http://david.abcc.ncifcrf.gov/)[25, 26] was applied to assess whether the gene ontology terms occurred more frequently than expected by chance in the set of genes dysregulated in BPH/5. The Functional Annotation Tool in DAVID was performed with the medium stringency setting (Kappa similarity term overlap ≥ 3 and threshold of 0.85; classification multiple linkage threshold of 0.5). For DAVID analyses, the significance of over-representation of functional categories was assessed with a p-value (from a modified Fisher Exact test) and with Benjamini correction of 0.05. This criterion was used to determine significance of enriched GO terms. All results are ranked based on p values and processes (Gene Ontology "Biological Process" category) with the highest enrichment are presented.

*Network analysis-IPA.*Ingenuity Pathway Analysis (IPA) assigns biological functions to genes using the Ingenuity Pathways Knowledge Base (Ingenuity Systems). IPA analysis was performed on array data from BPH/5 Class I, II and III compared to C57 (IPA version 8). The top 15 most dysregulated functional pathways were recorded

and the number of dysregulated genes within those pathways noted. Finally, network analysis was performed on the top ranking networks within each class.

RESULTS

BPH/5 fetoplacental units show a range of fetal health at e10.5. Previous studies show progressive fetal loss and a wide variation in fetoplacental health status within BPH/5 litters[6, 7]. Since we hypothesize that mRNA expression will vary with fetoplacental health status, we used ultra-high frequency ultrasound to phenotype and classify fetoplacental units prior to gene profiling. Initial experiments using 9 BPH/5 litters showed a wide range of fetal status at e10.5 compared to C57 gestation matched controls. Embryos were scored into three separate classes based on embryo size (crown-rump measurements), fetal heart rate, and cardiac development (Figure 3.1 A-D). Approximately 65% of BPH/5 fetuses were categorized as Class I which represent the healthiest of BPH/5 embryos (Figure 3.1E), with similar heart rate (Figure 3.1G) and developmental profiles as C57 time-matched counterparts, although they still showed reduced crown-rump measurements compared to C57 (Figure 3.1F). Class II embryos represent 23% of BPH/5 embryos, and they showed developmental delay in cardiac structure, bradycardic or irregular HR and extreme IUGR compared to both healthy littermates (Class I), and C57 controls (Figure 3.1 E-G). Finally, 12% of BPH/5 fetuses were Class III, with severely retarded development (although not necrotic) (Figure 3.1E).

Next we examined the histomorphology of different classes of fetoplacental units by isolectin staining to compare placental development. Class I (Figure 3.1H) embryos show normal formation of placental zones of labyrinth, spongiotrophoblast and decidua, whereas Class II (Figure 3.1I) embryos lack a unified formation of labyrinth, and Class III (Figure 3.1J) embryos show lack of placental development,

Table3.1. Primer Pairs Used for Real Time PCR Validation of Microarray Data

Gene	Accession No.	Primer sequence (5' to 3')	Tm (°C)	Amplicon size (bp)
AFP	NM_007423	AACAGGAGGCTATGCATCACCAGT	60.0 ºC	182
		TGCTCCTCTGTCAGTTCAGGCTTT	60.0 ºC	
Timp4	NM_080639	ACACGCCATTTGACTCTTCCCTCT	60.1 ºC	192
		AGCCACAGTTCTGGTGGTAGTGAT	59.7 ºC	
SP7	NM_130458	TGCAGCAAATTTGGCGGCTCTA	59.8 ºC	141
		TCCATTGGTGCTTGAGAAGGGA	58.2 ºC	
Ccnd2	NM_009829	ACGCATGTGGTGCCTGTTCAAA	59.9 ºC	142
		ATGTTGCAGGTACGCACACTCT	58.7 ºC	
Thbs2	NM_011581	ATGCAGCCTGGGCAAATGTGAT	59.8 ºC	195
		TCACGCTGACAGGGTTTGGTTT	59.2 ºC	
TNFRSF11B	NM_008764	CCACAATGAACAAGTGGCTGTGCT	60.0 ºC	155
		TAGGTAGGTGCCAGGAGCACATTT	59.8 ºC	
Sfrp4	NM_016687	TCATCACCAATTCCTCCTGCCAGT	60.1 ºC	182
		TGTTCTCTGCTGTTCCTGAAGCCT	60.0 ºC	
Adam12	NM_007400	AAGAATTGCCACTGTGAAGCCCAC	59.9 ºC	158
		ACAAATCCAGCAGCAAGCAGACAC	60.0 ºC	
Adam19	NM_009616	ATGGACCACAAGAGGAAGCCAAGA	60.0 ºC	176
		AAAGGTGCTCGTTCTTCTCCAGGT	60.0 ºC	
Casp2	NM_007610	TACATGACCAGACCGCACAGGAAA	60.0 ºC	130
		ACACCATAGATGCCACCTTCCACA	60.0 ºC	
Il1rl1	NM_001025602	ACACTTGTCAATTCACACACGCGG	59.9 ºC	222
		TAATCTGCCACAGGACATCAGCCA	60.0 ºC	
Itgb7	NM_013566	CACGGATACTGCAAATGCAACCGT	59.9 ºC	115
		ACTCTGCACAATCCCTGTACTGCT	59.9 ºC	
Cldn1	NM_016674	TGCAAAGTCTTCGACTCCTTGCTG	59.2 ºC	126
		CATGCACTTCATGCCAATGGTGGA	60.0 ºC	
Il1r2	NM_010555	AGATGAGCCAAGGATGTGGGTGAA	60.1 ºC	115
		CATTTGCTCACAGTGGGATGCGTT	60.0 ºC	
Tnfrsf22	NM_023680	TGTTTGGCTTCTTCTGCAGCTTGG	60.0 ºC	162
		ACCAGTATTCACCAGCGGGACATT	60.2 ºC	
Adamts5	NM_011782	ACTACGATGCAGCCATCCTGTTCA	60.1 ºC	187
		TGAGAAAGGCCAAGTAGATGCCCA	60.0 ºC	
Cyp39a1	NM_018887	TGCAGGTCATTCTGGAACCCTCTT	60.0 ºC	243
		CCTGCAGTGCCAAACACAGAAGAT	59.6 ºC	
Ccnd1	NM_007631	GCTGCAAATGGAACTGCTTCTGGT	60.1 ºC	199
		TACCATGGAGGGTGGGTTGGAAAT	60.0 ºC	
β-Actin	NM_007393	TCGTACCACAGGCATTGTGATGGA	60.1 ºC	200
		TGATGTCACGCACGATTTCCCTCT	60.2 ºC	

<u>Figure 3.1:</u> Ultrasonographic analysis reveals three classes of fetoplacental status in BPH/5 litters. Representative sonograms showing C57 controls (A) and three classes of embryos at e10.5 (B-D, Class I-III respectively). Caliper placement for crown- rump measurements illustrated in Class I (panel B). (E) Summary of the proportion of BPH/5 fetuses comprising each of the three classes (n=9 litters). (F) Summary of fetal HR (relative to maternal HR) reveals bradycardia in Class II (n=6) compared to Class I (n=26) and C57 (n=21). (G) Summary of crown rump length reveals reduced fetal size of Class I (n=20) and Class II embryos (n=5) compared to Class I and C57 (n=13). Representative images from isolectin stained fetoplacental units show a range of placental development from easily defined placenta in Class I (H), minimal placental definition in Class II (I), and no placental development in Class III (J). *$p<0.05$ vs C57, † $p<0.05$ vs Class I H, heart, U, umbilical cord, P, placenta.

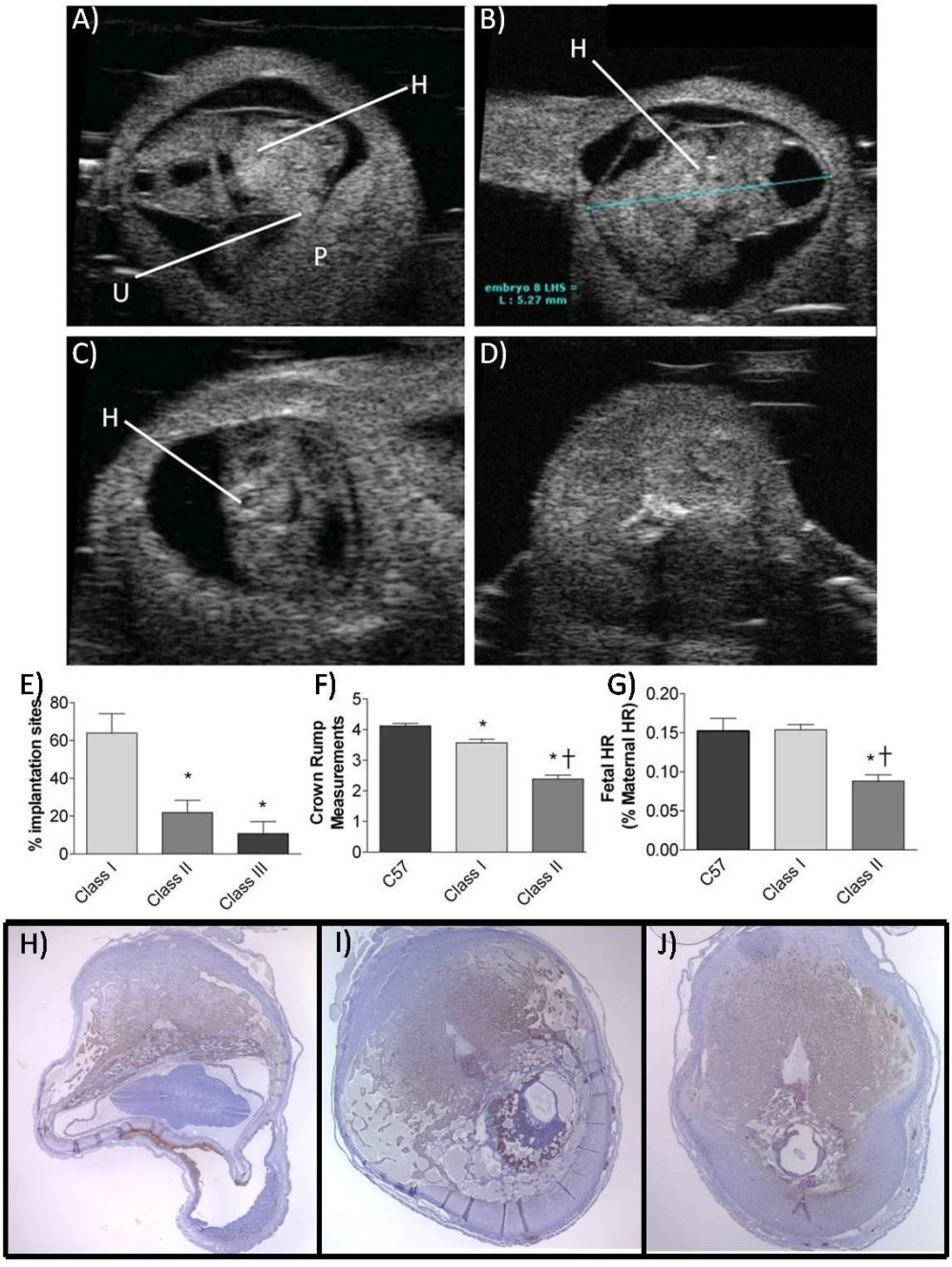
A)
H
P
U
B)
H
embryo 8 LHS =
L : 5.27 mm
C)
H
D)
E)
% implantation sites
80
60
40
20
0
*
*
Class I
Class II
Class III
F)
Crown Rump Measurements
5
4
3
2
1
0
*
*†
C57
Class I
Class II
G)
Fetal HR (% Maternal HR)
0.20
0.15
0.10
0.05
0.00
*†
C57
Class I
Class II
H)
I)
J)

and only a decidual response with a few scattered giant cells.

Scored fetoplacental units show unique genetic profiles. As three distinct classes of BPH/5 embryos are apparent at e10.5, gene expression microarray analysis was performed in these classes compared to C57 controls. The entire fetoplacental unit was used to remain consistent among all classes; as there is no embryo/placental development in Class III, we examined the entire implantation site including embryo, placenta and associated uterine tissue.

We performed a genome-wide expression study and identified 808, 1901 and 777 dysregulated genes in Class I, II and III, respectively, with the criteria of $p < 0.05$ and a fold-change greater than 1.5 compared to C57 controls (false discovery rate of less than 5%). The Venn diagram used to compare the expression pattern of all classes (Figure 3.2) showed that 287 genes were unique in Class I, 1098 genes were unique in Class II and only 104 genes were unique in Class III. A total of 275 genes were common in all three classes.

Microarray data validation with Quantitative Real Time RT-PCR. To validate the microarray expression profile, we performed real-time reverse transcription PCR for 16 genes, of which 9 are up-regulated and 7 down-regulated identified by microarray (Table 3.2). Validation confirmed the directionality of gene expression with slight differences in expression magnitude reflective of the difference between sensitivity of real time PCR with microarray[27].

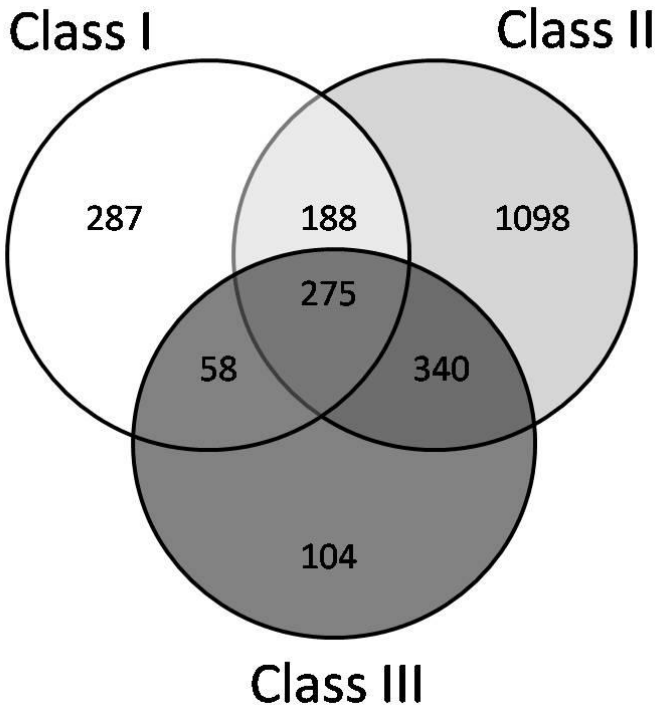

<u>Figure 3.2</u>: Microarray analysis revealed differential dysregulation of genes in BPH/5 fetoplacental units from each of the three embryonic health classes compared to C57 controls. Venn diagram summarizing the number of dysregulated mRNAs unique to each class and shared between Class I,II, and III. All genes considered have greater than 1.5-fold change difference from C57 fetoplacental controls, n=3, $p<0.05$ vs C57.

Table 3.2: Validation of microarray data from classed fetoplacental units with real time PCR

		Class I		Class II		Class III	
Gene Accession Number	**Gene Symbol**	**Microarray**	**Real Time PCR**	**Microarray**	**Real Time PCR**	**Microarray**	**Real Time PCR**
NM_007423	AFP	-3.1±1.2	-1.1±0.3	-5.1±0.3	-21.6±1.3	-21±2.6	-8.7±0.7
NM_080639	Timp4	-6.3±0.2	-2.0±0.1	-9.5±0.7	-15.2±0.8	-10.2±1.5	-6.1±1.0
NM_130458	SP7	-5.5±0.3	-1.5±0.4	-3.6±0.8	-7.9±0.6	-2.8±0.6	-2.5±0.4
NM_009829	Ccnd2	-1.8±0.7	-1.7±0.1	-2.4±0.3	-2.7±0.7	-3.1±0.5	-2.1±0.4
NM_011581	Thbs2	2.2±0.6	2.7±0.5	3.4±0.8	9.8±0.6	3.8±1.0	8.5±1.1
NM_008764	TNFRSF11B	2.4±0.6	8.0±0.6	4.4±0.6	9.3±0.5	4.0±0.9	12.3±0.3
NM_016687	Sfrp4	2.1±0.4	3.9±0.2	3.0±0.3	9.3±0.8	2.6±0.4	6.9±0.3
NM_007400	Adam12	2.1±0.5	6.0±0.5	3.2±0.4	6.9±2.0	2.7±0.3	6.0±0.5
NM_009616	Adam19	3.0±0.3	3.2±1.0	2.6±0.2	3.2±0.5	3.1±0.5	2.8±0.6
NM_007610	Casp2	-2.4±0.4	-1.6±0.04	-3.3±0.4	-2.8±0.2	-2.6±0.6	-2.1±0.2
NM_001025602	Il1rl1	-5.4±0.2	-7.1±0.02	-5.1±0.7	-9.7±0.02	-4.8±0.9	-8.5±0.08
NM_013566	Itgb7	2.4±0.3	5.9±1.2	2.1±0.5	4.9±0.8	2.7±0.6	4.9±1.0
NM_016674	Cldn1	3.1±0.2	6.7±2.0	3.2±0.5	5.9±1.1	3.6±0.7	8.1±2.0
NM_010555	Il1r2	3.7±0.2	4.7±1.2	7.1±1.0	7.8±0.7	6.5±1.4	7.5±0.7
NM_023680	Tnfrsf22	-2.7±0.5	-1.8±0.4	-2.4±0.4	-1.7±0.2	-2.0±0.4	-1.4±0.3
NM_011782	Adamts5	2.6±0.3	4.0±0.4	4.8±0.2	4.9±0.3	4.3±0.5	5.4±1.7
NM_007631	Ccnd1	-1.3±0.4	-2.5±0.4	-2.4±0.4	-5.5±0.2	-2.5±0.6	-6.1±0.2

Values are given as fold change vs C57 ± SEM. Negative values denote down regulated genes.

Gene Ontology analysis reveals common dysregulated pathways in classed BPH/5 fetoplacental units. To further analyze the data gathered by microarray, we performed gene ontology (GO) analysis using DAVID (Database for Annotation, Visualization and Integrated Discovery) to investigate how these dysregulated genes were classified into biological or physiological processes. Functional annotation clustering analysis was performed on all genes in Class I, Class II, Class III separately, as well as common genes shared in all classes. The GO analysis of the three functional groups with the highest enrichment scores are presented in Table 3.3, with selected genes from within those functional groups listed. Class I BPH/5 fetoplacental units show dysregulation in cell adhesion, development (predominantly bone development) and extracellular matrix organization (Table 3.3). In Class II, the biological processes with a markedly increased enrichment score include angiogenesis and blood vessel development, apoptosis and development. Finally, in Class III, the profile of biological processes resembles Class II with clusters in the processes of angiogenesis, apoptosis and embryonic development. Finally, the functional group analysis for genes common to all three classes show dysregulation in pathways involved in response to reactive oxygen species, extracellular matrix organization and apoptosis.

Gene network analysis-IPA analysis. An alternative method of examining the functional significance of dysregulated genes is to examine their function and grouping in Ingenuity Pathway Analysis, where genes are grouped into functional or disease-associated pathways. The top functional pathways generated from the unique genes dysregulated in each class are represented in panel A-C of Figure 3.3. The height of each bar graphs shows the significant degree of dysregulation of that

Table 3.3: GO analysis of classed fetoplacental units using DAVID software.

BPH/5 Class	Functional group ; Cluster	Enrichment score	Selected Genes
I	Cell adhesion ; cell-substrate adhesion, cell-matrix adhesion, integrin-mediated signaling pathway	2.74	CTGF, NPNT, ITGB7, ITGB5, ITGB3, ITGB1, ITGBL1, ADAM17, ADAMTS1, ADAM19,ADAMTS2
I	Development ; bone development, skeletal system development, ossification, cartilage development	2.25	MMP9, COL5A2, SP7,COL1A1,BMP7, BMP8A,
I	Extracellular Matrix ; extracellular matrix organization, collagen fibril organization, extracellular structure organization	2.03	MMP9, SERPINH1,TGFB2, COL5A2, TNFRSF11B, ADAMTS2,COL11A1,
II	Angiogenesis ;vasculature development, blood vessel development, blood vessel morphogenesis, angiogenesis	5.15	ENG, ANGPT2, ANG2, TGFBR2, LEPR, PEG3, MP14,TNFRSF12A,TGFBR2, FGF2, ANXA2
II	Apoptosis ; apoptosis, programmed cell death, cell death, death	4.90	CASP2, TNFRSF11B, PEG10, NFKB1, PAWR, PDCD4, DAPK1, PDCD6IP, CFLAR, DAP3, ID1, BRE, SIVA1
II	Development; skeletal system development, bone development, ossification, osteoblast differentiation	3.42	BMP4, SP7, BMP2, COL1A1, MMP14, BMP8A, IGF1, IGF2, IGFBP3, IGFBP5
III	Angiogenesis ;vasculature development, blood vessel development, blood vessel morphogenesis, angiogenesis	3.97	FGFR1, TNFRSF12A, LEPR, CTGF, ANGPT2, EPAS1, ANG2, TGFBR2, ANXA2, TNFAIP2
III	Apoptosis ; apoptosis, programmed cell death, cell death, death	3.31	TNFRSF21, TNFRSF11B, CASP2, CFLAR, GADD45G, PERP, PDCD6IP, HAND2
III	Embryonic development ; *in utero* embryonic development, chordate embryonic development, embryonic organ development	2.93	SFRS1, APOB, PRMT1, CCNB2, FGFR1, RUNX1, COL2A1, NCOR2
I,II, III	Response to Reactive Oxygen Species ; response to ROS, response to oxidative stress, response to hydrogen peroxide	2.86	CYP11A1,PRDX6,GPX3,MT1, PRDX2,COL1A1,PRNP,MT4
I, II, III	Extracellular Matrix ;collagen fibril organization, extracellular matrix organization, extracellular structure organization	2.24	COL11A1,ADAMTS2,SERPINH1,COL5 A2,TNFRSF11B
I, II, III	Apoptosis ; cell death, apoptosis, programmed cell death, death	2.13	CFLAR,TNFRSF21,TNFRSF1B,TNFRSF 11B,TNS1,HAND2,TNFAIP8, CASP2

Top three scoring processes are listed for each group, with selected dysregulated genes listed for each functional group.

Figure 3.3: Ingenuity pathways analysis of dysregulated genes in classed BPH/5 fetoplacental units compared to C57 controls. (A-C) Top 15 functional pathways dysregulated in gene sets unique to Class I, II, and III respectively. Numbers above bar graph indicate the number of genes dysregulated in that pathway. D) Network analysis showing Class I embryos have defects in cardiovascular system development and organismal development , (E) Class II fetoplacental units have dysregulation in cell death and embryonic development, (F) Class III fetoplacental units show dysregulation in cardiovascular system development and function, and cell cycle.

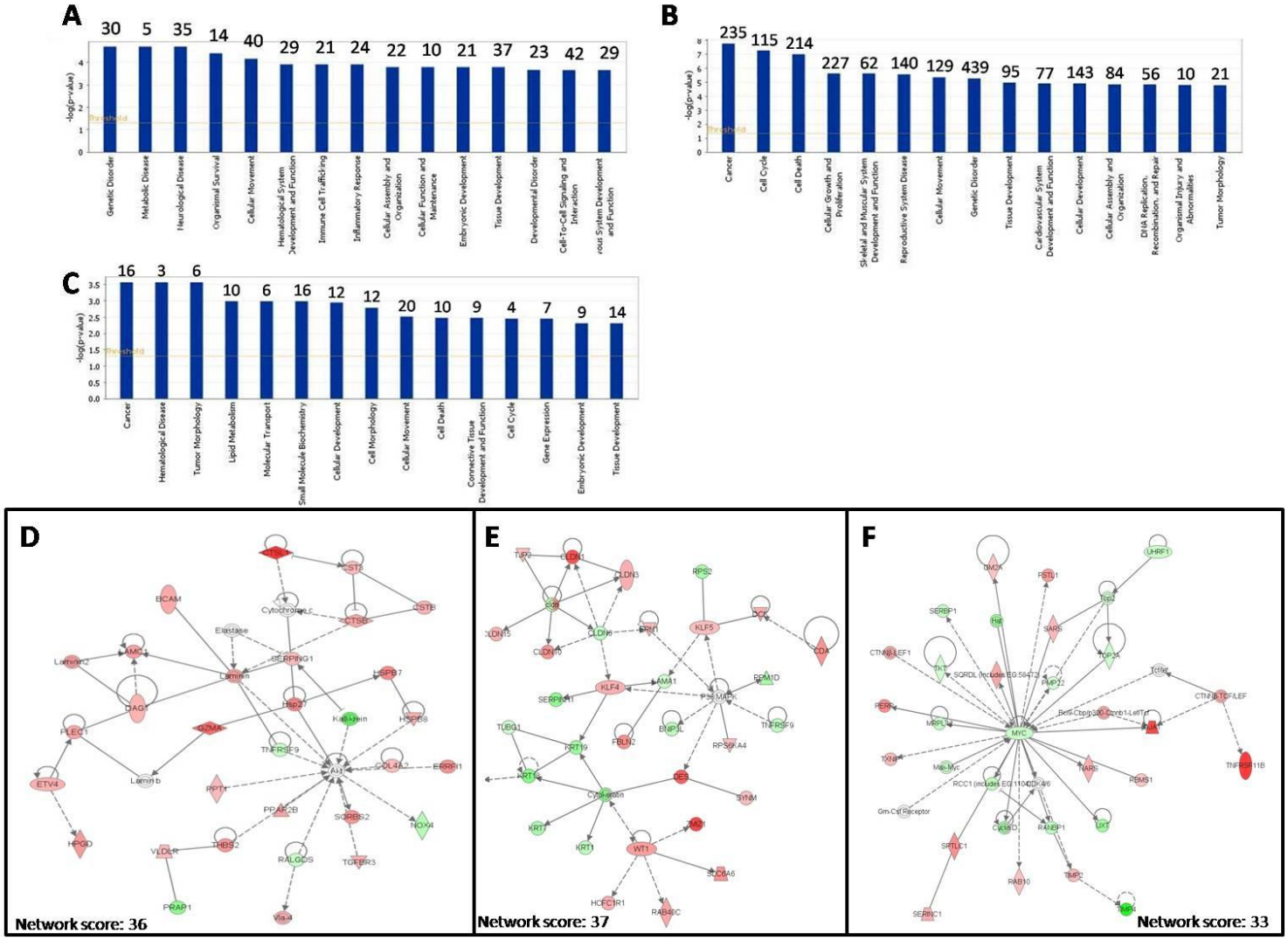
A
30 5 35 14 40 29 21 24 22 10 21 37 23 42 29
-log(p-value)
Genetic Disorder
Metabolic Disease
Neurological Disease
Organismal Survival
Cellular Movement
Hematological System Development and Function
Immune Cell Trafficking
Inflammatory Response
Cellular Assembly and Organization
Cellular Function and Maintenance
Embryonic Development
Tissue Development
Developmental Disorder
Cell-To-Cell Signaling and Interaction
Tissue Development
B
235 115 214 227 62 140 129 439 95 77 143 84 56 10 21
-log(p-value)
Cancer
Cell Cycle
Cell Death
Cellular Growth and Proliferation
Skeletal and Muscular System Development and Function
Reproductive System Disease
Cellular Movement
Genetic Disorder
Tissue Development
Cardiovascular System Development and Function
Cellular Development
Cellular Assembly and Organization
DNA Replication, Recombination, and Repair
Organismal Injury and Abnormalities
Tumor Morphology
C
16 3 6 10 6 16 12 12 20 10 9 4 7 9 14
-log(p-value)
Cancer
Hematological Disease
Tumor Morphology
Lipid Metabolism
Molecular Transport
Small Molecule Biochemistry
Cellular Development
Cell Morphology
Cellular Movement
Cell Death
Connective Tissue Development and Function
Cell Cycle
Gene Expression
Embryonic Development
Tissue Development
D
Network score: 36
E
Network score: 37
F
Network score: 33

pathway as a whole and the numbers above the bar graph show the number of dysregulated genes within each pathway. Additionally, network analysis reveals organismal development, cell death and embryonic development, and cell cycle defects in Class I, II and III respectively (Figure 3.3 D-F).

Imprinted Genes are a subset of dysregulated genes in BPH/5. Imprinted genes are known to be important in early mammalian development. Through the IPA and GO analysis, several imprinted genes emerged. We then sought to characterize these imprinted genes separately. Figure 3.4 illustrates the six dysregulated imprinted genes in the BPH/5 fetoplacental units. Four are paternally imprinted and two are maternally imprinted. As paternally imprinted genes largely determine the placental size and morphology[28], we hypothesized that these genes would be down-regulated in BPH/5 compared to C57. We validated the paternally imprinted genes by real-time PCR (Figure 3.4 panel A-D). True to our prediction, expression of all four paternally imprinted genes were significantly reduced in Class II and III compared to their healthier littermates (Class I), and/or C57 controls.

DISCUSSION

Pre-eclampsia (PE), a pregnancy specific syndrome that affects approximately 10% of pregnancies in the US each year, is characterized by late gestational hypertension and proteinuria (www.pre-eclampsia.org). Early fetal loss complicates anywhere from 10-25% of clinically recognized pregnancies each year (www.americanpregnancy.com). BPH/5, an inbred mouse strain, exhibits the cardinal symptoms of PE during pregnancy, and loses a significant number of pups throughout gestation due to fetal loss [6, 7]. This model provides a unique tool in examining how early pregnancy loss/distress may impact and play a role in the development of PE.

Imprinted Gene	Function	Maternal	Paternal
Igf2	Growth factor		X
Peg 3	Zinc finger transcription factor		X
Slc38a4	Amino acid transporter		X
Dlk-1	Function unknown		X
Dcn	Proteoglycan family	X	
H19	Non-coding RNA	X	

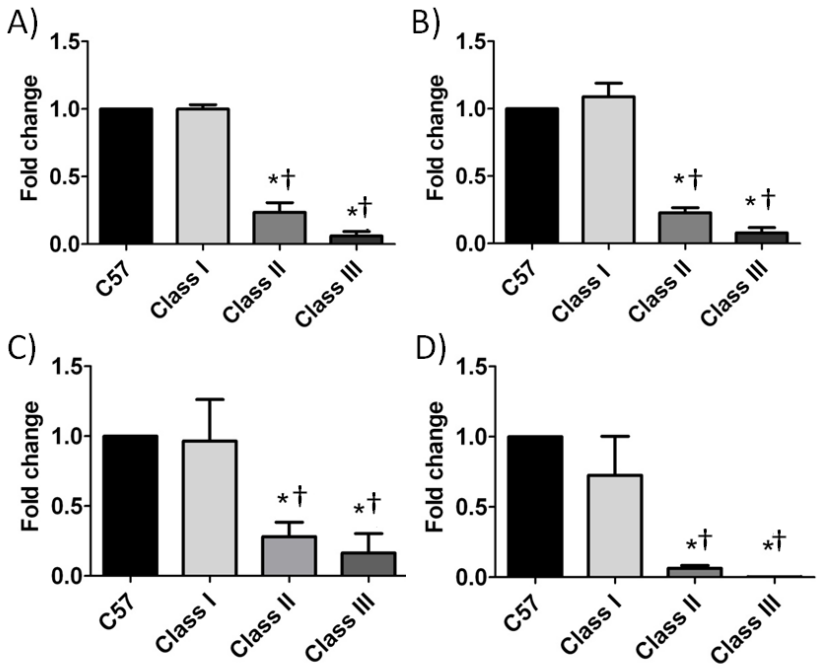

Figure 3.4: **Imprinted genes are among the dysregulated genes in BPH/5 classed fetoplacental units**. Table shows the imprinted genes that were dysregulated in our microarray analysis. Real time validation of paternally imprinted genes shows dysregulation in their expression in Class II and III embryos. Insulin-like growth factor 2 (Igf2, panel A), paternally expressed gene (Peg3, panel B), Slc38a4 (panel C) and delta-like 1 (Dlk-1, panel D) show a significant reduction in Class II and Class III embryos. n=5-6 *$p<0.05$ vs C57 and † $p<0.05$ vs Class I.

Using ultrasound classification, we observed signs of fetal stress apparent at e10.5 in a subset of BPH/5 embryos. Using ultrasound to score these fetoplacental units, microarrays were run comparing the healthiest embryos with their more challenged littermates and also compared to the C57Bl/6 strain, which does not exhibit significant fetoplacental stress. Pathways of angiogenesis, apoptosis and development were among pathways found to be highly dysregulated in fetoplacental units exhibiting developmental challenge in BPH/5.

Previous analysis of viable pups by necropsy revealed that fetal loss in BPH/5 began at e12.5 where resorption sites were first visible [7]. With the advances in high resolution imaging, such as ultra-high frequency ultrasound, structures as small as a murine embryo at e10.5 can be imaged with amazing clarity. We have shown that evidence of fetal demise in BPH/5 can be traced earlier than necropsy data and demonstrate that one third of embryos show significant fetal developmental challenge or delay as early as e10.5. From ultrasound data, we can classify embryos into three classes. The healthiest embryos (Class I), whose developmental status is closest to that of C57 controls, still show signs of IUGR, which has been previously documented in this model using neonatal weights[7]. Class II embryos show severe developmental delay as well as placental pathology characterized by a poor development of the labyrinth and junctional zones. Finally, Class III fetoplacental units show no evidence of placental or fetal development. These classed samples, made possible by ultrahigh frequency ultrasound, provide an excellent starting material for molecular profiling of fetal challenge in this model of PE.

Microarray analysis is a powerful tool to investigate the etiology of disease. In the past decade, over 20 researchers have used microarray technology to investigate the molecular profile of PE placentae in hopes of finding common mechanisms and

perhaps biomarkers. These studies often do not reveal the same results as sample sizes are often very small due to the limitations of human placenta availability from both normal and pre-eclamptic patients[11]. Also, it is becoming more widely recognized that the syndrome of PE can be subdivided into at least two separate pathologies, with an early onset and late onset classification, each with a unique profile and set of complications[1, 10, 29]. It is also known that the pathogenesis of pre-eclampsia begins long before the onset of maternal symptoms[5]. As such human placental samples available from term biopsies provide only the end results of PE and do not shed light on the early events at the onset of disease.

In this study, microarray analysis was used to determine the gene expression profile in fetoplacental units of varying status in the BPH/5 mouse model. Class I fetoplacental units, though they are the healthiest, still show dysregulation in genes involved in extracellular matrix remodeling and cell adhesion. These targets are most likely involved in the invasion and remodeling of the maternal uterine environment. Interestingly, targets found in this study such as COL5A2, COL1A1, ADAMTS2 were also found in a study linking fetal connective tissue defects to preterm birth[30]. Many of these may be targets that lead to shallow placental invasion into the decidua and reduced labyrinth formation characteristic of this model[6]. Class II fetoplacental units show dysregulation in genes involved in embryo development (predominantly bone), angiogenesis and apoptosis. Angiogenic factors have received much interest in the past few decades as both a mechanism behind placental pathologies such as reduced spiral artery remodeling in PE patients[31], and reduced levels have also been examined as a potential screening biomarker of women who go on to develop PE[32]. Previous work in our laboratory has shown a decrease in angiogenic potential that is present prior to the development of the PE symptoms in BPH/5 mice[33], and that increasing circulating levels of the angiogenic factor VEGF resolves many of the symptoms of

PE. Additionally, the area of bone development, a process very sensitive to circulating angiogenic levels, has significant dysregulation in Class I and II fetoplacental units, confirming the effects of our previous findings. Genes involved in apoptosis are also dysregulated in Class II and III embryos as they are probably so challenged that they are likely in the cohort that perish. Finally, Class III embryos again show defects in angiogenesis and apoptosis as well as embryo development. This is not surprising given the profound defects in both embryo and placental development common in this class of fetoplacental units. Several microarray studies have examined the role of hypoxia in gene regulation in the PE placenta[10, 11, 17, 34, 35]. The response to reactive oxygen species is a functional group that is highlighted in genes that are dysregulated in all classes of BPH/5 fetoplacental units, again highlighting the role of hypoxia in this model as it parallels the human studies. Our group has examined the role of reactive oxygen species and showed that the antioxidant Tempol ameliorated many of the PE symptoms in BPH/5 mice[36].

From our microarray work, we found several imprinted genes to be dysregulated in classed fetoplacental units of BPH/5. Imprinted genes are very important in early mammalian development, and are abundantly expressed in the placenta[37-39]. The Kinship theory states that paternally imprinted genes classically govern the size of the placenta in order to maximize the maternal resources acquired for the growing fetus, while the maternal imprinted genes generally conserve maternal resources for all of her current litter as well as future litters[28]. Studies reviewed by Angolioni and colleagues and Tycko and Morison, summarize the fetal and placental data acquired from several mouse knockout models[28, 38]. These knockout mouse models show drastic defects in placental anatomy and size or fetal size, depending on if a maternal or paternal gene is silenced. Additionally, recent studies have examined the role of imprinted genes and have found a significant correlation with altered

expression of imprinted genes in response to maternal underperfusion, a common phenotype of both IUGR and pre-eclampsia[40]. These include PLAGL1, PHLDA2, MEST, MEG3, LEP and IGF1. Interestingly, some linkage studies show the involvement of maternally expressed genes in some families with the occurrence of pre-eclampsia[41]. We hypothesized, given the placental defects in BPH/5, that paternal imprinted genes would be down-regulated, given their importance in placental development. Indeed several paternal genes, many of which have knockout models known, were downregulated in BPH/5 including *Dlk-1*, *Igf2*, *Peg3* and the amino acid transporter *Slc38a4*. Knockout models of these genes show the phenotype of abnormally large fetuses, and small placentae, indicative of the loss of the paternally imprinted stiumulus. Additionally the maternally imprinted genes decorin and H19 were also dysregulated in our model. Decorin, a proteoglycan, was highly upregulated in all of our classes (data not shown). Recently several studies indicate increased decorin expression in the umbilical vessels in pregnancies complicated with pre-eclampsia and have been speculated to alter the mechanics of fetal circulation[42]. Future studies to examine the methylation status of our imprinted genes in this model as well as spatiotemporal expression of these genes throughout the early gestation period would be helpful in characterizing how these genes affect placental development.

Using ultrasound-mediated scoring of implantation sites, we have identified numerous dysregulated pathways that shed light on the causes of fetal demise in our mouse model. It is interesting to speculate how these dysregulated pathways in healthy and compromised embryos contribute to the pathophysiology of PE in this model.

REFERENCES

1. Huppertz B. Placental origins of pre-eclampsia: Challenging the current hypothesis. *Hypertension*. 2008;51:970-975.

2. Cnattingius S, Haglund B, Kramer MS. Differences in late fetal death rates in association with determinants of small for gestational age fetuses: Population based cohort study. *BMJ*. 1998;316:1483-1487.

3. James JL, Whitley GS, Cartwright JE. Pre-eclampsia: Fitting together the placental, immune and cardiovascular pieces. *J Pathol*. 2010;221:363-378.

4. Roberts DJ, Post MD. The placenta in pre-eclampsia and intrauterine growth restriction. *J Clin Pathol*. 2008;61:1254-1260.

5. Roberts JM, Gammill HS. Pre-eclampsia: Recent insights. *Hypertension*. 2005;46:1243-1249.

6. Dokras A, Hoffmann DS, Eastvold JS, Kienzle MF, Gruman LM, Kirby PA, Weiss RM, Davisson RL. Severe feto-placental abnormalities precede the onset of hypertension and proteinuria in a mouse model of pre-eclampsia. *Biol Reprod*. 2006;75:899-907.

7. Davisson RL, Hoffmann DS, Butz GM, Aldape G, Schlager G, Merrill DC, Sethi S, Weiss RM, Bates JN. Discovery of a spontaneous genetic mouse model of pre-eclampsia. *Hypertension*. 2002;39:337-342.

8. Tanaka TS, Jaradat SA, Lim MK, Kargul GJ, Wang X, Grahovac MJ, Pantano S, Sano Y, Piao Y, Nagaraja R, Doi H, Wood WH,3rd, Becker KG, Ko MS. Genome-wide expression profiling of mid-gestation placenta and embryo using a 15,000 mouse developmental cDNA microarray. *Proc Natl Acad Sci U S A.* 2000;97:9127-9132.

9. Sood R, Zehnder JL, Druzin ML, Brown PO. Gene expression patterns in human placenta. *Proc Natl Acad Sci U S A.* 2006;103:5478-5483.

10. Sitras V, Paulssen RH, Gronaas H, Leirvik J, Hanssen TA, Vartun A, Acharya G. Differential placental gene expression in severe pre-eclampsia. *Placenta*. 2009;30:424-433.

11. Enquobahrie DA, Meller M, Rice K, Psaty BM, Siscovick DS, Williams MA. Differential placental gene expression in pre-eclampsia. *Am J Obstet Gynecol*. 2008;199:566.e1-566.11.

12. Toft JH, Lian IA, Tarca AL, Erez O, Espinoza J, Eide IP, Bjorge L, Draghici S, Romero R, Austgulen R. Whole-genome microarray and targeted analysis of angiogenesis-regulating gene expression (ENG, FLT1, VEGF, PlGF) in placentas from pre-eclamptic and small-for-gestational-age pregnancies. *J Matern Fetal Neonatal Med*. 2008;21:267-273.

13. Han JY, Kim YS, Cho GJ, Roh GS, Kim HJ, Choi WJ, Paik WY, Rho GJ, Kang SS, Choi WS. Altered gene expression of caspase-10, death receptor-3 and IGFBP-3 in preeclamptic placentas. *Mol Cells*. 2006;22:168-174.

14. Hansson SR, Chen Y, Brodszki J, Chen M, Hernandez-Andrade E, Inman JM, Kozhich OA, Larsson I, Marsal K, Medstrand P, Xiang CC, Brownstein MJ. Gene expression profiling of human placentas from preeclamptic and normotensive pregnancies. *Mol Hum Reprod*. 2006;12:169-179.

15. Nishizawa H, Pryor-Koishi K, Kato T, Kowa H, Kurahashi H, Udagawa Y. Microarray analysis of differentially expressed fetal genes in placental tissue derived from early and late onset severe pre-eclampsia. *Placenta*. 2007;28:487-497.

16. Reimer T, Koczan D, Gerber B, Richter D, Thiesen HJ, Friese K. Microarray analysis of differentially expressed genes in placental tissue of pre-eclampsia: Up-regulation of obesity-related genes. *Mol Hum Reprod*. 2002;8:674-680.

17. Founds SA, Conley YP, Lyons-Weiler JF, Jeyabalan A, Hogge WA, Conrad KP. Altered global gene expression in first trimester placentas of women destined to develop pre-eclampsia. *Placenta*. 2009;30:15-24.

18. Phoon CK. Imaging tools for the developmental biologist: Ultrasound biomicroscopy of mouse embryonic development. *Pediatr Res*. 2006;60:14-21.

19. Ji RP, Phoon CK, Aristizabal O, McGrath KE, Palis J, Turnbull DH. Onset of cardiac function during early mouse embryogenesis coincides with entry of primitive erythroblasts into the embryo proper. *Circ Res*. 2003;92:133-135.

20. Phoon CK, Aristizabal O, Turnbull DH. 40 MHz doppler characterization of umbilical and dorsal aortic blood flow in the early mouse embryo. *Ultrasound Med Biol*. 2000;26:1275-1283.

21. Slevin JC, Byers L, Gertsenstein M, Qu D, Mu J, Sunn N, Kingdom JC, Rossant J, Adamson SL. High resolution ultrasound-guided microinjection for interventional studies of early embryonic and placental development in vivo in mice. *BMC Dev Biol*. 2006;6:10.

22. Mu J, Slevin JC, Qu D, McCormick S, Adamson SL. In vivo quantification of embryonic and placental growth during gestation in mice using micro-ultrasound. *Reprod Biol Endocrinol*. 2008;6:34.

23. Duggan DJ, Bittner M, Chen Y, Meltzer P, Trent JM. Expression profiling using cDNA microarrays. *Nat Genet*. 1999;21:10-14.

24. Livak KJ, Schmittgen TD. Analysis of relative gene expression data using real-time quantitative PCR and the 2(-delta delta C(T)) method. *Methods*. 2001;25:402-408.

25. Da Wei Huang BTS, Lempicki RA. Systematic and integrative analysis of large gene lists using DAVID bioinformatics resources. *Nature protocols*. 2008;4:44-57.

26. Dennis Jr G, Sherman BT, Hosack DA, Yang J, Gao W, Lane HC, Lempicki RA. DAVID: Database for annotation, visualization, and integrated discovery. *Genome Biol*. 2003;4:P3.

27. Wang Y, Barbacioru C, Hyland F, Xiao W, Hunkapiller KL, Blake J, Chan F, Gonzalez C, Zhang L, Samaha RR. Large scale real-time PCR validation on gene expression measurements from two commercial long-oligonucleotide microarrays. *BMC Genomics*. 2006;7:59.

28. Angiolini E, Fowden A, Coan P, Sandovici I, Smith P, Dean W, Burton G, Tycko B, Reik W, Sibley C, Constancia M. Regulation of placental efficiency for nutrient transport by imprinted genes. *Placenta*. 2006;27 Suppl A:S98-102.

29. Roberts JM, Catov JM. Pre-eclampsia more than 1 disease: Or is it? *Hypertension*. 2008;51:989-990.

30. Anum EA, Hill LD, Pandya A, Strauss JF,3rd. Connective tissue and related disorders and preterm birth: Clues to genes contributing to prematurity. *Placenta*. 2009;30:207-215.

31. Khankin EV, Royle C, Karumanchi SA. Placental vasculature in health and disease. *Semin Thromb Hemost*. 2010;36:309-320.

32. Maynard S, Epstein FH, Karumanchi SA. Pre-eclampsia and angiogenic imbalance. *Annu Rev Med*. 2008;59:61-78.

33. Woods AK, Hoffmann DS, Weydert CJ, Butler SD, Zhou Y, Sharma RV, Davisson RL. Adenoviral delivery of VEGF121 early in pregnancy prevents spontaneous development of pre-eclampsia in BPH/5 mice. *Hypertension*. 2010.

34. Soleymanlou N, Jurisica I, Nevo O, Ietta F, Zhang X, Zamudio S, Post M, Caniggia I. Molecular evidence of placental hypoxia in pre-eclampsia. *J Clin Endocrinol Metab*. 2005;90:4299-4308.

35. Lee SB, Wong AP, Kanasaki K, Xu Y, Shenoy VK, McElrath TF, Whitesides GM, Kalluri R. Pre-eclampsia: 2-methoxyestradiol induces cytotrophoblast invasion and vascular development specifically under hypoxic conditions. *Am J Pathol*. 2010;176:710-720.

36. Hoffmann DS, Weydert CJ, Lazartigues E, Kutschke WJ, Kienzle MF, Leach JE, Sharma JA, Sharma RV, Davisson RL. Chronic tempol prevents hypertension, proteinuria, and poor feto-placental outcomes in BPH/5 mouse model of pre-eclampsia. *Hypertension*. 2008;51:1058-1065.

37. Ferguson-Smith AC, Moore T, Detmar J, Lewis A, Hemberger M, Jammes H, Kelsey G, Roberts CT, Jones H, Constancia M. Epigenetics and imprinting of the trophoblast -- a workshop report. *Placenta*. 2006;27 Suppl A:S122-6.

38. Tycko B, Morison IM. Physiological functions of imprinted genes. *J Cell Physiol*. 2002;192:245-258.

39. Isles AR, Holland AJ. Imprinted genes and mother-offspring interactions. *Early Hum Dev*. 2005;81:73-77.

40. Tycko B. Imprinted genes in placental growth and obstetric disorders. *Cytogenet Genome Res*. 2006;113:271-278.

41. Constancia M, Kelsey G, Reik W. Resourceful imprinting. *Nature*. 2004;432:53-57.

42. Gogiel T, Galewska Z, Jaworski S. Pre-eclampsia-associated alterations in wharton's jelly proteoglycans. *Acta Biochim Pol*. 2005;52:501-505.

CHAPTER FOUR:

PERI-IMPLANTATION DEFECTS AND ASYNCHRONOUS MATERNAL-FETAL INTERACTIONS IN A MURINE MODEL OF PRE-ECLAMPSIA, BPH/5

SUMMARY

BPH/5 mice develop the hallmarks of pre-eclampsia (PE), accompanied by placental defects and reduced litter sizes due to progressive fetal loss during gestation. We examined the peri-implantation period to see if placental defects could be traced to a defect at this time. We observed a significant delay in blastocyst development in BPH/5 compared to controls. We then hypothesized that this blastocyst delay in BPH/5 would impact implantation. Pontamine blue perfusions revealed a significant delay in implantation in BPH/5 vs C57Bl/6 controls, with a reduction in the number of implantation sites present at the beginning of the implantation window. Interestingly, later implanting embryos contribute to a clustering defect in BPH/5. Whereas C57 embryos were evenly spaced along the uterine horns, BPH/5 embryos were often crowded/clustered. To examine maternal-fetal interactions during implantation, reciprocal embryo transfers were used. Interestingly, clustering was only observed when BPH/5 embryos were placed in BPH/5 recipients. We next characterized the maternal endocrine profile and showed premature estrogen and progesterone signaling in BPH/5. To coordinate implantation events in BPH/5 the delayed implantation model was used. Using this model, embryo clustering was nearly completely resolved in BPH/5, suggesting a link between embryo maturation and maternal endocrine signaling and implantation defects observed in BPH/5. Additionally, synchronizing implantation had significant effects on placentation in this model. In summary, BPH/5 exhibit marked abnormalities in early gestational processes.

INTRODUCTION

The initiation of pregnancy and the implantation process is a highly intricate and coordinated set of maternal and fetal events. For implantation to occur, the uterus must be in a receptive phase, governed by the endocrine signaling of ovarian steroids estrogen and progesterone [1-3]. This timeframe has been coined the "window of receptivity." Additionally, the embryo must have reached the blastocyst stage and be activated for the crosstalk between the mature blastocyst and luminal epithelium of the uterus to occur [1, 4]. Several key growth factors, cytokines, homeotic genes, vasoactive factors and developmental genes are involved in the processes of embryo-uterine apposition, implantation and the initiation of the decidualization process (reviewed in Dey, 2004[2]). Although significant progress has been made toward understanding these early processes, further studies are needed to improve problems of infertility, pregnancy initiation and pregnancy loss.

The precise synchronization of embryo readiness and the "window of receptivity" is critical in pregnancy success and fetal heath. Wilcox and colleagues examined the rate of pregnancy success and the timing of implantation in the "window of implantation" and found an exponential increase in fetal loss when embryos implant even 24 hours outside the optimal implantation window [5]. This has significant repercussions for both naturally conceived pregnancies and many of the pregnancies that make use of assisted reproductive technologies (ART). ART pregnancies, specifically *in vitro* fertilization (IVF), involve coordinating the events from fertilization through to implantation artificially. As such, synchronization is key to the success of these pregnancies. Pregnancies initiated by ART require close monitoring as these pregnancies are often high risk, with increased rates of adverse maternal, fetal and placental outcomes. Historically, these complications were thought to be linked to

the increased rate of multiple pregnancies in ART [6], though the trends are holding true for singleton pregnancies as well[7]. Many pregnancies initiated by IVF show increased risk of preterm birth, low birth-weight fetuses, as well as increased placental abruption, placenta previa and an increased risk of pre-eclampsia (PE)[7-9]. As these pregnancies are initiated and implantation is coordinated artificially, these outcomes highlight the importance of the peri-implantation period in successful pregnancy outcomes.

One of the pregnancy outcomes that that is significantly increased in IVF pregnancies is the incidence of PE . PE is a pregnancy associated disorder that affects approximately 10% of pregnancies and is the leading cause of fetal and maternal deaths worldwide [10, 11]. It is characterized by new onset hypertension and proteinuria present during the third trimester. It has long been known as a disease that is closely tied to the placenta since. The symptoms resolve when the fetus, and more importantly, the placenta, are delivered. In addition, molar pregnancies, where the placenta is present but an embryo is absent, have been associated with PE, which links this organ to the etiology of the syndrome[12, 13]. Many of the placental defects present in PE pregnancies include shallow placental invasion and reduced spiral artery remodeling[10], both of which are linked to defects in cells from a single lineage, the trophoblast cells[14, 15]. As such, it has been argued that defects in placentation can be traced back to the establishment and activation of this important cell type. This sets the initiation of this pathological cascade to the peri-implantation period, a time frame far earlier than had been previously considered[16].

Studying a disease of human placentation such as PE is very difficult without the use of animal models. This is particularly true now as the focus of pathophysiological hypotheses is moving earlier and earlier to the peri-implantation period[16], when biomarkers and placental specimens are unattainable in human

pregnancies. BPH/5 is an inbred mouse strain that spontaneously exhibits the cardinal symptoms of PE during pregnancy [17]. This strain also has many of the placental phenotypes associated with the human disease, including reduced spiral artery remodeling and shallow trophoblast invasion[18], which begins before onset of maternal symptoms. Additionally, fetal demise and small pups also characterize this strain[17, 18]. As this model recapitulates many features of the human disease, including poor fetoplacental outcomes, BPH/5 mice provide a unique opportunity to examine the role of the peri-implantation period. We hypothesize that there are significant defects within the peri-implantation period, and that some of these defects may be causally linked to the placental defects observed in this model.

METHODS

Animals and Husbandry. Experiments were performed in 8-12 wk old BPH/5 and control C57Bl/6 (C57), 129, Balb/c, BPH/2 and BPN/3 mice obtained from in-house colonies. Animals were housed and maintained as previously described[17]. BPH/5 is an inbred strain derived from the spontaneously hypertensive BPH/2 strain, which was originally established through an eight-way cross that included C57Bl/6, 129 and Balb/c[17, 19]. Mice underwent strain-matched mating and presence of a vaginal plug in the morning was defined as gestational day e0.5[17]. All animal procedures were approved by the Institutional Animal Care and Use Committees at Cornell University, and are in accordance with the PHS Guide for the Care and Use of Laboratory Animals, USDA regulations and the AUMA panel on Euthanasia.

Early embryo isolation and culture. Embryos from e3.5 pregnant mice were flushed from the uterus in specialized media containing IMDM (Gibco),15% FBS, non-essential amino acids, β-mercaptoethanol, glutamine and penicillin-streptomycin.

Embryos were staged and then cultured individually in 48 well plates using complete media containing DMEM (Gibco), 15% FBS, non-essential amino acids, sodium pyruvate, penicillin-streptomycin and β-mercaptoethanol. Embryos were photographed and staged for 5 days. Embryos were classified as morula, blastocyst, hatched, plated (outgrowth present on the bottom of the dish), or dead.

Oocyte isolation and culture. Fertilized oocytes were collected from the oviduct from e0.5 pregnant mice. Eggs were dissociated from cumulus cells using standard hyaluronidase enzyme digestion (Sigma). Oocytes cultured individually in KSOM media (Millipore) for 5 days. Embryos were photographed and staged daily. Embryos were classified as fertilized, 2cell, 4cell, morula, blastocyst, or dead.

Pontamine blue perfusion. A single injection of 100µl of 0.1% pontamine blue (BDH) dissolved in saline was administered via tail vein injection into pregnant mice at e5.5 or where otherwise noted. After ten minutes, mice were euthanized via CO_2 asphyxiation and the uterus was dissected, fixed in 4% paraformaldehyde for 24 hours, and photographed. Clusters were defined as embryos that were spaced less than one embryo width apart from each other. For time course experiments, pontamine blue perfusions were carried out at 0 00h e4.5, 7 00h e4.5, 19 00h e4.5 and 10 00h e5.5.

Histology and morphometric analyses. Whole implantation sites including embryos at e5.5 were excised, fixed in 10% neutral buffered formalin, and embedded in paraffin using standard procedures. The entire implantation site was serially sectioned at 5µm, mounted on slides, and stained with H&E using standard protocols. Analyses were carried out on the sections in which the embryo area was greatest. Quantification

of the area of the embryo, the area of decidualization, and the length of the embryo to the antimesometrial pole was measured using Image J software (version 1.33, NIH).

Additional morphometric analyses were carried out on e12.5 fetoplacental units. Samples were isolated and processed as stated above. Sections were stained using isolectin B4 staining as previously described [18]. Implantation depth was analyzed using Image J software (version 1.33, NIH) as previously described [18].

***Embryo transfer studies*.** Embryo transfer experiments were carried out using standard procedures. Donor female mice from C57 and BPH/5 strains were mated and embryos were isolated at e3.5 as above. Alongside donor mice, recipient mice were mated with vasectomized males to initiated pseudopregnancy. Recipient females were anaesthetized at e2.5 using ketamine (100mg/kg) and xylazine (10mg/kg) and two small dorsal incisions were made to exteriorize the distal uterine horns. Eight to ten donor embryos were injected per uterine horn. Mice were allowed to recover and pontamine blue studies were carried out as above at e5.5 of pseudopregnancy.

Blood collection and endocrine assays. Blood was collected for endocrine measures via cardiac puncture at 7 00h and 19 00h for a time course beginning at e1.5 at 19 00h through e4.5 at 7 00h. Blood was left at room temperature to clot for 90 minutes prior to centrifugation at 3500 RPM for 20 minutes. Serum was immediately frozen at -80ºC. An estrogen ELISA (Calbiotech) was performed according to manufacturer's instructions. The sensitivity of this assay is 3pg/mL. Progesterone levels were measured by RIA at the Ligand Assay and Analysis Core Laboratory at the University of Virginia. The sensitivity of this assay is 0.05ng/mL

Delayed implantation studies. Ovariectomies were performed on the afternoon of e2.5 in pregnant C57 and BPH/5 mice. Mice were anaesthetized with ketamine (100mg/kg) and xylazine (10mg/kg) and dorsal incisions were made to exteriorize and remove the ovaries. After recovery, mice received daily subcutaneous injections of progesterone (P4) (Watson) at a dose of 1mg/mouse. To initiate implantation, estrogen (25ng/mouse, Sigma) was injected subcutaneously. Mice then received daily progesterone injections until the time of sample collection. All hormones were dissolved in sesame oil (Sigma).

Quantitative Real time PCR. Entire implantation sites, including uterine tissue and embryo, were dissected from clustered and spaced embryos from BPH/5 and C57 samples at e5.5, or the equivalent gestation day for delayed implantation mice. RNA was extracted using a standard Trizol method and total RNA content quantified by spectrophotometry. Several candidate genes were assayed based on their importance in developmental processes. For a complete list of target genes and primers, see Table 4.1. Quantitation of gene expression levels were performed by amplification of cDNA (equivalent to 25 ng input RNA) using SYBR Green (Quanta) and primers specific to each gene. Primers were designed and validated using Primer Quest software (IDT). All primers were purchased from integrated DNA technologies (IDT) (see Table 4.1 for primer sequences). Samples were subjected to forty cycles of PCR (50°, 2 min; 95°, 10 min; 40X [95°, 0:15 min; 60°, 1 min]) followed by a dissociation protocol. Each sample was run in duplicate and gene expression was analyzed using the ddCt method. mRNA levels were normalized to *β-actin* (to generate dCt) and compared to respective C57 controls, either by natural mating or delayed implantation model (to generate ddCt). Sequence-specific amplification was confirmed by a single peak during the dissociation protocol following amplification.

***Ultrasound assessment of fetal health*.** Pregnant mice at e12.5 were anaesthetized using 2%isofluorane. The Vevo 770 ultrahigh frequency ultrasound was used to examine fetal health (Visualsonics). A ventral incision was made to exteriorize the uterus and examine individual implantation sites using a 40MHz probe. Body temperature of the pregnant females was maintained and monitored throughout the recording procedure. Fetal heart rates were measured and reported as a ratio of fetal heart rate to maternal heart rate to control for minor variations in anesthetic efficacy. Umbilical blood flow was measured using Doppler measurements of the umbilical vessels. After recording, the pregnant mice were euthanized via cervical dislocation and implantation sites were dissected and fixed for histological examination as stated above.

Statistical Analyses. All data are expressed as mean ± SEM ANOVA followed by Newman-Keuls test for significance was performed for all data sets. $p<0.05$ was considered statistically significant.

RESULTS

BPH/5 embryo show marked pre-implantation embryo maturation delay. Previous studies in the BPH/5 mice show marked placental defects and evidence of fetal demise starting as early as e9.5 of gestation [18] (also Chapter 3). We postulated that these abnormalities could have their origin in the peri-implantation period. We first sought to examine the pre-implantation embryos from both mouse strains. Whereas C57 control embryos flushed from the uterus at e3.5 (referred to as Day 1) were at the expected blastocyst stage [20], embryos isolated from BPH/5 mice at this time point were predominantly at the morula stage or younger (see Figure 4.1A for C57 and B for BPH/5). On Day 1, approximately 85% of embryos in C57 were in the

Table 4.1: Primer sequences for genes in early developmental processes.

Gene	Peri-Implantation Function	Primer Sequence
Areg	Growth factor in uterine epithelium	5’ TCT GCC ATC ATC CTC GCA GCT ATT 3’
		5’CGG TGT GGC TTG GCA ATG ATT CAA 3’
Bmp2	Developmental gene involved in decidualization	5’TGT GGG CCC TCA TAA AGA AGC AGA 3’
		5’AGC AAG CTG ACAGGT CAG AGA ACA 3’
CB1	GPCR on blastocyst surface	5’CCA CTG TGC AGT TGC TGT TTC CTT 3’
		5’ TTG GCC ATC GAG GCC TGA AAT CTA 3’
c-Myc	Gene highly expressed in activated blastocysts	5’ ACT TAC AAT CTG CGA GCC AGG ACA 3’
		5’ GCC CAA AGG AAA TCC AGC CTT CAA 3’
Cyclin B	Cell cycle mediator in maintenance of mitotic cell cycle	5’TGT GTG TGA ACC AGA GGT GGA ACT 3’
		5’ AGA TGT TTC CAT CGG GCT TGG AGA3’
Cyclin D3	Cell cycle mediator in decidualizing stromal cells	5’AAA CAG ATG TCC TGC AGC GAG AGA3’
		5’ TTC TGG AAG GTC TTG CTG GTC CAT 3’
Fkbp52	Immunophilin in uterine stroma	5’AGC TGG AGC AGA GCA ACA TAG TGA3’
		5’TCA GGT GAC ACA TGG CCA GAT TGA 3’
Hegfl	Growth factor in early recognition of uterus to attaching blastocyst	5’TTA TCC TGC TGT TCT TCG GGT GCT 3’
		5’ TCA ACT CCA AAG CTC CCT GCT CTT 3’
Hoxa-10	Transcription factor in uterine stroma	5’TTA GCT AAA GGG CTT GAC CTG GCT 3’
		5’AGA GAG GTT TCC TTC TCT TGC CCA 3’
Lif	Cytokine in uterine glands and stroma surrounding implanting blastocyst	5’TCA GCG ACA AAG TTA CTC CAC CGT 3’
		5’AAG TGA TGA CAA AGC CCA ACA GGC3’
Ptgs1	Murine Cox1, vasoactive factor in luminal epithelium and glands of uterus	5’CTT TGC ACA ACA CTT CAC CCA CCA 3’
		5’TTG AAG AGC CGC AGG TGA TAC TGT 3’
Ptgs2	Murine Cox2, vasoactive factor in luminal epithelium of uterus	5’ACT GGG CCA TGG AGT GGA CTT AAA 3’
		5’AAC TGC AGG TTC TCA GGG ATG TGA 3’
Wnt3a	Developmental gene activated during blastocyst maturity	5’ATG CCT CAG AGA TGT TGC CTC ACT 3’
		5’ TCA GAT GGG TCC TGA AAC AAC CCT 3’
Wnt4	Developmental gene involved in decidualization	5’GCA GAT GTG CAA ACG GAA CCT TGA 3’
		5’ACA CCT GCT GAA GAG ATG GCG TAT 3’
β-actin	Housekeeping gene	5’ CAT CCT CTT CCT CCC TGG AGA AGA 3'
		5’ACA GGA TTC CAT ACC CAA GAA GGA AGG3’

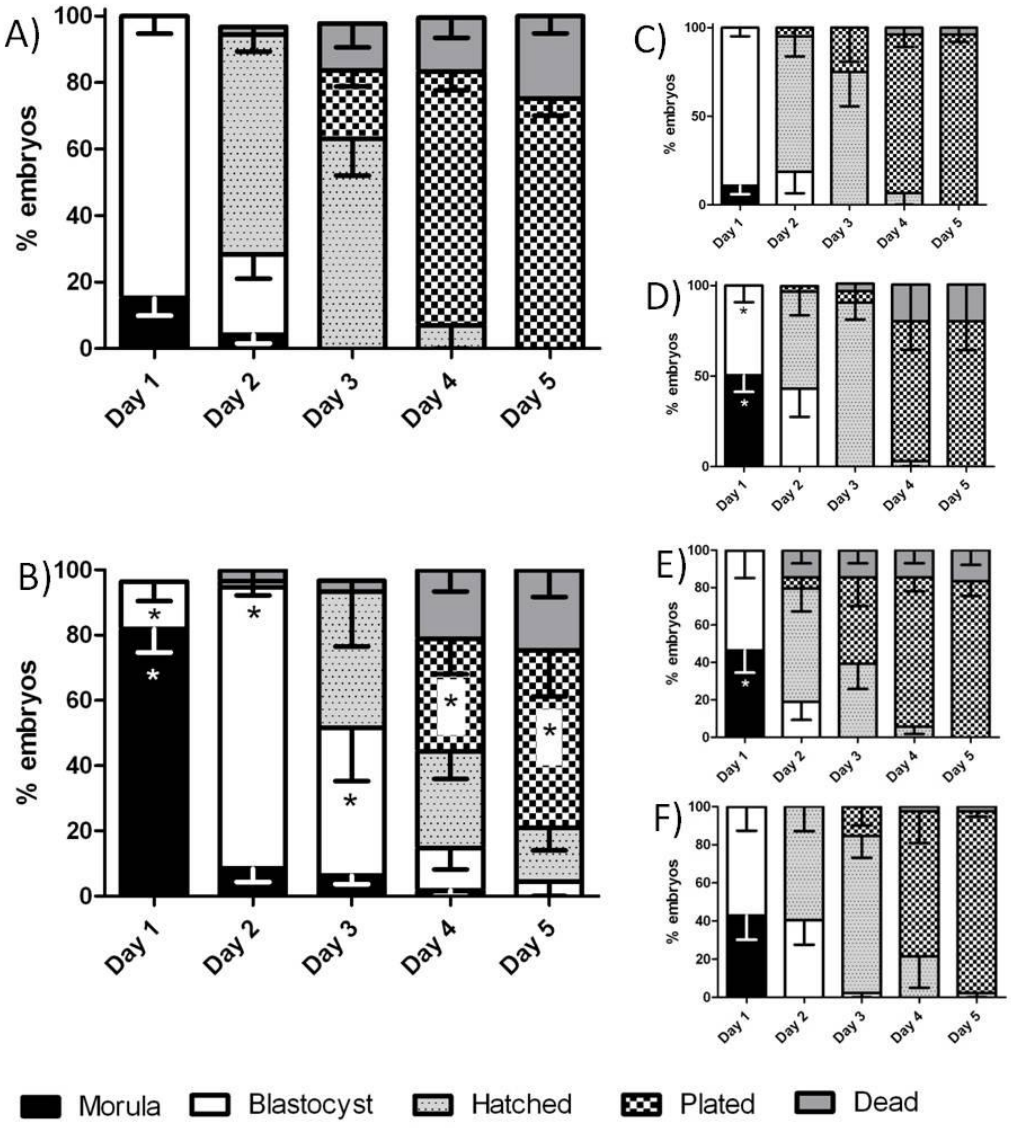

<u>Figure 4.1</u>: BPH/5 embryos show delayed pre-implantation and slowed *in vitro* embryo maturation kinetics compared to related strains. Summary of percentages of embryos at various stages when cultured *in vitro* for 5 days after e3.5 isolation. C57 (A) and BPH/5 (B) are shown along with related parental strains 129 (C), Balb/c (D), BPH/2 (E), and BPN/3 (F). n=5-7 litters per strain. *p<0.05 vs C57 stage- and day-matched control.

blastocyst stage, where inner cell mass and trophoblast lineages are first segregated. This is in contrast to Day 1 of BPH/5 isolation, were 82% of embryos were still in the morula stage, where cells destined for trophoblast and inner cell mass fates have not segregated. To determine the maturation kinetics of these strains, we cultured these embryos *in vitro* for five days. By the second day in culture, 66% C57 embryos had begun to hatch while the BPH/5 population was only just reaching the blastocyst stage. This significant delay in BPH/5 embryo maturation continued throughout the culturing period, with the BPH/5 embryos showing a ~24 hour delay compared to their C57 counterparts. In order to rule out simple strain differences, BPH/5 parental strains 129 and Balb/c were characterized as these strains were part of the original 8-way cross in establishing the BPH sublines[17, 19]. We also examined the closely related BPH/2 (the high blood pressure related strain from which BPH/5 was derived as a subline) and BPN/3 (normotensive subline from the original 8way cross) strains (Figure 4.1 C-F, respectively)[19]. Interestingly, while Balb/c and BPH/2 strains showed a significant morula population the first day of isolation (Figure 4.1D and E), the kinetics soon resolved to mature at a rate similar to C57 controls. BPH/5 was the only strain to show such a sustained and significant delay.

BPH/5 embryos do not show maturation defect at the fertilization step. As a significant delay was found in embryos isolated at e3.5, we wanted to rule out a deficiency in oocyte integrity. A similar strategy was adopted as the previous studies, where fertilized oocytes were isolated from the oviduct at e0.5 and cultured *in vitro* for five days. There were no differences in the number of oocytes ovulated between BPH/5 and C57 control mice (Figure 4.2 A). Furthermore, there was no significant difference in the progression from fertilized oocyte to the two- cell stage between the strains (Figure 4.2B and C), with only 20% of BPH/5 oocytes remaining in the single

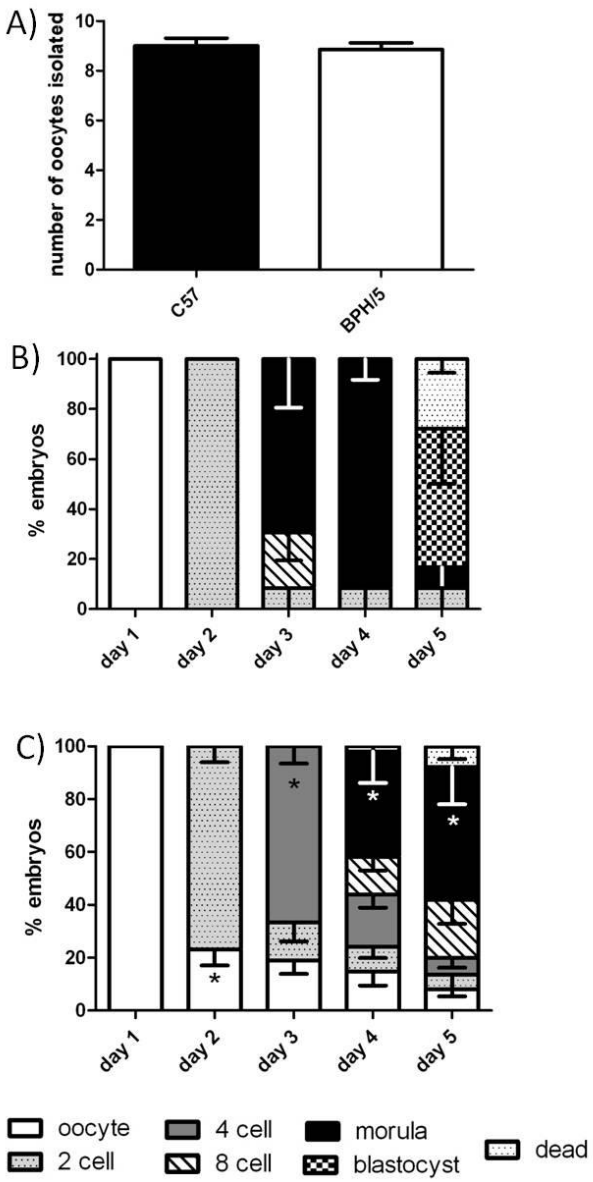

<u>Figure 4.2:</u> BPH/5 fertilized embryos progress to the 2 cell stage at a similar rate to C57 controls. Summary of number of fertilized oocytes isolated from each strain (A). Summary of staged fertilized embryos from C57 (B) and BPH/5 (C) cultured *in vitro* for 5 days post e0.5 isolation. n=4-5 litters per strain*$p<0.05$ vs C57 stage- and day-matched control.

cell stage on Day 2. The more marked embryo maturation delay in BPH/5 seems to originate in the progression from the 4 to 8-cell stage. This is where the BPH/5 delay starts and leads to differences observed in Figure 4.1.

BPH/5 exhibit embryo clustering. We have demonstrated in the above data sets significant pre-implantation maturation delay in BPH/5 embryos compared to C57 controls. We hypothesized that these pre-implantation defects may translate to defects in the implantation process *in vivo*. To test this, we examined implantation sites at e5.5 using the pontamine blue perfusion method. This method allows for the detection of early implantation sites along the uterine horn where the uterine decidualization reaction causes the blue dye to be trapped in the tissue, facilitating imaging and quantification of these sites. Figure 4.3A and B show representative photomicrographs of uteri from C57 and BPH/5 mice, respectively. C57 show even spacing between embryos along both uterine horns, which is consistent with what has been reported previously for this strain [21]. In contrast, BPH/5 show a marked implantation site spacing defect (Figure 4.3B and inset). Although the number of implantation sites is similar between the strains (Figure 4.3C), summary data presented in Figure 4.3D reveal that BPH/5 embryos implant in a clustered arrangement nearly 40% of the time. Embryo clustering is extremely rare in C57 controls (Figure 4.3D).

As we established a significant delay in BPH/5 embryo maturation *in vitro* (Figure 4.1), we decided to perform a more detailed examination of the window of implantation kinetics *in vivo* by performing a time-course beginning at e3.5 midnight through to the morning of e5.5. As seen in Figure 4.3E, BPH/5 showed a significant reduction in the number of implantation sites present at the beginning of the window

Figure 4.3: BPH/5 exhibit increased clustering/crowding of implantation sites. Representative Pontamine blue stained uteri of C57 (A) and BPH/5 (B) with inset at higher magnification and arrows indicating implantation sites. Summary showing the total number of implantation sites (C), and the percentage of embryos observed in a cluster at e5.5 (D). Summary of the implantation time-course reflecting the number of implantation sites (E) and the percentage of embryos in a cluster (F) during several stages within the window of implantation. Summary data of the percentage of embryos in a cluster across closely strains closely related to BPH/5, BPH/2 and BPN/3 (G). n=5-6, *$p<0.05$ vs C57.

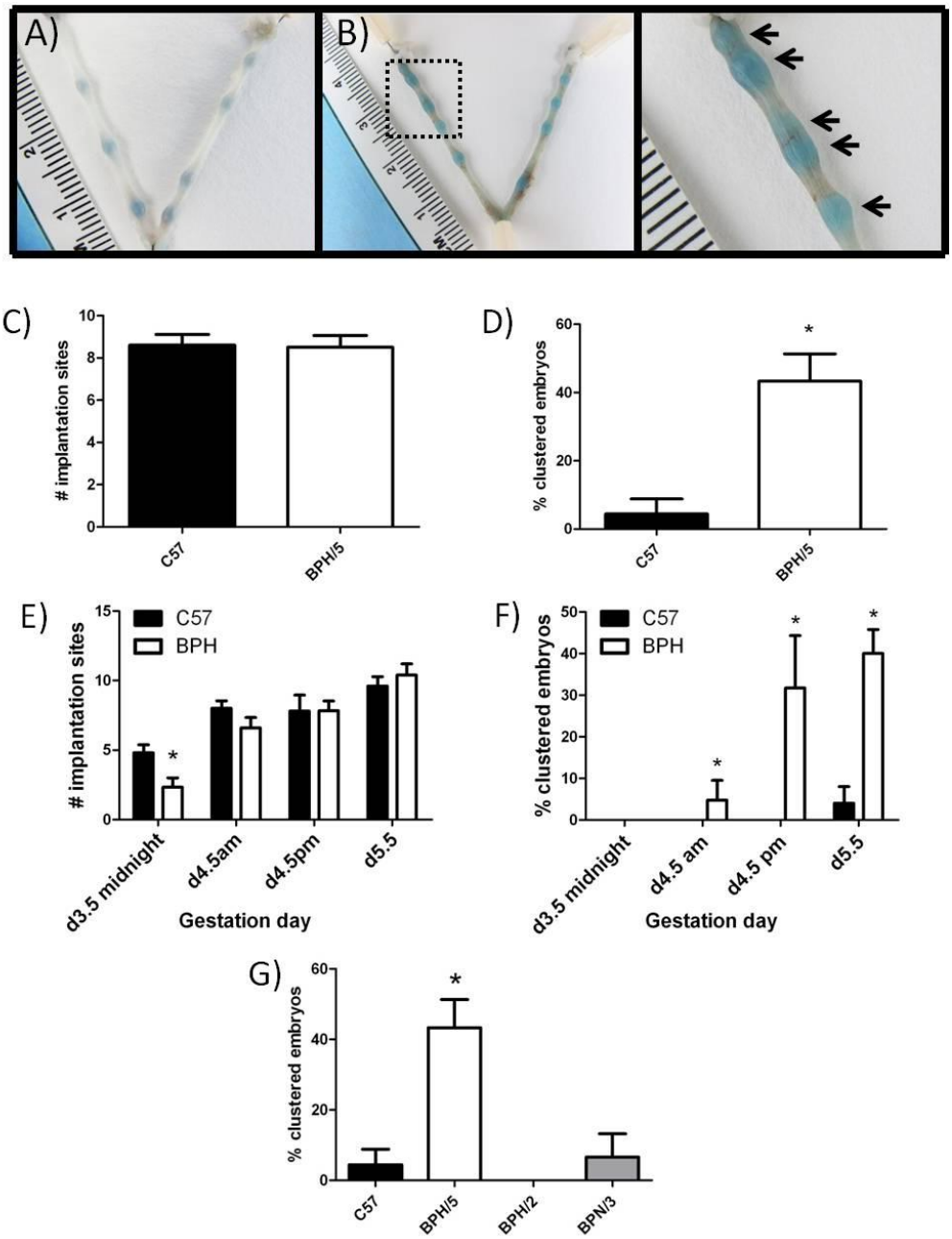
A)
B)
C)
implantation sites
C57
BPH/5
D)
% clustered embryos
C57
BPH/5
E)
C57
BPH
implantation sites
d3.5 midnight
d4.5am
d4.5pm
d5.5
Gestation day
F)
C57
BPH
% clustered embryos
d3.5 midnight
d4.5 am
d4.5 pm
d5.5
Gestation day
G)
% clustered embryos
C57
BPH/5
BPH/2
BPN/3

of implantation (Figure 4.3E). This delay is resolved by the beginning e4.5am measurement, and both strains' implantation rates remain similar through to the end of the implantation window. Interestingly, the embryos that implant later during the implantation window are more likely to be in a cluster (Figure 4.3F). Pontamine blue perfusions were also carried out in the closely related BPN/3 and BPH/2 strains, where no clustering of implantation sites was observed (Figure 4.3G), again suggesting that these peri-implantation defects are unique to BPH/5.

Morphometric analysis reveals abnormalities in implantation sites of BPH/5 mice. We next examined BPH/5 implantation sites using histology. Serial sectioning of e5.5 implantation sites from both clusters and normally spaced embryos revealed significant morphometric abnormalities. First, BPH/5 implantation sites show the presence of a persistent lumen (Figure 4.4A) along the mesometrial pole of the implantation sites. This characteristic is common to all BPH/5 implantation sites, regardless of embryo spacing. The quantification of implantation site sections show decreased area of decidualization surrounding the embryo and a smaller embryo in BPH/5 implantation sites compared to C57 (Figure 4.4B and C respectively). This was observed in both clustered and normally spaced BPH/5 implantation sites. We next examined the spacing of embryos to the antimesometrial pole to examine the depth of implantation. BPH/5 embryos that are spaced normally and C57 embryos implant to the same depth, where as clustered embryos show a more shallow invasion (Figure 4.4D).

Implantation defects in BPH/5 require both an embryonic and maternal contribution. As implantation requires synchronization of maternal and embryonic contributions, we decided to dissect the maternal and embryo components using an

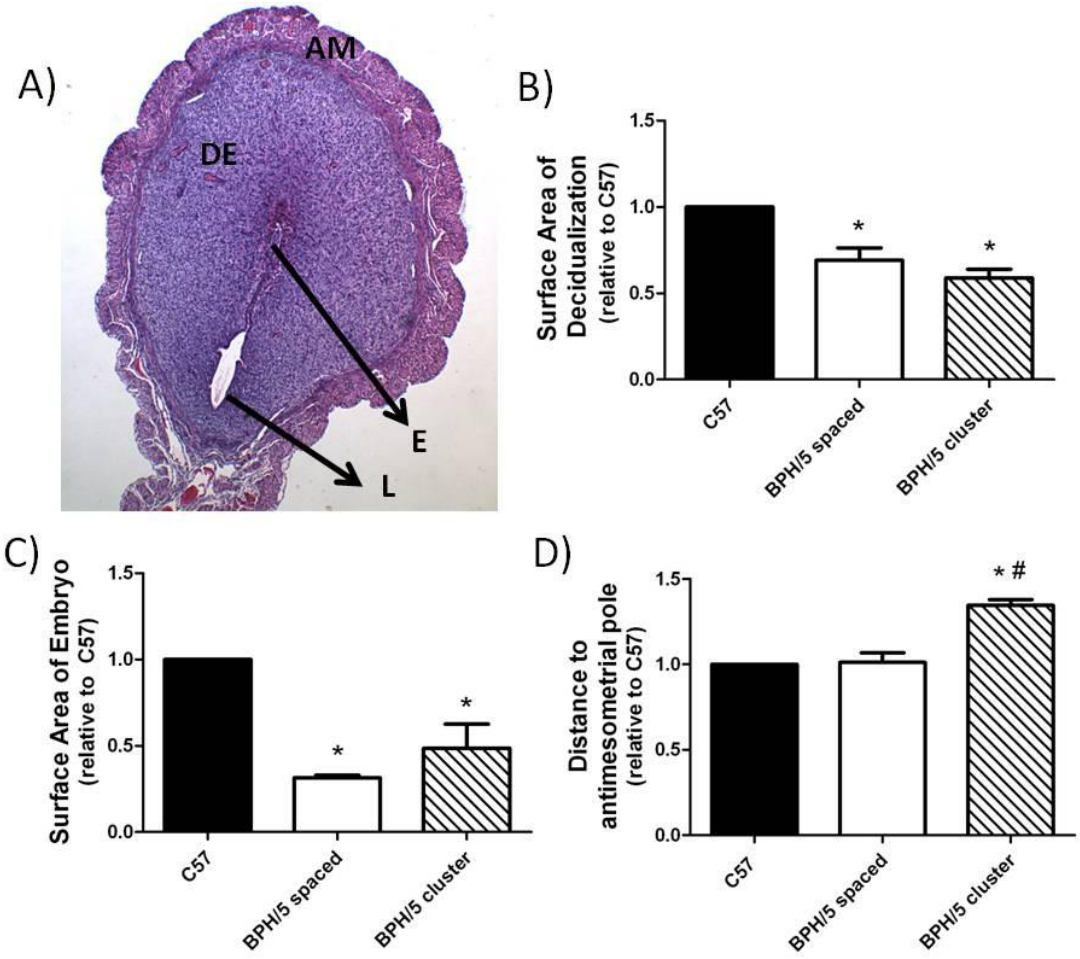

<u>Figure 4.4:</u> BPH/5 implantation sites at e5.5 show significant morphometric defects. Representative cross section of BPH/5 implantation sites stained with H&E (A). Summary of the surface area of decidualization surrounding the embryo (B), the surface area of the embryo (C) and the distance from the embryo to the antimesometrial pole (D) in C57 implantation sites, BPH/5 individually spaced implantation sites as well as BPH/5 embryos in a cluster. n=4-6, *p<0.05 vs C57, #p<0.05 vs BPH/5 spaced embryos. AM-antimesometrial pole, L=lumen, E=embryo, DE=decidua

embryo transfer strategy. We performed a series of transfers where separate pools of embryos from either BPH/5 or C57 strains were implanted along separate uterine horns within the same pseudopregnant recipients. This allowed us to examine the effect of the embryo maturation on implantation. By having both strains within the same recipient we were able to control for the maternal uterine environment. If clustering is an embryo-driven phenotype, then any recipient receiving BPH/5embryos would not space them evenly. If clustering is a defect in the maternal uterine environment, BPH/5 mothers would not be able to space embryos, independent of strain origin and maturation state. Schematic representation of the results is shown in Figure 4.5A, where clustering was observed only when BPH/5 embryos were transferred into BPH/5 uteri. Figure 4.5B shows a summary of the percentage of clustered embryos present in all the respective crosses. BPH/5 embryos in BPH/5 mothers were the only combinations where clustering was observed, implicating both a maternal and embryo contribution to implantation defects.

Examination of the maternal endocrine contribution shows premature signaling for implantation. Embryo transfer experiments implicate the maternal component, at least in part, in the embryo spacing defect observed in BPH/5. Since the maternal endocrine profile determines the period of uterine receptivity [20], we decided to examine the maternal endocrine signaling surrounding the implantation period. Serum was collected at 700h and 1900h beginning at e1.5 through e4.5. Estrogen levels were measured by ELISA and show a significant shift in BPH/5 estrogen signaling. The estrogen surge is earlier in BPH/5 mice compared to C57 controls, with a significant increase in this hormone at e2.5am then returning to baseline at e2.5pm. This is in contrast to C57 estrogen surge which begins at e2.5pm and does not return to baseline until e3.5pm (Figure 4.6A). Progesterone measured by RIA reveals a marked

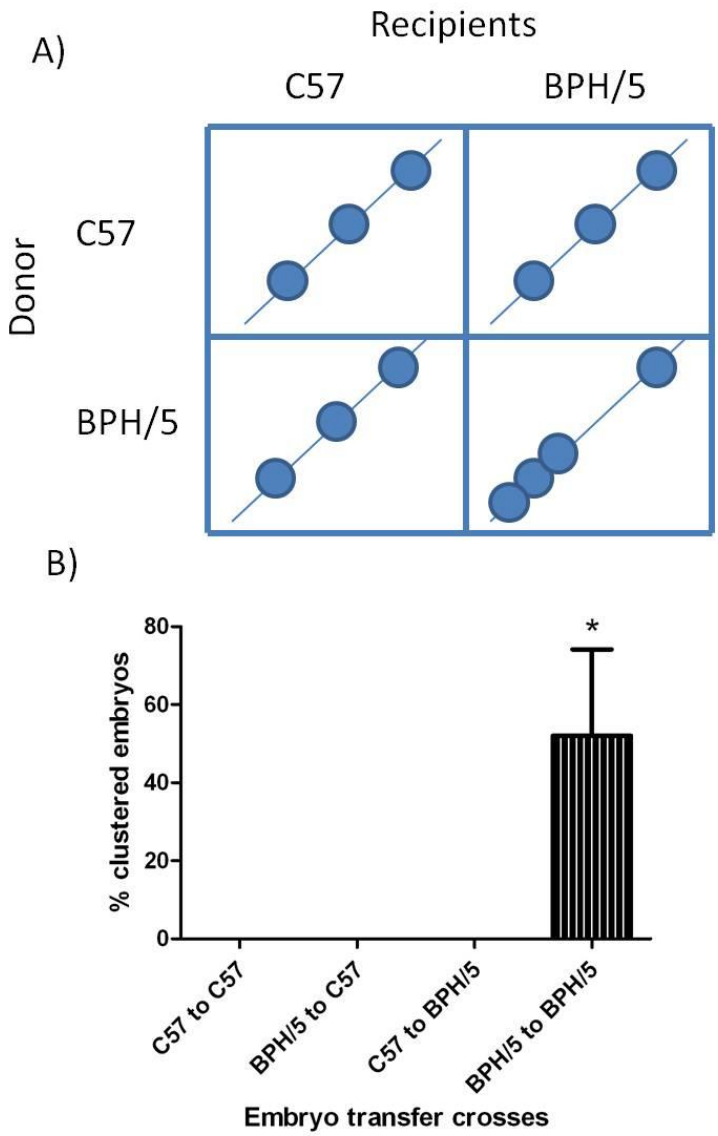

<u>Figure 4.5:</u> Clustering defects are only present when BPH/5 mothers carry BPH/5 embryos. Schematic representation of the results of embryo transfer experiments illustrating the occurrence of clustering when C57 or BPH/5 embryos were placed in C57 or BPH/5 recipients (A). Summary of the percentage of clustered embryos at e5.5 with all embryo transfer experiments is shown in (B). n=4 embryo transfers/recipient strain. *$p<0.05$ vs C57 to C57 cross.

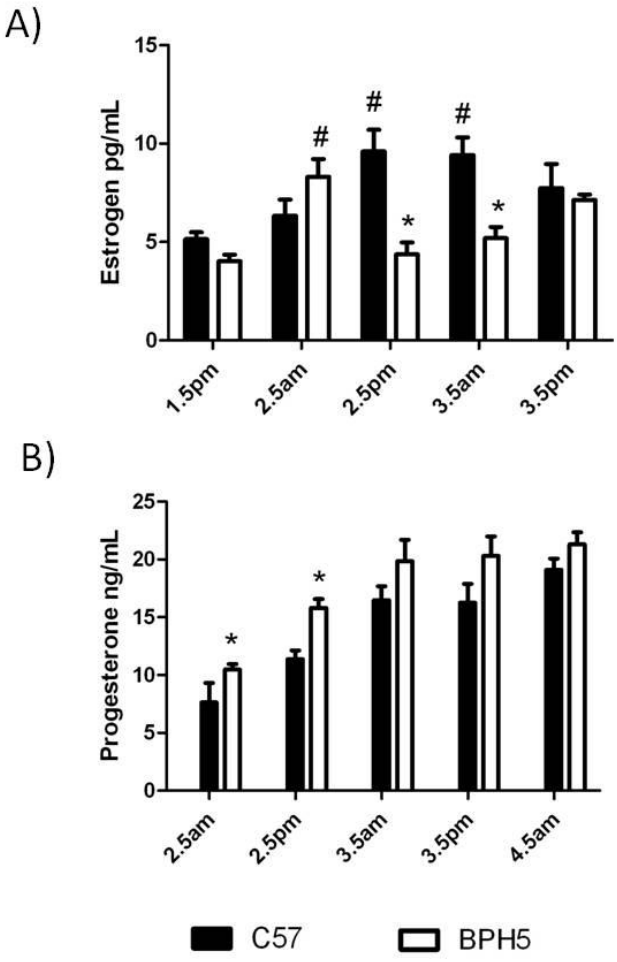

<u>Figure 4.6</u>: BPH/5 endocrine signaling shifts the window of implantation early in this strain compared to C57 controls. Summary of estrogen (A) and progesterone (B) levels determined over the timecourse indicated. n=4-10, *$p<0.05$ vs time matched C57 controls, # $p<0.05$ vs strain matched baseline levels.

increase in progesterone levels in BPH/5 by e2.5 (Figure 4.6B) that resolves by e3.5 1900h. This combined hormone profile reveals a premature endocrine surge in BPH/5 compared to C57 controls.

Artificially synchronizing maternal uterine receptivity and embryo maturation resolves implantation defects in BPH/5. Our studies have demonstrated both a delay in embryo maturation and premature maternal hormonal signaling. To determine if there is a functional link between these asynchronous events and implantation defects in BPH/5, we made use of the delayed implantation model. This procedure allows for the elongation of the window of receptivity through exogenous progesterone hormone supplementation and for implantation to be elicited in a coordinated fashion through a single estrogen injection[22]. Importantly, this procedure had no effect on implantation success in either BPH/5 or C57 mice (Figure 4.7A). Interestingly, there was a significant reduction in the BPH/5 clustering defect when peri-implantation events are synchronized (Figure 4.7B).

Genes in early development are dysregulated in natural BPH/5 pregnancies but are rescued in delayed implantation BPH/5 mice. To examine the molecular profile and potentially determine the mechanism of implantation defects in BPH/5, we performed real-time PCR to examine the expression of several candidate genes known to be involved in early developmental processes (see Table 4.1). We performed these studies using implantation sites from both natural pregnancies and synchronized pregnancies. Many of the dysregulated genes in the natural BPH/5 implantation sites include genes directly linked to endocrine signaling (*Areg, Fkbp52* and *Lif;* Figure 4.8A, B, C respectively) or downstream of initial endocrine signaling

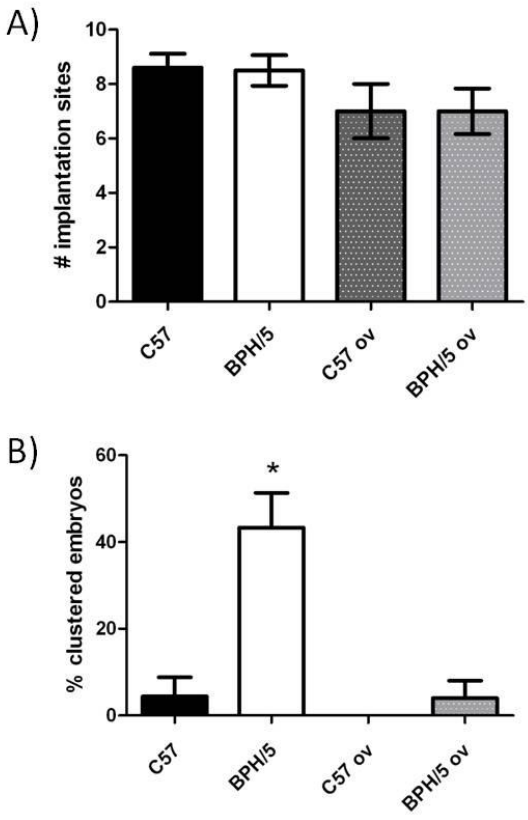

<u>Figure 4.7:</u> Artificially synchronizing embryo maturation with uterine receptivity resolves implantation defects. Summary of the number of implantation sites from mice receiving an ovariectomy (ov) and daily hormone supplementation compared to natural matings (A). Summary data of the percentage of clustered embryos in naturally mated C57 and BPH/5 compared to strain matched pregnancies that received an ovariectomy (B). n=5-6, *$p<0.05$ vs respective C57 controls.

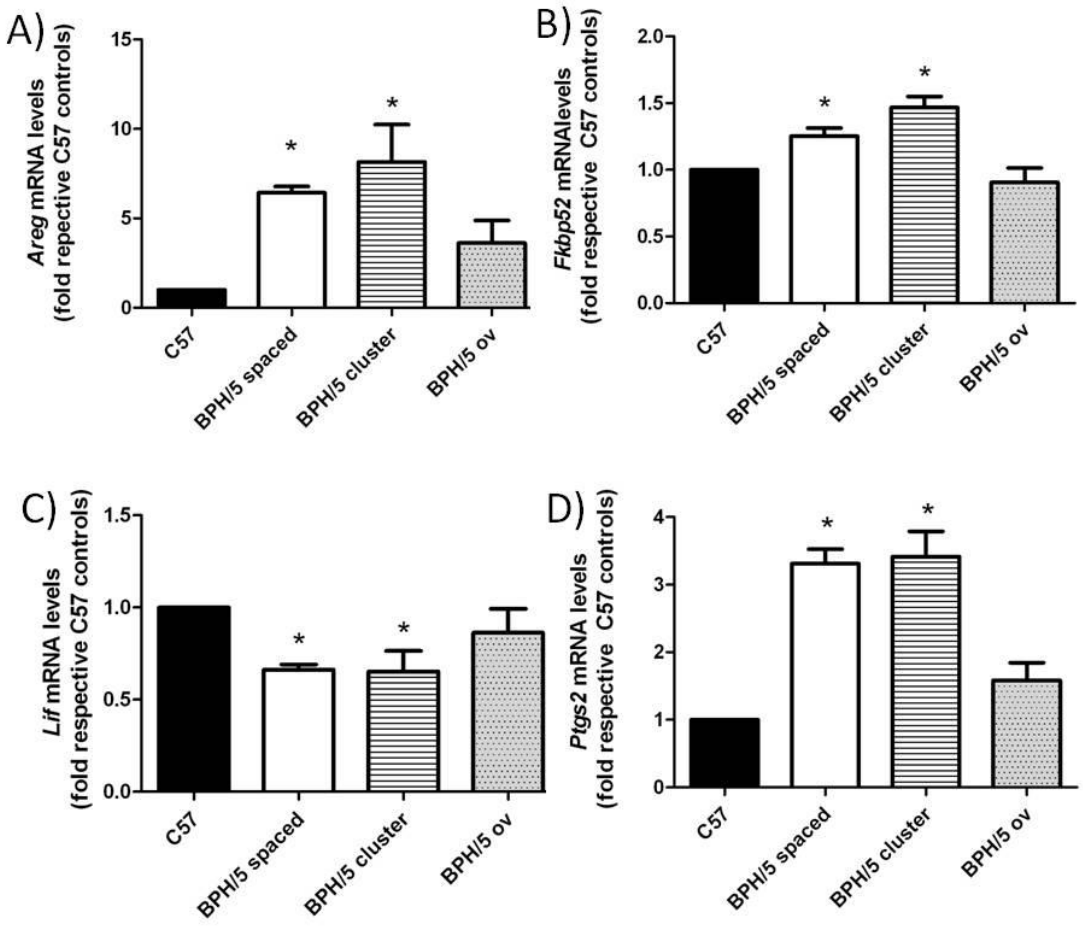

<u>Figure 4.8:</u> Synchronizing embryo maturation and uterine receptivity resolves molecular defects in implantation sites. Summary of mRNA levels of *Areg* (A), *Fkbp52* (B), *Lif* (C) and *Ptgs2* (D) in natural pregnancies of BPH/5 clustered and spaced embryos as well as BPH/5 implantation sites from artificially synchronized pregnancies. n=5-6, *$p<0.05$ vs respective C57 controls.

(Ptgs2; Figure 4.8D). Progesterone sensitive targets *Areg* and *Fkbp52* were significantly elevated in both spaced and clustered implantation sites from natural pregnancies compared to control C57s (Figure 4.8 A-B). Estrogen sensitive *Lif* showed a decrease in gene expression in natural BPH/5 implantation sites, both spaced and clustered (Figure 4.8C). Finally, *Ptgs2* showed a significant increase in transcript levels in BPH/5 implantation compared to C57 controls (Figure 4.8D). As with morphometric analyses, individually spaced embryos and clusters were indistinguishable in their molecular profile. Interestingly, by synchronizing implantation events, all of these molecular differences in natural BPH/5 implantation sites were resolved to control C57 levels (Figure 4.8 A-D).

Synchronization of implantation events has beneficial effects on placentation in BPH/5. As we have demonstrated significant improvement in spacing defects and candidate gene expression when maternal and embryo components are synchronized, we decided to continue some of these pregnancies to e12.5 to examine the effects of synchronization on fetoplacental outcomes. We began by examining fetal health in these synchronized embryos using ultra-high frequency ultrasound (see Chapter 3). As shown in Chapter 3, fetal heart rates, expressed as a ratio to maternal heart rate, were were significantly lower in BPH/5 than in C57 controls, and synchronization of implantation events had no effect on this developmental defect (Figure 4.9A). However, umbilical blood flow was significantly altered by synchronization. As seen in Figure 4.9B, BPH/5 embryos from natural pregnancies showed diminished umbilical blood flow compared to C57 controls. Synchronizing implantation events significantly improved this parameter in BPH/5 such that umbilical blood flow was now similar to that observed in C57 controls (Figure 4.9B). Importantly, the artificial

<u>Figure 4.9:</u> Rescuing implantation processes improves placental defects in BPH/5. Summary of fetal heart rates (expressed as a ratio of fetal to maternal heart rate) (A) and umbilical blood flow (B) gathered from ultrasound measurements of embryos at e12.5 of naturally mated and ovariectomized (ov) BPH/5 and C57. Representative images of isolectin stained C57 (C) BPH/5 natural (D) and implantation synchronized mice. (E) Summary data of quantification of placental depth (F). n=4-6,or where indicated, $p<0.05$ vs C57 controls, #$p<0.05$ vs BPH/5 natural mating. P=placenta, De=decidua

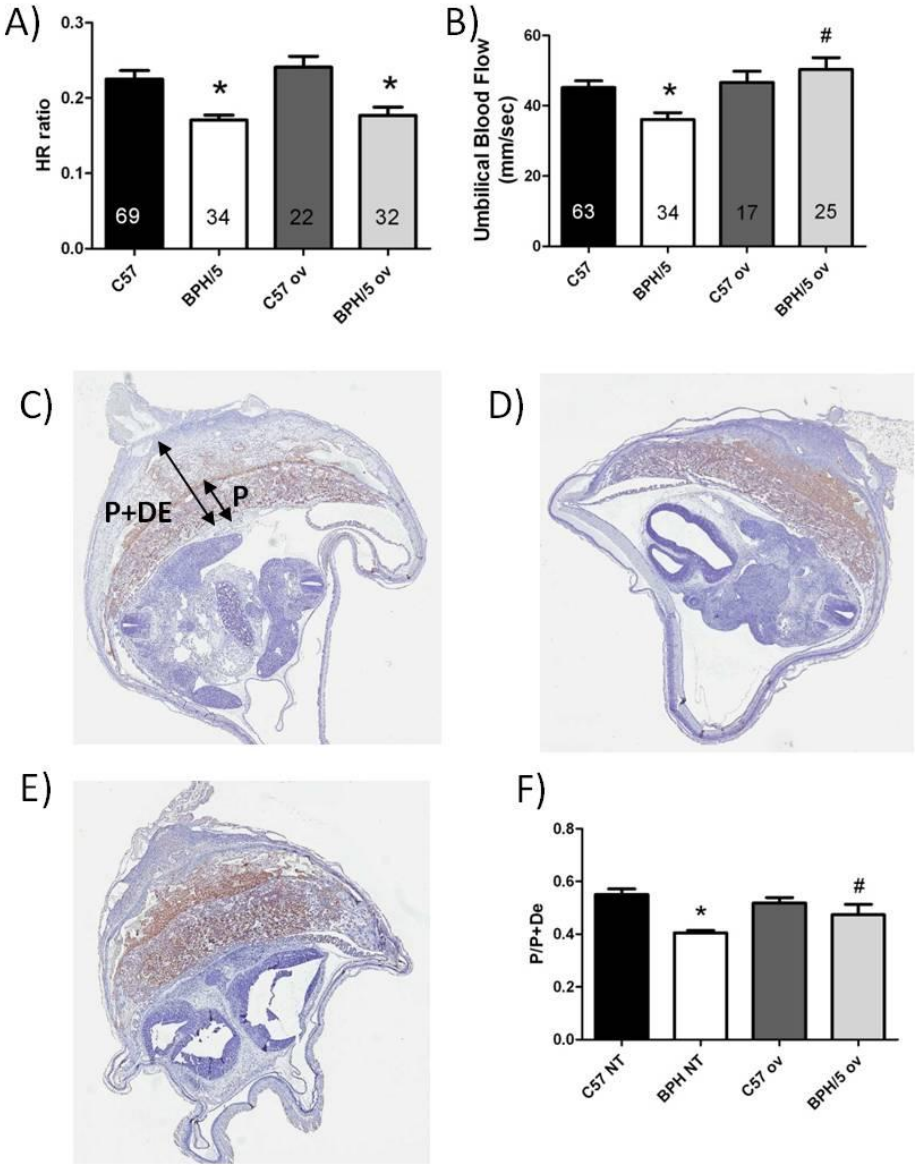
A)
HR ratio
0.3
0.2
0.1
0.0
*
*
69
34
22
32
C57
BPH/5
C57 ov
BPH/5 ov
B)
Umbilical Blood Flow (mm/sec)
60
40
20
0
*
#
63
34
17
25
C57
BPH/5
C57 ov
BPH/5 ov
C)
P+DE
P
D)
E)
F)
P/P+De
0.8
0.6
0.4
0.2
0.0
*
#
C57 NT
BPH NT
C57 ov
BPH/5 ov

synchronization procedure had no effect on fetal heart rates or umbilical blood flow in C57.

BPH/5 mice have well characterized placental defects, including shallow invasion of the trophoblast into the maternal decidua [18]. We next examined whether synchronization altered this endpoint in BPH/5. Isolectin stained sections showed shallow expansion into the maternal decidua in natural BPH/5 placentae (Figure 4.9D) compared to C57 controls (Figure 4.9C), consistent with previous findings[18]. This was measured by comparing the length of the labyrinth and junctional zones in relation to the depth of the placenta and decidua as a whole as described[18]. Interestingly, placentae from pregnancies where implantation events were synchronized showed increased placental expansion and labyrinth development (Figure 4.9E). The ratios of the fetoplacental components to the depth of the whole placental disk are quantified in Figure 4.9F, using methods previously described[18].

DISCUSSION

Implantation requires the correct synchronization of embryo maturation and uterine receptivity. When this process is altered, as is the case with IVF pregnancies, there are increased risks of adverse pregnancy outcomes including an increased risk of PE. BPH/5, a mouse model of PE, show profound placental defects that precede the development of PE-like symptoms later in gestation[17, 18]. Placental defects in PE have been associated with defects in trophoblast invasion and remodeling of maternal spiral arteries [16]. The trophoblast lineage is established in the pre-implantation period. As such, the current study asked the question whether the placental defects in BPH/5could be traced back to the peri-implantation period. This study systematically examined the peri-implantation period in BPH/5 mice, taking into account both embryo maturation and maternal endocrine signaling that determines the window of implantation. We

have found asynchronous maternal and fetal events that lead to implantation defects in this mouse model. Implantation sites in BPH/5 are clustered, and show significant morphological and molecular defects compared to control C57s. Artificially synchronizing blastocyst competency and maternal endocrine signaling rescues many of these implantation defects, with beneficial effects on later placentation.

BPH/5 mice showed a drastic delay in embryo maturation during the pre-implantation period (Figure4. 1 and 4.2). Close examination of related strains showed that this delay is unique to the BPH/5 inbred strain. This suggests either an embryo deficiency in BPH/5 or the effect of a suboptimal oviduct or uterine environment. Several groups have highlighted the importance of the oviduct and uterine milieu in the development of the embryo[23, 24]. Interestingly, in superovulated mice, delayed embryo maturation is observed in the progression to the blastocyst stage and hatching kinetics in contrast to naturally cycling controls [25]. Additionally, stimulation of the oviductal environment had detrimental effects on embryo implantation and fetal viability, resulting in an IUGR phenotype and increased resorption rate in these mice [25, 26]. These traits show significant resemblance to BPH/5 phenotypes of embryo maturation delay, implantation defects, fetal demise and IUGR in this model. Such striking similarities draws future work to examine the endocrine signaling at the time of ovulation, and a more thorough characterization of oocyte quality in these mice.

One of the most marked implantation phenotypes in BPH/5 mice was the clustering of embryos along the uterine horn. This was in contrast to evenly spaced embryos in control C57s as well as other related strains (Figure 4.3). Our embryo transfer experiments also highlight the coordinated role of both embryo and maternal components in the development of this defect, as clustering is only present when BPH/5 embryos are implanted in a BPH/5 mother (Figure 4.5). The phenomenon of

embryo spacing can be a determinant of embryo success and survival. Many polytocous species space implantation sites evenly within the uterus perhaps to maximize the maternal resources surrounding each embryo [27]. Overcrowding of implantation sites has been linked to several placental defects [21, 28]. The mechanism of embryo spacing however is largely unknown. Studies using an inhibitor of myometrial contractions, relaxin, highlighted the role of maternal uterine contractions in separating/aligning the embryos prior to implantation[29, 3031]. Additionally, the use of transgenic mice has greatly improved our molecular understanding of this process[21,32-34]. Recent work from the Arai lab demonstrates the involvement of lisophosphatidic acid (LPA) in embryo spacing[21]. LPA deficient mice show clustering of implantation sites, and treatment with an LPA agonist induces rapid uterine contractions in wild type mice, but not LPA deficient mice. This highlights LPA as a mediator of the uterine contractions in embryo spacing [32]. Other candidates include Wnts where Mohammed and colleagues recently examined their role in potentially mediating uterine smooth muscle cell contraction[33, 35]. Mice deficient in prostaglandin signaling, such as *cPla2* knockout mice, also show defects in embryo spacing as well as delayed implantation rates [34]. This highlights a potential functional link between delayed implantation and clustering of implantation sites. Interestingly, Ptgs2, an enzyme downstream of cPLA2, is among the dysregulated genes in BPH/5 implantation sites, implicating this pathway as a potential mediator of this implantation defect in BPH/5 mice.

The pathway beginning with cPLA2, via Ptgs2 and ultimately prostaglandin signaling has received quite a bit of attention for its role in implantation and early decidualization events. During implantation the uterine stroma undergoes decidual transformation where stromal cells proliferate and differentiated into decidual cells, ultimately becoming the maternal portion of the placenta [36] . This reaction is specific

to areas surrounding the implanting blastocyst. Prostaglandins are thought to be involved in initial vascular changes by increasing vascular permeability as well as early decidualization [36]. The enzymes Ptgs1 and Ptgs2 (murine COX1 and COX2) mediate the conversion of arachadonic acid to downstream prostaglandin synthesis. Ptgs1 is the constitutively active isoform in the uterus, whereas Ptgs2 is inducible in response to cytokines and growth factors [37]. In knockout Ptgs2 mice, reproductive effects include failure of blastocyst implantation and decidualization in some strains[38]. Interestingly, Ptgs2 has been demonstrated to affect the window of implantation in mice [34, 39]. In studies using low doses of pharmacological inhibitors of both Ptgs1 and Ptgs2, implantation shifted later by more than 24hrs [39]. This led embryos to implant out of the optimal window of implantation, leading to significant fetal loss later in pregnancy. Additionally, mice with a null mutation in the upstream enzyme cytosolic phospholipase A2 (which produces the arachidonic acid substrate for Ptgs2), also show a shift in the timing of the window of receptivity, delayed implantation, abnormal uterine spacing as well as defects in fetoplacental growth and development[34]. Many of these implantation defects as a result of a shifting of implantation timing show marked similarities to BPH/5 implantation kinetics. However, BPH/5 implantation sites show an elevation in Ptgs2 compared to controls (Figure 4.8), which is not predicted by these previous studies. A more thorough examination of Ptgs2 signaling and localization within the implantation sites is warranted to resolve this discrepancy.

Histological analysis of BPH/5 implantation sites revealed morphometric defects, most notably the presence of a lumen in the implantation sites. In rodents, the period of uterine receptivity is characterized by generalized edema as the uterine walls close around the blastocyst [40]. This process is largely mediated by

progesterone [40] and estrogen[41]. As we have shown altered endocrine signaling in the implantation period (Figure 4.6), this may explain the incomplete closure of the uterine tissue surrounding the implantation site. This period of implantation is also characterized by increased vascular permeability in uterine tissue surrounding the embryo, as well as the onset of decidualization. Interestingly, other mouse models where a persistent uterine lumen is present include models where NO signaling is pharmacologically altered [42], or VEGF signaling silenced [41], highlighting the importance of vasodilation in the uterine edema characteristic of this time. The BPH/5 implantation sites also show reduced decidualization and embryo growth compared to controls. Interestingly, the morphological parameters examined were similar between spaced embryos and those embryos in a cluster (Figure 4.4). Additionally, the molecular signature of all BPH/5 sites, irrespective of spacing, is similar (Figure 4.8). This suggests that the clustering phenotype is a representation of global implantation defects.

Several of our implantation phenotypes are linked to aberrant pre-implantation maternal endocrine signaling. Direct analysis of the ovarian steroids estrogen and progesterone revealed premature endocrine signaling, shifting the window of receptivity earlier in BPH/5 (Figure 4.6). This, when matched with delayed embryo maturation, leads to asynchronous implantation timing between embryo and uterus. The molecular profile of natural BPH/5 implantation sites shows significant defects in genes downstream of endocrine mediators (see Figure4.9 8). For example, *Lif* is a potent downstream target of estrogen signaling. In fact, an injection of LIF can be substituted for nidatory estrogen surge to elicit implantation in mice[43], and *Lif* knockout mice are sterile due to implantation failure[44]. Downstream mediators of progesterone signaling include amphiregulin[45], and the immunophilin FKBP52[46].

Each of these targets has a significant role in fertility and implantation success [44-46]. As BPH/5 show significant dysregulation of all of these genes, this may play a role in our implantation defects in this model.

Over the past few decades, mice have proven to be an invaluable resource in the study of the various contributions to implantation and our knowledge of mammalian development[20]. As we have demonstrated a lack of synchronization between embryo maturation and uterine receptivity in BPH/5, the use of the delayed implantation model has proved indispensible in examining the specific defects in this mouse strain. By artificially prolonging uterine receptivity, we have allowed BPH/5 embryos to mature *in vivo*, and then elicited implantation in a synchronized manner. By coordinating implantation events, we have resolved not only the proximal implantation defects such as clustering of implantation sites and the altered molecular signature of these implantation sites (Figure 4.8), but also later placental defects characteristic of this mouse model (Figure 4.9). By synchronizing implantation events, BPH/5 placentae show improved invasion into the decidua, and more developed labyrinth and spongiotrophoblast layers compared to natural pregnancies, confirming our previous findings [18]. This suggests that implantation defects in the natural pregnancy affect the trophoblast cell lineage, as these cells are critical in these processes [14, 15]. This work highlights the importance of examining placentation defects by tracing events back to the peri-implantation period.

This study emphasizes the importance of the peri-implantation period in pregnancy success using a murine model of a relatively common pregnancy disorder, PE. PE has long been characterized as a disease of placentation, but more recent theory suggests a deficiency at the time of implantation may be the origin of this disorder [16]. The BPH/5 mouse model of PE shows asynchronous implantation events

that cause implantation defects, leading to poor placental outcomes and fetal demise in this model. Future work would examine the effect of rescuing implantation defects on the development of the maternal late gestational hypertension and proteinuria, the hallmark symptoms of PE. By focusing our efforts to better understanding of the peri-implantation cascade, greater improvements could be made in our understanding of the etiology of PE in women.

REFERENCES

1. Carson DD, Bagchi I, Dey SK, Enders AC, Fazleabas AT, Lessey BA, Yoshinaga K. Embryo implantation. *Dev Biol*. 2000;223:217-237.

2. Dey SK, Lim H, Das SK, Reese J, Paria BC, Daikoku T, Wang H. Molecular cues to implantation. *Endocr Rev*. 2004;25:341-373.

3. Paria BC, Reese J, Das SK, Dey SK. Deciphering the cross-talk of implantation: Advances and challenges. *Science*. 2002;296:2185-2188.

4. Paria BC, Song H, Dey SK. Implantation: Molecular basis of embryo-uterine dialogue. *Int J Dev Biol*. 2001;45:597-605.

5. Wilcox AJ, Baird DD, Weinberg CR. Time of implantation of the conceptus and loss of pregnancy. *N Engl J Med*. 1999;340:1796-1799.

6. Gelbaya TA. Short and long-term risks to women who conceive through in vitro fertilization. *Hum Fertil (Camb)*. 2010;13:19-27.

7. Kalra SK, Molinaro TA. The association of in vitro fertilization and perinatal morbidity. *Semin Reprod Med*. 2008;26:423-435.

8. Jackson RA, Gibson KA, Wu YW, Croughan MS. Perinatal outcomes in singletons following in vitro fertilization: A meta-analysis. *Obstet Gynecol*. 2004;103:551-563.

9. Shevell T, Malone FD, Vidaver J, Porter TF, Luthy DA, Comstock CH, Hankins GD, Eddleman K, Dolan S, Dugoff L, Craigo S, Timor IE, Carr SR, Wolfe HM, Bianchi DW, D'Alton ME. Assisted reproductive technology and pregnancy outcome. *Obstet Gynecol*. 2005;106:1039-1045.

10. Maynard S, Epstein FH, Karumanchi SA. Pre-eclampsia and angiogenic imbalance. *Annu Rev Med*. 2008;59:61-78.

11. Roberts JM, Pearson G, Cutler J, Lindheimer M, NHLBI Working Group on Research on Hypertension During Pregnancy. Summary of the NHLBI working group on research on hypertension during pregnancy. *Hypertension*. 2003;41:437-445.

12. Goldstein DP, Berkowitz RS. Current management of complete and partial molar pregnancy. *J Reprod Med*. 1994;39:139-146.

13. Chun D, Braga C, Chow C, Lok L. Clinical observations on some aspects of hydatidiform moles. *J Obstet Gynaecol Br Commonw*. 1964;71:180-184.

14. Red-Horse K, Zhou Y, Genbacev O, Prakobphol A, Foulk R, McMaster M, Fisher SJ. Trophoblast differentiation during embryo implantation and formation of the maternal-fetal interface. *J Clin Invest*. 2004;114:744-754.

15. Goldman-Wohl D, Yagel S. Regulation of trophoblast invasion: From normal implantation to pre-eclampsia. *Mol Cell Endocrinol*. 2002;187:233-238.

16. Huppertz B. Placental origins of pre-eclampsia: Challenging the current hypothesis. *Hypertension*. 2008;51:970-975.

17. Davisson RL, Hoffmann DS, Butz GM, Aldape G, Schlager G, Merrill DC, Sethi S, Weiss RM, Bates JN. Discovery of a spontaneous genetic mouse model of pre-eclampsia. *Hypertension*. 2002;39:337-342.

18. Dokras A, Hoffmann DS, Eastvold JS, Kienzle MF, Gruman LM, Kirby PA, Weiss RM, Davisson RL. Severe feto-placental abnormalities precede the onset of hypertension and proteinuria in a mouse model of pre-eclampsia. *Biol Reprod*. 2006;75:899-907.

19. Schlager G, Sides J. Characterization of hypertensive and hypotensive inbred strains of mice. *Lab Anim Sci*. 1997;47:288-292.

20. Wang H, Dey SK. Roadmap to embryo implantation: Clues from mouse models. *Nat Rev Genet*. 2006;7:185-199.

21. Ye X, Hama K, Contos JJ, Anliker B, Inoue A, Skinner MK, Suzuki H, Amano T, Kennedy G, Arai H, Aoki J, Chun J. LPA3-mediated lysophosphatidic acid signalling in embryo implantation and spacing. *Nature*. 2005;435:104-108.

22. Paria BC, Huet-Hudson YM, Dey SK. Blastocyst's state of activity determines the "window" of implantation in the receptive mouse uterus. *Proc Natl Acad Sci U S A*. 1993;90:10159-10162.

23. Ertzeid G, Storeng R. Adverse effects of gonadotrophin treatment on pre- and postimplantation development in mice. *J Reprod Fertil*. 1992;96:649-655.

24. Ertzeid G, Storeng R, Lyberg T. Treatment with gonadotropins impaired implantation and fetal development in mice. *J Assist Reprod Genet*. 1993;10:286-291.

25. Van der Auwera I, D'Hooghe T. Superovulation of female mice delays embryonic and fetal development. *Hum Reprod*. 2001;16:1237-1243.

26. Van der Auwera I, Pijnenborg R, Koninckx PR. The influence of in-vitro culture versus stimulated and untreated oviductal environment on mouse embryo development and implantation. *Hum Reprod*. 1999;14:2570-2574.

27. Wellstead JR, Bruce NW, Rahima A. Effects of indomethacin on spacing of conceptuses within the uterine horn and on fetal and placental growth in the rat. *Anat Rec*. 1989;225:101-105.

28. Li M, Yee D, Magnuson TR, Smithies O, Caron KM. Reduced maternal expression of adrenomedullin disrupts fertility, placentation, and fetal growth in mice. *J Clin Invest*. 2006;116:2653-2662.

29. Pusey J, Kelly WA, Bradshaw JM, Porter DG. Myometrial activity and the distribution of blastocysts in the uterus of the rat: Interference by relaxin. *Biol Reprod*. 1980;23:394-397.

30. Rogers PA, Murphy CR, Squires KR, MacLennan AH. Effects of relaxin on the intrauterine distribution and antimesometrial positioning and orientation of rat blastocysts before implantation. *J Reprod Fertil*. 1983;68:431-435.

31. Rogers RJ, Monnier JM, Nick HS. Tumor necrosis factor-alpha selectively induces MnSOD expression via mitochondria-to-nucleus signaling, whereas interleukin-1beta utilizes an alternative pathway. *J Biol Chem*. 2001;276:20419-20427.

32. Hama K, Aoki J, Inoue A, Endo T, Amano T, Motoki R, Kanai M, Ye X, Chun J, Matsuki N, Suzuki H, Shibasaki M, Arai H. Embryo spacing and implantation timing are differentially regulated by LPA3-mediated lysophosphatidic acid signaling in mice. *Biol Reprod*. 2007;77:954-959.

33. Mohamed OA, Jonnaert M, Labelle-Dumais C, Kuroda K, Clarke HJ, Dufort D. Uterine Wnt/beta-catenin signaling is required for implantation. *Proc Natl Acad Sci U S A*. 2005;102:8579-8584.

34. Song H, Lim H, Paria BC, Matsumoto H, Swift LL, Morrow J, Bonventre JV, Dey SK. Cytosolic phospholipase A2alpha is crucial [correction of A2alpha deficiency is crucial] for 'on-time' embryo implantation that directs subsequent development. *Development*. 2002;129:2879-2889.

35. Chen Q, Zhang Y, Lu J, Wang Q, Wang S, Cao Y, Wang H, Duan E. Embryo-uterine cross-talk during implantation: The role of wnt signaling. *Mol Hum Reprod*. 2009;15:215-221.

36. Kennedy TG, Gillio-Meina C, Phang SH. Prostaglandins and the initiation of blastocyst implantation and decidualization. *Reproduction*. 2007;134:635-643.

37. Chakraborty I, Das SK, Wang J, Dey SK. Developmental expression of the cyclo-oxygenase-1 and cyclo-oxygenase-2 genes in the peri-implantation mouse uterus and their differential regulation by the blastocyst and ovarian steroids. *J Mol Endocrinol*. 1996;16:107-122.

38. Lim H, Paria BC, Das SK, Dinchuk JE, Langenbach R, Trzaskos JM, Dey SK. Multiple female reproductive failures in cyclooxygenase 2-deficient mice. *Cell*. 1997;91:197-208.

39. Pakrasi PL, Jain AK. Effect of cyclooxygenase on "window of implantation" in mouse. *Prostaglandins Leukot Essent Fatty Acids*. 2007;77:147-153.

40. Tranguch S, Smith DF, Dey SK. Progesterone receptor requires a co-chaperone for signalling in uterine biology and implantation. *Reprod Biomed Online*. 2006;13:651-660.

41. Rockwell LC, Pillai S, Olson CE, Koos RD. Inhibition of vascular endothelial growth factor/vascular permeability factor action blocks estrogen-induced uterine edema and implantation in rodents. *Biol Reprod*. 2002;67:1804-1810.

42. Wei P, Yuan JX, Jin X, Hu ZY, Liu YX. Molsidomine and N-omega-nitro-L-arginine methyl ester inhibit implantation and apoptosis in mouse endometrium. *Acta Pharmacol Sin*. 2003;24:1177-1184.

43. Chen JR, Cheng JG, Shatzer T, Sewell L, Hernandez L, Stewart CL. Leukemia inhibitory factor can substitute for nidatory estrogen and is essential to inducing a receptive uterus for implantation but is not essential for subsequent embryogenesis. *Endocrinology*. 2000;141:4365-4372.

44. Stewart CL, Kaspar P, Brunet LJ, Bhatt H, Gadi I, Kontgen F, Abbondanzo SJ. Blastocyst implantation depends on maternal expression of leukaemia inhibitory factor. *Nature*. 1992;359:76-79.

45. Das SK, Chakraborty I, Paria BC, Wang XN, Plowman G, Dey SK. Amphiregulin is an implantation-specific and progesterone-regulated gene in the mouse uterus. *Mol Endocrinol*. 1995;9:691-705.

46. Tranguch S, Wang H, Daikoku T, Xie H, Smith DF, Dey SK. FKBP52 deficiency-conferred uterine progesterone resistance is genetic background and pregnancy stage specific. *J Clin Invest*. 2007;117:1824-1834.

CHAPTER FIVE:

DISCUSSION

Summary of Findings

Prior to this thesis, significant work had been carried out by Hoffmann and colleagues to define and characterize many aspects of the BPH/5 mouse model of pre-eclampsia (PE). Multiple phenotyping studies proved the presence of the hallmark maternal symptoms of PE, along with the placental pathology associated with human PE in the BPH/5 mice[1, 2]. Initial studies found significant fetal demise as determine by necropsy, and poor fetoplacental outcomes including small litters of low birth-weight pups. These studies were instrumental in establishing this inbred mouse strain as an important model for the study the pathogenesis PE.

Building on this, this thesis sought to answer three major questions: 1) Do BPH/5 mice show an angiogenic profile during pregnancy that mimics that of women who are at increased risk of developing PE? 2) What are some potential underlying causes of fetal demise and poor fetoplacental outcomes as determined by molecular profiling of BPH/5 fetoplacental units? 3) And finally, can the placentation defects previously characterized in BPH/5 be traced to the peri-implantation period?

In Chapter 2, we examined the role of angiogenic factors in the pathology of PE in BPH/5. Initially, we examined the levels of circulating angiogenic factors and found a significant decrease in factors VEGF and PGF in BPH/5 compared to controls, and that the decrease in these factors was independent of sFLT1 antagonism. Though human studies show an increase in sFLT1 levels, these generally occur later in gestation. Next we performed a gene transfer rescue study in which we delivered adenovirus encoding a diffusible isoform of VEGF early in pregnancy. This had significant effects on attenuating the development of the hallmarks of PE, as well as improving fetal outcomes in BPH/5. Additionally, preliminary data suggests that the VEGF therapy acts at the level of the placenta by improving spiral artery remodeling.

In Chapter 3, we examined the question of early fetal status in BPH/5. By using ultrasound-mediated scoring of implantation sites, we were able to identify three classes of fetoplacental units that differed based on various fetal status parameters. This served as a platform to examine at the molecular level why some implantation sites may survive to term, while others perish. Even the healthiest BPH/5 embryos showed significant defects in cell adhesion and extracellular matrix remodeling pathways, which is not surprising given the placental defects present in this model. Interestingly, BPH/5 embryos also showed a defect in bone morphogenesis, a process very intimately linked to circulating angiogenic factors, highlighting our findings in Chapter 2. Finally, the two most challenged fetoplacental classes showed global defects in embryo development as well as an increase in apoptotic genes, suggesting that these embryos are part of the group of embryos that perish during gestation.

Finally, in Chapter 4, we examined the peri-implantation period in BPH/5 to examine whether causes of the later placental phenotypes may have originated from defects at this stage. Pre-implantation BPH/5 embryos showed a significant delay in their maturation compared to C57 controls. Additionally, this was juxtaposed against an implantation endocrine profile that is premature in BPH/5. The combination of delayed embryo development with premature maternal hormonal signaling leads to implantation defects including abnormal morphology and spacing of implantation sites. These defects can be rescued when embryo maturation and maternal endocrine signaling are synchronized artificially. Excitingly, the fetoplacental units from the pregnancies with artificially synchronized implantation events also show significantly improved later fetoplacental phenotypes, including placental expansion and umbilical blood flow, compared to naturally mated BPH/5.

Proposed Model:

These studies have provided important advances in our understanding of the BPH/5 model and how some of these findings may translate to the human disease. The schematic in Figure 1 synthesizes the important findings from this thesis as well as highlights areas of future study. The discussion to follow will progress through each component of the figure.

1) Asynchronous peri-implantation events

The studies presented in this thesis suggest that the pathological cascade in BPH/5 may begin as early as the pre-implantation period, a time point that had not been previously examined in this or other models of PE. My studies have shown significant delays in BPH/5 embryo development prior to implantation and that these delays have significant repercussions on implantation (Chapter 4: Figure 1 and 3). Additionally, I examined the in vitro growth kinetics of embryos isolated from the point of fertilization onwards to check oocyte quality (Chapter 4: Figure2). The embryos progress from the fertilized oocyte stage to the 2 cell stage normally, suggesting no major compromise in oocyte integrity. The maturation delay in BPH/5 embryos seems to begin around the progression from 4 to 8 cell stage. My studies have defined the kinetics of this delay, but further characterization of genetic defects at this stage is definitely warranted. Several candidates for stem cell and lineage development have been explored over the recent decades and may provide insight into the specific maturation delay observed in our studies. As the BPH/5 embryonic delay seems to begin at the conversion from 4-8cell stage, one of the main targets expressed at that time is *Oct4*[3]. The expression of this transcription factor increases at the 4-8cell stage where it is expressed in all nuclei. Interestingly, from this point forward, the

Figure 5.1: Schematic of the proposed pathological cascade in the development of PE in BPH/5. Asynchronous maternal signaling and embryo maturation (1) leads to implantation defects including the presence of a persistent lumen (2). The persistent lumen may alter the hypoxic state of the implantation site leading to impaired trophoblast differentiation, invasion and activation of immune cells. This leads to inadequate spiral artery remodeling and altered hemodynamic characteristics (3). The proximity of the implantation site to the lumen may have adverse effects on fetoplacental health (4). The lack of spiral artery remodeling impacts placental perfusion, and together with hemodynamic parameters(3) of the placenta leading to potential secretion of trophoblast debris, may contribute to the development of the maternal syndrome.

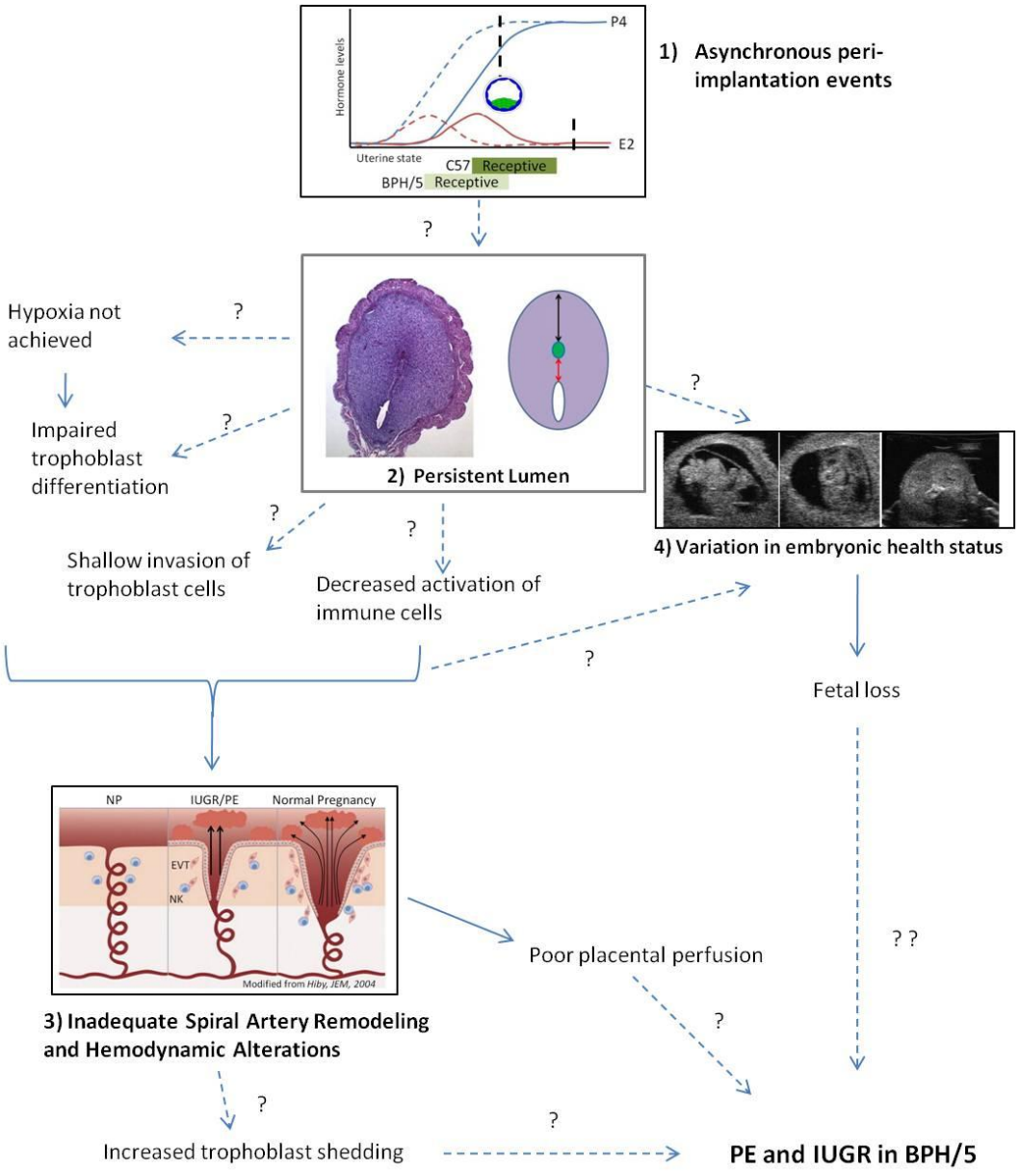
P4
Hormone levels
E2
Uterine state
C57 Receptive
BPH/5 Receptive
1) Asynchronous peri-implantation events
?
Hypoxia not achieved
?
Impaired trophoblast differentiation
?
2) Persistent Lumen
?
4) Variation in embryonic health status
?
Shallow invasion of trophoblast cells
?
Decreased activation of immune cells
?
Fetal loss
NP
IUGR/PE
Normal Pregnancy
EVT
NK
Modified from Hiby, JEM, 2004
3) Inadequate Spiral Artery Remodeling and Hemodynamic Alterations
Poor placental perfusion
? ?
?
?
?
Increased trophoblast shedding
PE and IUGR in BPH/5

relative expression of this transcription factor within the cell determines its lineage: with the greatest expression leading to extra-embryonic endoderm and mesoderm lineages and lowest expression in trophectoderm cells, and a maintained expression level remaining part of the embryonic stem cell lineage[3]. In *Oct4* knockout models, blastocysts fail to form and cells show properties of trophectoderm lineages[4]. An additional transcription factor, Nanog, shares expression in the embryonic stem cells with Oct4[5]. Interestingly, when this transcription factor is knocked out, all stem cells differentiate to a primitive endoderm phenotype[6]. Numerous factors that determine the trophoblast cell lineage have been studied by Rossant and colleagues over the years. A key factor includes *Cdx2*, one of the earliest acting trophoblast markers, and is suggested to be at the top of the hierarchy of transcription factors determining this fate[5, 7]. *Cdx2* mutants are lethal at the preimplantation stage due to failure at the blastocyst stage[7]. Later trophoblast lineage markers, including *Eomes*, are downstream of *Cdx2* and confer post-implantation trophoblast lineages. *Eomes* mutants are lethal at the early post-implantation stage[7, 8]. Additionally, future studies should consider early markers of oocyte integrity such as *MATER* and *Filia*, proteins encoded by the maternal genome that are part of a subcortical maternal complex and aid in pre-implantation embryo development[9, 10]. Interestingly, studies using null *Filia* embryos show delayed pre-implantation embryo development [11], highly reminiscent of BPH/5 kinetics. I am confident that many of these targets will show differential gene expres+sion in BPH/5 embryos. Whether they reflect simply a kinetic shift or a differentiation defect would be very useful in studies moving forward. Though I tried to perform a molecular profile of BPH/5 pre-implantation embryos, our RNA extraction techniques and the tissue limitations for this kind of analysis, have proved challenging. Though microarray strategies would be useful in identifying dysregulated targets, acquiring sufficient RNA from pre-implantation embryos for this

type of assay would be very difficult. Future studies may consider immuno-staining to better characterize these embryo defects.

My studies have also examined the maternal role in implantation defects observed in BPH/5. Characterization of the time-course of maternal endocrine signaling through assaying estrogen and progesterone levels showed a shift in signaling that is earlier than C57 controls (Chapter 4: Figure 6). This begs the question as to why this would happen in a strain that already shows delayed embryo maturation, especially since the combination of early endocrine signaling and delayed embryo maturation would give rise to implantation defects. One might hypothesize that this is a compensatory mechanism; providing an early endocrine cue can perhaps accelerate embryo maturation at the expense of moderate implantation defects. A number of studies have illustrated that estrogen signaling is the key event that leads to implantation [12-14]. In the absence of estrogen surge, blastocysts hatch but remain dormant in the uterus until this signal is given[13]. This is the basis of the delayed implantation model, a technique very readily employed in the study of murine implantation. Estrogen signaling (mediated by Lif), is also required for blastocyst activation and its preparation for implantation [15-18]. As this is such a potent signal for the final stages of blastocyst maturity, perhaps by providing an early cue (as in BPH/5 mice), this may help accelerate the delayed embryo maturation in this strain. This hypothesis can be tested by culturing BPH/5 embryos in vitro with varying amounts of estrogen in the media to see if the growth kinetics are accelerated due to this external stimulus.

Linking pre-implantation defects to implantation defects

Stemming from the endocrine signaling and embryo maturation defects, my studies show an implantation defect in BPH/5. This defect most strikingly manifests as

clustering of implantation sites (Chapter 4: Figure3).However, upon further analysis, clustered embryos have similar morphological and molecular signatures (Chapter 4: Figure 4 and 7), suggesting that perhaps clustering is only a visual cue to a greater implantation defect affecting all BPH/5 implantation sites. Studies not presented in this thesis tested the hypothesis that clustered implantation sites resulted in some of our previously scored Class II and III embryos (methods from Chapter 3). These studies involved performing pontamine studies (e5.5) on anaesthetized mice to identify early implantation site spacing followed by recovery from this procedure and examination of fetoplacental health using ultrasound at e10.5. Contrary to our hypothesis, Class I, II and III embryos were distributed among spaced and clustered implantation sites, with only a slightly increased incidence of Class II and III embryos in a cluster. The cause(s) of clustering however is an important question that has seen very little study. The spacing of implantation sites in litter-bearing species is important in maximizing the allocation of maternal resources per embryo[19]. Clustering of implantation sites has resulted in many placental defects such as hypertrophy, twinning and fetal demise [20-22]. Potential mechanisms behind clustering include failure in maternal uterine contractions [23, 24], and roles for lisophosphatidic acid (lPA), cytosolic phopholipase A2 (cPLA2) and their downstream products [21, 25, 26]. Alternative hypotheses include the role of Wnt signaling in explaining this phenomenon[27, 28]. Wnt pathways are transiently expressed in uterine smooth muscle prior to implantation [28], suggesting a potential role in uterine contractions used to separate blastocysts. I would hypothesize that the clustering defect in BPH/5 is resulting from embryos implanting outside the receptive window of the uterus. I have demonstrated premature maternal endocrine signaling in BPH/5 mothers (Chapter 4: Figure 6), and that later implanting embryos are more likely to be in a cluster (Chapter 4: Figure 3). This suggests that the embryos may be implanting outside the natural window of

implantation, perhaps a time when maternal contractions have stopped. This may lead to clustering of these implantation sites. Further examination of maternal uterine contractions is warranted in the peri-implantation period.

2) Persistent Lumen

Morphometric analyses of implantation sites from BPH/5 embryos showed significant morphological differences in embryos compared to controls. Most striking is the persistence of a lumen in the implantation sites (Chapter 4 : Figure 4). When comparing the cross sections of implantation sites between BPH/5 embryos and C57 controls, the location of the embryo with respect to the antimesometrial and mesometrial poles are similar, indicating that the location of implantation of BPH/5 embryos in the uterus is normal. The distance from the antimesometrial pole is denoted as a black arrow in Figure 5.1. I believe the distance to the lumen is key to embryo survival in BPH/5 (red arrow).

Before we consider the effects of a persistent lumen during the implantation period, future studies may consider the causes of the lumen. During normal implantation, this process is characterized by a time of generalized uterine edema, as the uterine walls close around the blastocyst [29]. As a uterine event, it is governed by ovarian steroids used to coordinate uterine receptivity [29, 30]. As we have demonstrated premature endocrine signaling in BPH/5, this process may be shifted as well, leading to an incompatible embryo-uterine cross-talk at this time. Other models where a persistent lumen is present involve defects in vasodilatory mediators such as nitric oxide and vascular endothelial growth factor, highlighting their importance in this process [30, 31]. It is interesting that VEGF may be a player at this time, as we have shown significant defects in VEGF signaling throughout the remainder of pregnancy (Chapter 2). Numerous investigators have characterized several genes necessary for

implantation and decidualization including adhesion molecules, extracellular matrix remodeling factors, vasoactive factors, growth factors, cytokines, homeobox genes, cell cycle regulators, endocannabinoid signaling, and developmental genes (reviewed in Dey, 2004[32]). Not surprisingly, many are downstream of estrogen and progesterone signaling including *Lif, Fkbp52, Areg, Hoxa-10, cyclins D* and *E, Hif* and potentially *Vegf*[32-39]. In our studies, *Fkbp52, Areg* and *Lif* were dysregulated in BPH/5 implantation sites, correlating with our premature endocrine signaling (Chapter 4: Figure 6 and 7). One can hypothesize that the signal for decidualization (linked very closely to implantation timing and endocrine-driven preparedness), is offset in BPH/5, leading to a decrease in the rapid proliferation of uterine cells causing a decreased area of decidualization as shown in Chapter 4 Figure: 4. Further characterization of the spatial distribution of decidualization targets including BMP2, PTGS2 and PTGS1 (murine Cox2 and Cox1), and perhaps additional targets involved in uterine edema including VEGF and NO signaling, may hint at a mechanism surrounding the presence of the uterine lumen.

Linking persistent lumen to the altered state of hypoxia and impaired trophoblast differentiation

How then does the persistent lumen provide the initiating cascade in the pathology of PE in BPH/5? In human pregnancy, the early post-implantation stage of the utero-embryo milieu is characterized by a period of hypoxia [40, 41]. Endovascular cytotrophoblast cells migrate and plug maternal spiral arteries resulting in a low oxygen environment. After the plugs are dislodged at 12 weeks, the oxygen tension rises roughly threefold (2.5% to 8.5%)[42]. Early trophoblast differentiation and proliferation requires a hypoxic environment. Many of the differentiation pathways are governed by hypoxia-inducible factor-1α (HIF-1α) mediated pathways[43]. Whereas

hypoxia stimulates the proliferative phenotype of trophoblast cells, increased oxygen concentrations drive differentiation towards a more invasive phenotype[44]. Very little is known about the oxygen environment in early murine implantation sites. A study by Pringle and colleagues used the hypoxia marker primonidazole and showed levels of hypoxia in implantation sites from e5.5-7.5 mice[45]. I believe that the presence of the lumen may alter the hypoxic environment necessary for these essential early events. To test this hypothesis, a similar strategy to the study by Pringle and colleagues would be adopted, where primonidazole would be administered to BPH/5 and C57 mice and e5.5-7.5 implantation sites examined. That would tell us whether the lumen altered the hypoxic state of the implantation site. Additionally, hypoxia-sensitive targets such as HIF1α and its downstream genes *Vegf* and the glucose transporter *Slc2a1* need to be examined in implantation sites. In murine studies, oxygen tension had a significant effect on trophoblast lineage specification, as demonstrated by an increase in spongiotrophoblast cells when ectoplacental cone explants were grown in low oxygen environment[45]. If the lumen in BPH/5 mice altered the hypoxia sensitive genes, future studies should also consider the effects on trophoblast lineage specification.

Hypoxia, oxidative stress and trophoblast lineage abnormalities are each associated with human PE. Preeclamptic placentae show an abundance of proliferative intermediate trophoblasts [46]. This suggests an inadequate conversion at ~10-12weeks to the invasive phenotype perhaps resulting from prolonged hypoxia exposure, leading to decreased invasiveness and spiral artery remodeling. The area of early implantation trophoblast lineage defects in PE pregnancies remains entirely unknown. This is where murine models will be invaluable.

Linking persistent lumen to shallow invasion of trophoblast cells

If the hypothesis that the persistent lumen was altering trophoblast differentiation and proliferation were true, it follows that this would impact the invasion of these cell types into the maternal uterine tissue. Shallow invasion is both a characteristic of early onset PE placentae as well as in the BPH/5 model [2, 47]. Excitingly, my research shows that when the implantation period is synchronized artificially, we rescue the shallow invasion phenotype observed in BPH/5 (Chapter 4: Figure 8). This would suggest that by resolving implantation defects, we have provided the optimal conditions for trophoblast differentiation, and these cells invade the maternal decidua to the same depth as the control strain.

Linking persistent lumen to decreased activation of immune cells

A consequence of shallow invasion may also be poor recruitment and activation of immune cells necessary for the early placentation and invasion processes. Uterine NK cells as well as macrophages are an important source of angiogenic factors as well as cytokines necessary to promote trophoblast invasion [48, 49]. Preliminary data from our VEGF studies shows a significant improvement in spiral artery remodeling in BPH/5 when treated with VEGF (Chapter 2: Figure 7). A potential reason for this improvement is that we are supplementing a system with VEGF where this might normally be provided by NK cells. Therefore, we may be bypassing the deficient NK cell population by VEGF administration, thus rescuing the process of spiral artery remodeling. A thorough examination of the immune cells, especially the natural killer cells, would greatly benefit our understanding of the immunologic role in the placental defects and PE symptoms in BPH/5.

As I have observed a significant defect in implantation in BPH/5, moving forward, microarray work may help identify some of the key players in these specific defects of embryo clustering and the presence of the lumen. Microarray work, however, has its limitations in that the volume of data acquired from these experiments often poses challenges for future analyses. Ideally, one would choose the most basic starting material to examine genetic differences. Following that theory, the initial defects that we see are in the pre-implantation embryo. However, acquiring sufficient RNA from 4/8cell or morula stage embryos for a microarray would be nearly impossible. Therefore we should consider early implantation sites as our microarray starting material. As we have shown, implantation sites have pathology of persistent lumen, decreased decidualizaion and embryo growth as well as the clustering of these implantation sites (Chapter 4: Figure 3, 4, 7). The implantation site itself, however is large enough to provide enough RNA for microarray studies. In our case, early implantation samples would presumably show defects in decidualization, trophoblast differentiation and potentially hypoxia sensitive genes. Additionally, when thinking of the application of microarray generated targets, the goal is to provide a means of rescuing a genetic defect. In a placentally-driven disease such a PE, we would want our intervention to happen as early as possible, if not the pre-implantation period, then early implantation. Lentiviral mediated targeting of trophoblast cells, is an exciting new technology that would enable the rescue of specific placental defects [50]. By infecting pre-implantation embryos with at the blastocyst stage with lentiviral-encoded targets, recent studies have shown the specific localization of these targets to trophoblast lineages, with no non-specific infection of embryo lineages[51, 52]. This technology is being developed in our laboratory and will be incredibly valuable in this model.

5.3 **Spiral artery remodeling and hemodynamic outcomes**

Previous work in our lab has demonstrated defects in spiral artery remodeling in the BPH/5 model. My studies have shown that even the healthiest embryos (Class I), and the most likely to survive, exhibit these defects. Trophoblast defects in maturation and proliferation whether due to lack of sustained hypoxia during development caused by a persistent lumen during implantation, or other factors, can lead to decreased invasion and activation of immune cells leading to a lack of spiral artery remodeling. Spiral artery remodeling defects is one of the hallmark features of human PE placentae [47]. The obvious consequence of reduced spiral artery remodeling is reduced blood flow to the intervillous space. However, recent hypotheses suggest that it is not simply the quantity of blood flow but the quality of blood flow that is problematic[53, 54]. In the normal placenta, spiral arteries are dilated leading to increased blood flow. The blood flow however is under low pressure and is thought to gently bathe the intervillous space. This is beneficial for the exchange of nutrients across the delicate fetal/maternal interface. Diffusion rates are improved when the distance between two compartments is minimized. Therefore, in pregnancy, a thin layer (the syncytiotrophoblast) separates maternal and fetal circulations, allowing oxygen, nutrients and waste products to be freely diffused[53]. Additionally, a positive pressure differential favoring a fetal to maternal direction results in higher pressures in the fetal capillaries compared to the intervillous space. This pressure gradient prevents compression of fetal vessels[55]. This is under marked contrast from the PE placentae, where the arteries are not remodeled, and lead to less blood flow but under a significantly higher pressure[56]. Therefore, the beneficial fetal to maternal pressure gradient is lessened, which could lead to fetal nutrition defects. Additionally, instead of smoothly bathing the intervillous space, the "jet-like" blood flow can cause significant damage to the delicate syncytiotrophoblast layer[53, 57]. This can lead to

increased levels of turnover and sloughing of synctiotrophoblast knots into the maternal circulation[53, 58]. The phenomenon of increased trophoblast debris in the maternal circulation has been correlated with increased risk of PE, through mediation of the immune response[58].

A thorough examination of spiral artery remodeling in BPH/5 is currently being examined in the lab with the use of vascular casting and MicroCT. This work will provide a marked improvement from histological examination as it will consider the vessels in the entire placental bed, instead of single vessels in a histological section. We will be able to examine the number of spiral arteries per placenta as well as the volume of maternal blood flow to the placenta, providing a unique perspective to the placental perfusion question. Additionally the specific 3D architecture of the vessel bed as well as individual measures of spiral artery tortuosity will further our ability to characterize the placental defects of BPH/5. Future work might also examine the vasculature differences from the pregnancies where implantation was synchronized artificially. As we have rescued invasion defects in placentation, perhaps we have also improved some of the vasculature defects in this model.

Trophoblast and syncytiotrophoblast turnover is not something that has been examined in BPH/5. With the current hemodynamic theory, this would be an interesting venue to examine. Examining the quantity of trophoblast debris in the maternal circulation, as well as the known inflammatory cytokines known to be activated by this process (IL-6), would give a systemic inflammatory perspective to placental stress. Flow cytometry protocols have been established for the measurements of these syncytiotrophoblast knots in circulation[59]. It would be interesting to quantify not only the number of particles shed, but the nature of these particles, whether they have been generated by apoptotic or necrotic pathways. Chen

and colleagues have demonstrated an abundance of particles generated by necrotic pathways that induce an inflammatory response in PE pregnancies[58].

5.4 Variation in embryonic health status

Linking persistent lumen to variations in embryonic health status.

We know that implantation defects are present in BPH/5 and that there is also a variation in fetoplacental health as characterized by ultrasound at e10.5. The spacing between the implantation site and the lumen may also lead to the variation in fetoplacental health. In fact, in both systems where a uterine lumen is present (VEGF silencing and NO signaling alteration), significant effects were found in pregnancy success[30, 31]. If this hypothesis is true, then the embryos closest to the lumen would have significant trophoblast differentiation defects leading to global development attenuation, perhaps as reflected in Class III and ultimately fetal demise in these embryos. In contrast, the embryos furthest from the lumen, may show improved fetal outcomes as reflected in Class I, but maintain the trophoblast driven placental defects known in this model, resulting from the suboptimal implantation environment

One strategy for determining whether there is a link between embryo-lumen spacing and the fetoplacental variation in BPH/5 would be the use of the viral strategy to target individual embryos with a specific marker (LacZ or GFP). These labeled embryos would then be implanted in a pseudopregnant female and the implantation characteristics would be examined. These experiments would help test many of the hypotheses generated to date. Initially, one would label a specific set of embryos (either the most mature, or least mature). For the purpose of this discussion, let us consider labeling the most mature embryos with an adenovirus encoding LacZ. We hypothesize that the most mature embryos implant the farthest from the lumen, and

become what we consider Class I embryos (the healthiest). Therefore, we would examine the implantation sites of all embryos (both labeled mature embryos, and unlabeled immature embryos) for the distance of the embryo to the lumen and co-staining for the presence of LacZ. In parallel, the same viral mediated labeling would be performed but these pregnancies would be allowed to continue until e10.5. Embryos could then be scored with the ultrasound, and subsequently stained for LacZ activity to correlate the health of the embryo with the presence of absence of the marker. This would be an important set of experiments highlighting the effects of embryo proximity to the lumen on embryo maturation and implantation defects, as well as linking those implantation defects to later fetoplacental health. A challenge to these experiments is that they would require embryo transfers (to isolate and infect embryos, then implant into pseudopregnant females). This procedure adds its own set of complications (success rate, shifted blastocyst and maternal timing).

5.5 Linking it all together: thoughts on the development of PE in BPH/5.

In Chapter 4, I examined the implantation defects in a mouse model where placentation defects are also present[2]. In the final figure of Chapter 4 (Figure 8), I have demonstrated the effects of coordinating implantation events on placentation. Excitingly, by synchronizing implantation, placentation defects of shallow trophoblast invasion are rescued in this model. How defects in placentation are linked to the development of PE is still a major unknown in the study of pre-eclampsia. Many defects in placentation are shared with IUGR pregnancies, and yet some women develop PE while others have relatively uncomplicated pregnancies. A common theory is that there is a threshold effect; that maternal constitutional factors, in combination with placental stress, may take an uncomplicated pregnancy to a PE

pregnancy. Ultimately, the study of the link between placental defects and maternal symptomology would definitely provide an invaluable step forward in understanding this disease.

Placental samples at term in patients and animal models have provided us an important starting point to examine some of cascades that may lead to the development of PE. Unlike other rodent models of PE, BPH/5 exhibits many of these placental defects early in gestation, and provides a unique tool for the linking of placental defects to the development of the maternal syndrome. Placental perfusion defects are present in PE pregnancies[47]. How these defects are produced may provide insight into how placental perfusion is linked to PE symptomology. The role of diminished angiogenic factors have been shown to play an important role in the development of PE symptoms in various rodent models[60, 61], including this study in BPH/5 (Chapter 2). These factors have both local and systemic effects, by being instrumental in placental maternal vessel remodeling, and systemic effects of altering global vascular reactivity and kidney function.

Poor placental perfusion is very closely linked to shallow invasion of trophoblast cells into the maternal uterine tissue. This can be mediated by several immune cells. Recently, studies show that autoantibodies to the angiotensin 1 receptor (AT1-AAs) have significant effects of diminishing trophoblast invasion (mediated by plasminogen activator inhibitor-1)[62], and also have the capability for inducing hypertension and proteinuria in rodent models[63]. This is also a promising candidate that has both placental and systemic targets.

Recent work from our group links placental oxidative stress to the development of PE in BPH/5. Attenuation of this placental ROS damage through Tempol treatment also suggests a link driven by oxidative stress and the development of PE in BPH/5[64].

One of the most promising links between placental stress and maternal systemic immune activation is the shedding of trophoblast knots. This provides a definitive link between perfusion defects and hemodynamic results, leading to increased placental debris. This overwhelms the maternal immune cell capabilities to dispose of the debris, leading to a global immune and increased endothelial cell activation[53, 58, 65].

Finally, in BPH/5 we show significant fetal demise throughout gestation in a fraction of the embryos in a litter [1, 2](Chapter 3). Though the links between this fetal demise and the development of PE symptoms is less clear, it cannot be ruled out. Though there are undoubtedly links between a distressed embryo and the maternal environment, it is not advantageous to respond to such stimuli that may lead to compromise of the remaining litter. However, apoptotic remains of resorbed implantation sites may contribute to an already overwhelmed systemic inflammatory response.

5.6 Perspectives:

This thesis has advanced our understanding of the development of PE in BPH/5 mice. These studies have provided important mechanistic insights into pathological events observed in BPH/5 at different gestational stages. Microarray work has examined the molecular signature of BPH/5 fetoplacental units and provides some clues as to the reason some of these embryos perish. We have elucidated the role of angiogenic factors in the development of the symptomology of PE in BPH/5, and illustrated how closely our model resembles the human condition in this regard. Finally, and most importantly, this thesis argues for a shift in focus on the initiation of the PE cascade to the peri-implantation period. By concentrating future studies to this

timeframe, we may provide an important intervention early in the development of PE, thereby preventing rather than treating an established disorder.

REFERENCES

1. Davisson RL, Hoffmann DS, Butz GM, Aldape G, Schlager G, Merrill DC, Sethi S, Weiss RM, Bates JN. Discovery of a spontaneous genetic mouse model of pre-eclampsia. *Hypertension*. 2002;39:337-342.

2. Dokras A, Hoffmann DS, Eastvold JS, Kienzle MF, Gruman LM, Kirby PA, Weiss RM, Davisson RL. Severe feto-placental abnormalities precede the onset of hypertension and proteinuria in a mouse model of pre-eclampsia. *Biol Reprod*. 2006;75:899-907.

3. Stewart CL. Oct-4, scene 1: The drama of mouse development. *Nat Genet*. 2000;24:328-330.

4. Nichols J, Zevnik B, Anastassiadis K, Niwa H, Klewe-Nebenius D, Chambers I, Scholer H, Smith A. Formation of pluripotent stem cells in the mammalian embryo depends on the POU transcription factor Oct4. *Cell*. 1998;95:379-391.

5. Rossant J. Stem cells and lineage development in the mammalian blastocyst. *Reprod Fertil Dev*. 2007;19:111-118.

6. Mitsui K, Tokuzawa Y, Itoh H, Segawa K, Murakami M, Takahashi K, Maruyama M, Maeda M, Yamanaka S. The homeoprotein nanog is required for maintenance of pluripotency in mouse epiblast and ES cells. *Cell*. 2003;113:631-642.

7. Strumpf D, Mao CA, Yamanaka Y, Ralston A, Chawengsaksophak K, Beck F, Rossant J. Cdx2 is required for correct cell fate specification and differentiation of trophectoderm in the mouse blastocyst. *Development*. 2005;132:2093-2102.

8. Russ AP, Wattler S, Colledge WH, Aparicio SA, Carlton MB, Pearce JJ, Barton SC, Surani MA, Ryan K, Nehls MC, Wilson V, Evans MJ. Eomesodermin is required for mouse trophoblast development and mesoderm formation. *Nature*. 2000;404:95-99.

9. Ohsugi M, Zheng P, Baibakov B, Li L, Dean J. Maternally derived FILIA-MATER complex localizes asymmetrically in cleavage-stage mouse embryos. *Development*. 2008;135:259-269.

10. Li L, Baibakov B, Dean J. A subcortical maternal complex essential for preimplantation mouse embryogenesis. *Dev Cell*. 2008;15:416-425.

11. Zheng P, Dean J. Role of filia, a maternal effect gene, in maintaining euploidy during cleavage-stage mouse embryogenesis. *Proc Natl Acad Sci U S A*. 2009;106:7473-7478.

12. Ma WG, Song H, Das SK, Paria BC, Dey SK. Estrogen is a critical determinant that specifies the duration of the window of uterine receptivity for implantation. *Proc Natl Acad Sci U S A*. 2003;100:2963-2968.

13. Paria BC, Huet-Hudson YM, Dey SK. Blastocyst's state of activity determines the "window" of implantation in the receptive mouse uterus. *Proc Natl Acad Sci U S A*. 1993;90:10159-10162.

14. Wang H, Dey SK. Roadmap to embryo implantation: Clues from mouse models. *Nat Rev Genet*. 2006;7:185-199.

15. Paria BC, Reese J, Das SK, Dey SK. Deciphering the cross-talk of implantation: Advances and challenges. *Science*. 2002;296:2185-2188.

16. Paria BC, Das SK, Dey SK. Embryo implantation requires estrogen-directed uterine preparation and catecholestrogen-mediated embyronic activation. *Adv Pharmacol*. 1998;42:840-843.

17. Stewart CL, Kaspar P, Brunet LJ, Bhatt H, Gadi I, Kontgen F, Abbondanzo SJ. Blastocyst implantation depends on maternal expression of leukaemia inhibitory factor. *Nature*. 1992;359:76-79.

18. Hamatani T, Daikoku T, Wang H, Matsumoto H, Carter MG, Ko MS, Dey SK. Global gene expression analysis identifies molecular pathways distinguishing blastocyst dormancy and activation. *Proc Natl Acad Sci U S A*. 2004;101:10326-10331.

19. Wellstead JR, Bruce NW, Rahima A. Effects of indomethacin on spacing of conceptuses within the uterine horn and on fetal and placental growth in the rat. *Anat Rec*. 1989;225:101-105.

20. Li M, Yee D, Magnuson TR, Smithies O, Caron KM. Reduced maternal expression of adrenomedullin disrupts fertility, placentation, and fetal growth in mice. *J Clin Invest*. 2006;116:2653-2662.

21. Ye X, Hama K, Contos JJ, Anliker B, Inoue A, Skinner MK, Suzuki H, Amano T, Kennedy G, Arai H, Aoki J, Chun J. LPA3-mediated lysophosphatidic acid signalling in embryo implantation and spacing. *Nature*. 2005;435:104-108.

22. Wimsatt WA. Some comparative aspects of implantation. *Biol Reprod*. 1975;12:1-40.

23. Rogers PA, Murphy CR, Squires KR, MacLennan AH. Effects of relaxin on the intrauterine distribution and antimesometrial positioning and orientation of rat blastocysts before implantation. *J Reprod Fertil*. 1983;68:431-435.

24. Pusey J, Kelly WA, Bradshaw JM, Porter DG. Myometrial activity and the distribution of blastocysts in the uterus of the rat: Interference by relaxin. *Biol Reprod*. 1980;23:394-397.

25. Hama K, Aoki J, Inoue A, Endo T, Amano T, Motoki R, Kanai M, Ye X, Chun J, Matsuki N, Suzuki H, Shibasaki M, Arai H. Embryo spacing and implantation timing are differentially regulated by LPA3-mediated lysophosphatidic acid signaling in mice. *Biol Reprod*. 2007;77:954-959.

26. Song H, Lim H, Paria BC, Matsumoto H, Swift LL, Morrow J, Bonventre JV, Dey SK. Cytosolic phospholipase A2alpha is crucial [correction of A2alpha deficiency is crucial] for 'on-time' embryo implantation that directs subsequent development. *Development*. 2002;129:2879-2889.

27. Chen Q, Zhang Y, Lu J, Wang Q, Wang S, Cao Y, Wang H, Duan E. Embryo-uterine cross-talk during implantation: The role of wnt signaling. *Mol Hum Reprod*. 2009;15:215-221.

28. Mohamed OA, Jonnaert M, Labelle-Dumais C, Kuroda K, Clarke HJ, Dufort D. Uterine Wnt/beta-catenin signaling is required for implantation. *Proc Natl Acad Sci U S A*. 2005;102:8579-8584.

29. Tranguch S, Smith DF, Dey SK. Progesterone receptor requires a co-chaperone for signalling in uterine biology and implantation. *Reprod Biomed Online*. 2006;13:651-660.

30. Rockwell LC, Pillai S, Olson CE, Koos RD. Inhibition of vascular endothelial growth factor/vascular permeability factor action blocks estrogen-induced uterine edema and implantation in rodents. *Biol Reprod*. 2002;67:1804-1810.

31. Wei P, Yuan JX, Jin X, Hu ZY, Liu YX. Molsidomine and N-omega-nitro-L-arginine methyl ester inhibit implantation and apoptosis in mouse endometrium. *Acta Pharmacol Sin*. 2003;24:1177-1184.

32. Dey SK, Lim H, Das SK, Reese J, Paria BC, Daikoku T, Wang H. Molecular cues to implantation. *Endocr Rev*. 2004;25:341-373.

33. Das SK, Chakraborty I, Paria BC, Wang XN, Plowman G, Dey SK. Amphiregulin is an implantation-specific and progesterone-regulated gene in the mouse uterus. *Mol Endocrinol*. 1995;9:691-705.

34. Tranguch S, Wang H, Daikoku T, Xie H, Smith DF, Dey SK. FKBP52 deficiency-conferred uterine progesterone resistance is genetic background and pregnancy stage specific. *J Clin Invest*. 2007;117:1824-1834.

35. Lim H, Ma L, Ma WG, Maas RL, Dey SK. Hoxa-10 regulates uterine stromal cell responsiveness to progesterone during implantation and decidualization in the mouse. *Mol Endocrinol*. 1999;13:1005-1017.

36. Daikoku T, Matsumoto H, Gupta RA, Das SK, Gassmann M, DuBois RN, Dey SK. Expression of hypoxia-inducible factors in the peri-implantation mouse uterus is regulated in a cell-specific and ovarian steroid hormone-dependent manner. evidence for differential function of HIFs during early pregnancy. *J Biol Chem*. 2003;278:7683-7691.

37. Yang ZM, Chen DB, Le SP, Harper MJ. Differential hormonal regulation of leukemia inhibitory factor (LIF) in rabbit and mouse uterus. *Mol Reprod Dev*. 1996;43:470-476.

38. Geum D, Sun W, Paik SK, Lee CC, Kim K. Estrogen-induced cyclin D1 and D3 gene expressions during mouse uterine cell proliferation in vivo: Differential induction mechanism of cyclin D1 and D3. *Mol Reprod Dev*. 1997;46:450-458.

39. Prall OW, Sarcevic B, Musgrove EA, Watts CK, Sutherland RL. Estrogen-induced activation of Cdk4 and Cdk2 during G1-S phase progression is accompanied by increased cyclin D1 expression and decreased cyclin-dependent kinase inhibitor association with cyclin E-Cdk2. *J Biol Chem*. 1997;272:10882-10894.

40. Burton GJ, Caniggia I. Hypoxia: Implications for implantation to delivery-a workshop report. *Placenta*. 2001;22 Suppl A:S63-5.

41. Jauniaux E, Watson AL, Hempstock J, Bao YP, Skepper JN, Burton GJ. Onset of maternal arterial blood flow and placental oxidative stress. A possible factor in human early pregnancy failure. *Am J Pathol*. 2000;157:2111-2122.

42. Pringle KG, Kind KL, Sferruzzi-Perri AN, Thompson JG, Roberts CT. Beyond oxygen: Complex regulation and activity of hypoxia inducible factors in pregnancy. *Hum Reprod Update*. 2010;16:415-431.

43. Maltepe E, Krampitz GW, Okazaki KM, Red-Horse K, Mak W, Simon MC, Fisher SJ. Hypoxia-inducible factor-dependent histone deacetylase activity determines stem cell fate in the placenta. *Development*. 2005;132:3393-3403.

44. Caniggia I, Winter J, Lye SJ, Post M. Oxygen and placental development during the first trimester: Implications for the pathophysiology of pre-eclampsia. *Placenta*. 2000;21 Suppl A:S25-30.

45. Pringle KG, Kind KL, Thompson JG, Roberts CT. Complex interactions between hypoxia inducible factors, insulin-like growth factor-II and oxygen in early murine trophoblasts. *Placenta*. 2007;28:1147-1157.

46. Redline RW, Patterson P. Pre-eclampsia is associated with an excess of proliferative immature intermediate trophoblast. *Hum Pathol*. 1995;26:594-600.

47. Maynard S, Epstein FH, Karumanchi SA. Pre-eclampsia and angiogenic imbalance. *Annu Rev Med*. 2008;59:61-78.

48. Ahn H, Park J, Gilman-Sachs A, Kwak-Kim J. Immunologic characteristics of pre-eclampsia, a comprehensive review. *Am J Reprod Immunol*. 2010.

49. Trundley A, Moffett A. Human uterine leukocytes and pregnancy. *Tissue Antigens*. 2004;63:1-12.

50. Cross JC. Lentiviruses to the placental rescue. *Nat Biotechnol*. 2007;25:190-191.

51. Okada Y, Ueshin Y, Isotani A, Saito-Fujita T, Nakashima H, Kimura K, Mizoguchi A, Oh-Hora M, Mori Y, Ogata M, Oshima RG, Okabe M, Ikawa M. Complementation of placental defects and embryonic lethality by trophoblast-specific lentiviral gene transfer. *Nat Biotechnol*. 2007;25:233-237.

52. Georgiades P, Cox B, Gertsenstein M, Chawengsaksophak K, Rossant J. Trophoblast-specific gene manipulation using lentivirus-based vectors. *BioTechniques*. 2007;42:317-8, 320, 322-5.

53. James JL, Whitley GS, Cartwright JE. Pre-eclampsia: Fitting together the placental, immune and cardiovascular pieces. *J Pathol*. 2010;221:363-378.

54. Burton GJ, Charnock-Jones DS, Jauniaux E. Regulation of vascular growth and function in the human placenta. *Reproduction*. 2009;138:895-902.

55. Karimu AL, Burton GJ. The effects of maternal vascular pressure on the dimensions of the placental capillaries. *Br J Obstet Gynaecol*. 1994;101:57-63.

56. Toal M, Chan C, Fallah S, Alkazaleh F, Chaddha V, Windrim RC, Kingdom JC. Usefulness of a placental profile in high-risk pregnancies. *Am J Obstet Gynecol*. 2007;196:363.e1-363.e7.

57. Hutchinson ES, Brownbill P, Jones NW, Abrahams VM, Baker PN, Sibley CP, Crocker IP. Utero-placental haemodynamics in the pathogenesis of pre-eclampsia. *Placenta*. 2009;30:634-641.

58. Chen Q, Ding JX, Liu B, Stone P, Feng YJ, Chamley L. Spreading endothelial cell dysfunction in response to necrotic trophoblasts. soluble factors released from endothelial cells that have phagocytosed necrotic shed trophoblasts reduce the proliferation of additional endothelial cells. *Placenta*. 2010;31:976-981.

59. Knight M, Redman CW, Linton EA, Sargent IL. Shedding of syncytiotrophoblast microvilli into the maternal circulation in pre-eclamptic pregnancies. *Br J Obstet Gynaecol*. 1998;105:632-640.

60. Gilbert JS, Verzwyvelt J, Colson D, Arany M, Karumanchi SA, Granger JP. Recombinant vascular endothelial growth factor 121 infusion lowers blood pressure and improves renal function in rats with placentalischemia-induced hypertension. *Hypertension*. 2010;55:380-385.

61. Li Z, Zhang Y, Ying Ma J, Kapoun AM, Shao Q, Kerr I, Lam A, O'Young G, Sannajust F, Stathis P, Schreiner G, Karumanchi SA, Protter AA, Pollitt NS. Recombinant vascular endothelial growth factor 121 attenuates hypertension and improves kidney damage in a rat model of pre-eclampsia. *Hypertension*. 2007;50:686-692.

62. Irani RA, Zhang Y, Zhou CC, Blackwell SC, Hicks MJ, Ramin SM, Kellems RE, Xia Y. Autoantibody-mediated angiotensin receptor activation contributes to pre-eclampsia through tumor necrosis factor-alpha signaling. *Hypertension*. 2010;55:1246-1253.

63. Zhou CC, Zhang Y, Irani RA, Zhang H, Mi T, Popek EJ, Hicks MJ, Ramin SM, Kellems RE, Xia Y. Angiotensin receptor agonistic autoantibodies induce pre-eclampsia in pregnant mice. *Nat Med*. 2008;14:855-862.

64. Hoffmann DS, Weydert CJ, Lazartigues E, Kutschke WJ, Kienzle MF, Leach JE, Sharma JA, Sharma RV, Davisson RL. Chronic tempol prevents hypertension, proteinuria, and poor feto-placental outcomes in BPH/5 mouse model of pre-eclampsia. *Hypertension*. 2008;51:1058-1065.

65. Huppertz B, Frank HG, Kingdom JC, Reister F, Kaufmann P. Villous cytotrophoblast regulation of the syncytial apoptotic cascade in the human placenta. *Histochem Cell Biol*. 1998;110:495-508.